Applied Battery Research for Transportation
(B&R No. VT-1102000)

Progress Report
for
Second Quarter FY 2013

Contributions from
Argonne National Laboratory
Army Research Laboratory
Brookhaven National Laboratory
Idaho National Laboratory
Jet Propulsion Laboratory
Lawrence Berkeley National Laboratory
National Renewable Energy Laboratory
Oak Ridge National Laboratory
Sandia National Laboratories

June 2013

Applied Battery Research for Transportation Program
Second Quarter Progress Report for FY 2013

This quarterly progress report describes the activities being conducted in support of DOE's Applied Battery Research for Transportation (ABR) Program. This program focuses on helping the industrial developers to overcome barriers for Li-Ion batteries for use in plug-in hybrid electric vehicles (PHEVs). In its goal of developing low-emission high fuel economy light-duty HEVs and PHEVs, the DOE and U.S. DRIVE established requirements for energy storage devices in these applications. The Vehicle Technologies Program at DOE has focused the efforts of this applied battery R&D program on the PHEV application.

Through the U.S. DRIVE Partnership, DOE is currently supporting the development of advanced Li-Ion batteries with industry for HEV, PHEV, and EV applications. The industrial developers have made significant progress in developing such batteries for HEV applications and there are new challenges associated with developing viable battery technologies for the PHEV application, especially when targeting the 40-mile all electric range. In addition to the calendar life, abuse tolerance, and cost challenges that exist for Li-Ion batteries in the HEV application, now the issue of providing sufficient energy within the weight and volume requirements becomes a huge challenge, as does cycle life. Also, the abuse tolerance and cost challenges become even greater. The Applied Battery Research for Transportation program is directed at assisting the industrial developers to identify the major factors responsible for the technical barriers and to find viable cost-effective solutions to them. The goal is to facilitate the development of low-cost cell chemistries that can simultaneously meet the life, performance, abuse tolerance, and cost goals that have been established by the U.S. DRIVE Partnership.

The ABR Program is organized to identify and develop advanced electrochemical couples, and further to efficiently move promising electrochemical couples from the research environment to industrial developers for evaluation. An overview of this process is given in Figure 1. Argonne has joined with other national laboratories, universities, and industry to create an integrated team to accomplish the program goals. There is a significant effort within the program to develop promising advanced electrochemical couples. As these electrochemical couples or others identified from outside the program exhibit reproducible cutting-edge results in small lab cells, the component materials are scaled-up as needed by the Materials Engineering Research Facility (MERF) and prototype cells are built by the Cell Fabrication Facility (CFF). The advanced prototype cells are thoroughly tested, examined, and characterized by a broad spectrum of studies, including utilizing the Electrochemical Analysis and Diagnostic Laboratory (EADL) and the Post-Test Facility (PTF). This information is fed back to the material researchers, and further offered to industrial developers along with prototype cells and scaled materials.

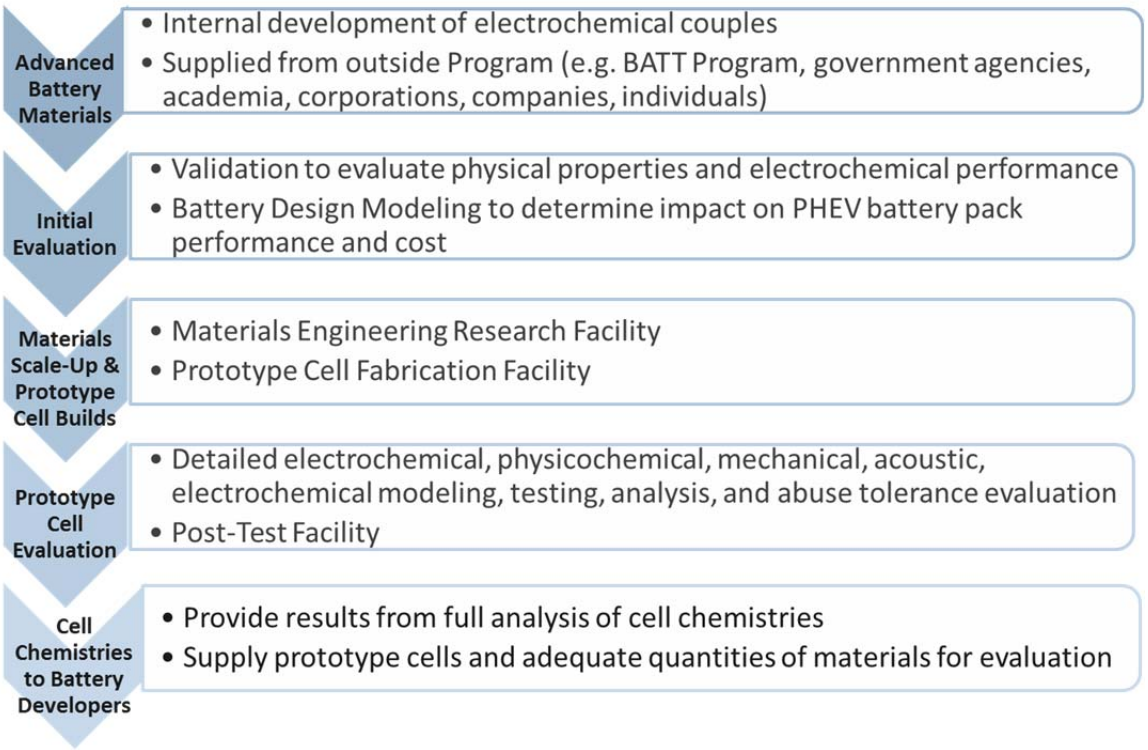

Figure 1. High level view of ABR program.

Initially, the ABR Program was organized into three main technical task areas to address the challenges for PHEVs:

(1) Battery Cell Materials Development—focuses on research, development, and engineering of advanced materials and cell chemistries that simultaneously address the life, performance, abuse tolerance, and cost issues.
(2) Calendar & Cycle Life Studies—deals with understanding the factors that limit life in different Li-Ion cell chemistries, which are used as feedback to Task 1. This task also deals with the establishment and operation of in-program cell fabrication capabilities for use in these life studies.
(3) Abuse Tolerance Studies—deals with understanding the factors that limit the inherent thermal and overcharge abuse tolerance of different Li-ion cell materials and chemistries, as well as developing approaches for enhancing their abuse tolerance.

The ABR Program is currently going through a major reorganization. The broad range of projects is being further integrated into core facility teams and efforts, along with larger electrochemical couples and electrolyte development projects. As part of the restructuring a crosscutting project focused on enabling the Argonne high energy composite layered cathode $xLi_2MnO_3 \bullet (1-x)LiMO_2$ (M = Ni, Mn, Co), also referred to as lithium and manganese rich NMC material (LMR-NMC), for the 40-mile PHEV (PHEV-40) application. This class of materials offers the potential for capacities exceeding

250mAh/g, excellent cycle and calendar life, and outstanding abuse tolerance. However, the material currently possesses a voltage fade issue (and other related issues) that affects its long-term cycle life and needs to be resolved. The voltage fade project results are reported under Task 1 although they cover activities in Task 2 also.

The list of current projects is given in the table, with the individual reports compiled in the Appendix.

Organization	AMR Project ID	AOP Project ID	Title	PI/Contact Point	Page Number
			Task 1: Battery Cell Materials Development		
ANL	ES161	1.2	Voltage Fade in the LMR-NMC Materials	Anthony Burrell	6
ANL	ES167	IV. E.1.1	Process Development and Scale up of Advanced Cathode Materials	Gregory Krumdick	25
ANL	ES168	IV. E.1.2	Process Development and Scale up of Advanced Electrolyte Materials	Gregory Krumdick	29
ARL	ES024		High Voltage Electrolytes for Li-ion Batteries	Kang Xu and Richard Jow	33
JPL	ES026		Electrolytes for Use in High Energy Li-Ion Batteries with Wide Operating Temperature Range	Marshall Smart	36
INL	ES027		Novel Phosphazene Compounds for Enhancing Electrolyte Stability and Safety of Lithium-ion Cells	Kevin Gering	45
LBNL	ES029	1.2.2	Scale-up and Testing of Advanced Materials from the BATT Program	Vincent Battaglia	53
ORNL	ES164	18502	Overcoming Processing Cost Barriers of High Performance Lithium Ion Battery Electrodes	David Wood	56
NREL	ES162		Development of Industrially Viable Battery Electrode Coatings	Robert Tenent	64
NREL	ES196	25194	Evaluate ALD Coatings of LGCPI Cathode Materials and Electrodes	Shriram Santhanagopalan	68

Organization	AMR Project ID	AOP Project ID	Title	PI/Contact Point	Page Number
			Task 2: Calendar & Cycle Life Studies		
ANL	ES030	1.1	Cell Fabrication Facility Team Production and Research Activities	Andrew Jansen	71
LBNL	ES033	1.1.1 and 2.4	Strategies to Enable the Use of High-Voltage Cathodes and Diagnostic Evaluation of ABRT Program Lithium Battery Chemistries	Robert Kostecki	93
BNL	ES034	1.1, 2.4, and 3.3	Life and Abuse Tolerance Diagnostic Studies for High Energy Density PHEV Batteries	Xiao-Qing Yang	96
ORNL	ES165	18502	Roll-to-Roll Electrode Processing NDE and Materials Characterization for Advanced Lithium Secondary Batteries	David Wood	99
			Task 3: Abuse Tolerance Studies		
SNL	ES036	3.2	Abuse Tolerance Improvements	Chris Orendorff	108
LBNL	ES037	3.3	Overcharge Protection for PHEV Batteries	Guoying Chen	113

APPENDIX

Individual Project Progress Reports

TASK 1
Battery Cell Materials Development

Project Number: 1.2 (ES161)

Project Title: Voltage Fade in the LMR-NMC Materials

Project PI, Institution: Anthony Burrell, Argonne National Laboratory

Collaborators (include industry): Ali Abouimrane, Daniel Abraham, Khalil Amine, Mahalingam Balasubramanian, Javier Bareno Garcia-Ontiveros, Ilias Belharouak, Roy Benedek, Ira Bloom, Zonghai Chen, Dennis Dees, Kevin Gallagher, Hakim Iddir, Brian Ingram, Christopher Johnson, Wenquan Lu, Dean Miller, Yang Ren, Michael Thackeray, Lynn Trahey, and John Vaughey all from Argonne National Laboratory

Project Start/End Dates: March 2012 / September 2014

Objectives: The objective of the work is to enable the Argonne high energy composite layered cathode $xLi_2MnO_3 \bullet (1-x)LiMO_2$ (M = Ni, Mn, Co), also referred to as lithium and manganese rich NMC material (LMR-NMC), for the 40-mile PHEV (PHEV-40) application. This class of materials offers the potential for capacities exceeding 250mAh/g, excellent cycle and calendar life, and outstanding abuse tolerance. This material currently possesses a voltage fade issue (and other related issues) that effects its long-term cycle life and this issue needs to be resolved.

Approach: Bring together a diverse technical team that will share data and expertise to "fix" voltage fade in the LMR-NMC cathode materials. This will be a single team effort – not multiple PI's working independently on the same problem.

- Definition of the problem and limitations of the composite cathode materials.
- Data collection and review of compositional variety available using combinatorial methods.
- Modeling and Theory.
- Fundamental characterization of the composite cathode materials.
- Understand the connections between electrochemistry and structure.
- Synthesis.
- Post treatment/system level fixes.

Milestones:

(a.) Determine if coatings have a positive effect on voltage fade – go/no-go on coatings within this project.
(b.) Determine the origin of the enhanced capacity in the LMR-NMC materials.
(c.) Determine the effect of synthesis (if any) on voltage fade.
(d.) Synthesize, characterize and optimize the composition of 'layered-layered-' and 'layered-layered-spinel' electrodes and to determine the causes for, and to counter, the voltage fade phenomenon;

(e.) Using first principles identify strategies for designing high-capacity VF-free cathode materials, and calculate properties of candidate materials that implement these strategies.
(f.) Determine compositions that mitigate voltage fade in the LMR-NMC materials.

Financial data: $4000K/year

PROGRESS TOWARD MILESTONES

(a) Summary of work in the past quarter related to milestone (a).
Argonne, the National Renewable Energy Laboratory and Oak Ridge National Laboratory and the Jet Propulsion Laboratory collaborated to devise methods to arrest voltage fade. The effect of the coatings, Al_2O_3, $LiAlO_x$, ZrO_2, TiO_2, $AlPO_4$, LiPON and AlF_3, and of the electrolyte additives, 3-hexylthiophene and lithium difluorooxalatoborate (LiDFOB), on the voltage fade phenomenon in lithium-manganese-rich, Li-Ni-Mn-Co-O cathodes was investigated. Cells containing these materials or additives were cycled according to a standard protocol at room temperature between 2.0 and 4.7 V vs. Li^+/Li. As expected, the cells containing either an additive or a coated cathode displayed less capacity loss than that in cells containing an uncoated cathode and no additive. The voltage fade phenomenon was quantified in terms of change in the parameter, average cell voltage (Wh/Ah). The results indicate that, within experimental error, there was little-to-no effect regarding voltage fade.

General. All positive electrodes contained the same, commercially-available LMR-NMC material, $0.5Li_2MnO_3 \bullet 0.5LiNi_{0.375}Mn_{0375}Co_{0.25}O_2$ (Toda Kogyo, Japan; referred to as HE5050). It was used as-received in cells and for coating.

Laminate coatings. Atomic-layer deposition (ALD) coatings of Al_2O_3, TiO_2, ZrO_2, and $LiAlO_x$ were applied to HE5050 laminate sheets (see below for the composition of the laminate), some of which were made by the Argonne Cell Fabrication Facility. The ALD coatings were performed under nitrogen. All coatings were done in 6 cycles and total less than 3 nm per coating (per 6 cycles), as determined from previous studies. The time at temperature for 6 cycles averaged less than 30 minutes. Laminates were stored in an argon glovebox after coating. Cells were then made and cycled in duplicate.

Al_2O_3. Ultrathin films of alumina were grown directly on the laminated HE5050 electrodes. The precursors for the Al_2O_3 ALD coating were trimethylaluminium (97%, Aldrich) and H_2O (HPLC grade, Sigma-Aldrich). The coating was obtained using the sequential and self-limiting surface reactions, shown in (A) and (B) below.

(A) surface-OH $+Al(CH_3)_3 \rightarrow$ surface $-O-Al(CH_3)_2 + CH_4$
(B) surface $-O-Al(CH_3)^* + H_2O \rightarrow$ surface-O-Al-OH $+ CH_4$

Each ALD cycle consists of these two reactions. The typical growth rate for the Al_2O_3 coating was ~1.1Å per cycle; however, the growth may be enhanced for the high-surface area, torturous electrodes. These ALD reactions were conducted at 120°C.

TiO_2, ZrO_2, and $LiAlO_x$. The ALD coating of TiO_2 was grown on the HE5050 laminate at both 100 and 150°C using titanium tetraisopropoxide ($Ti(OCH(CH_3)_2)_4$, Sigma-Aldrich) and H_2O as precursors. The coating was obtained using the reactions shown in (C) and (D) below.

(C) 2 surface -OH + $Ti(OCH(CH_3)_2)_4$ (g) → surface $-O_2-Ti(OCH(CH_3)_2)_2$ + $2(CH_3)_2CHOH$ (g)
(D) surface-O_2-$Ti(OCH(CH_3)_2)_2$ + $2H_2O$ (g) → surface-O_2-$Ti(OH)_2$ + $2(CH_3)_2CHOH$ (g)

The ALD coating of ZrO_2 was grown on the HE5050 laminate at both 100 and 150°C using tetrakis(dimethylamido)zirconium ($Zr(NMe_2)_4$, Sigma-Aldrich) and H_2O as precursors. The coating was obtained using the reactions shown in (E) and (F) below.

(E) surface-OH + $Zr(NMe_2)_4$ (g) → surface-O-$Zr(NMe_2)_3$ + $HNMe_2$ (g)
(F) surface-O-$Zr(NMe_2)_3$ + $3H_2O$ (g) → surface-O-Zr-$(OH)_3$ + $3HNMe_2$ (g)

The ALD coating of LiAlOx was was made by combining two sequential subprocesses, Al-O followed by Li-O, in a ratio of 1:1, per deposition cycle. The Al-O ALD subprocess was the same as that given in (A) and (B), above. The Li-O subprocess used lithium tert-butoxide ($LiOC(CH_3)_3$, Strem Chemicals) as precursor; the reactions used are given in (G) below.

(G) surface –O-Al-OH + $LiOC(CH_3)_3$ (g) → surface-O-Al-O-Li + $HOC(CH_3)_3$ (g)

Single particle coatings.

$AlPO_4$. The active, cathode material was mixed with aluminum nitrate ($Al(NO_3)_2 \bullet 9H_2O$) in $(NH_4)_2HPO_4$ solution. The aluminum phosphate ($AlPO_4$) precipitate was deposited on the surface of active material. The resulting slurry was filtered and dried in an oven at 100°C for 12 hours. The dried powder was annealed at 400°C for 4 hours before electrode fabrication.

LiPON. The LiPON layer was applied to the cathode powder by using RF-magnetron sputtering. Electrodes were then cast from the coated materials.

AlF_3. The material was applied using the methods described previously. The coated material was assembled into a coin cell using the procedure described below.

Electrolyte additive. The concentration of 3-hexylthiophene was 0.1wt% %, and that of LiDFOB (Central Glass Co., Japan), 2.0 wt% in the carbonate-based electrolyte (see Cell Construction).

Cell construction. For each 2032 coin cell, cathode laminates were prepared with a specific active mass loading of 6 to 7 mg/cm^2. The laminates contained 92 wt% active material, 4 wt% C45 (Timcal) conductive additive, and 4 wt% Solvey 5130 binder. The calendared laminate thickness was 46 µm, and the calculated final porosity was 36.1%. The anode consisted of lithium metal. The electrolyte consisted of 1.2 M $LiPF_6$ in EC:EMC (3:7 by wt). Celgard 2325 was used as the separator.

Cell construction at NREL. The 2032 coin cells using ALD-coated cathodes (mass loading ~6 to 7 mg/cm^2) were assembled in an argon-filled dry box with Li metal as the counter electrode. The laminates consisted of 84 wt% active material, 8 wt% PVDF binder, 8 wt% Super P carbon black. The anode consisted of lithium metal. A 1 M $LiPF_6$ electrolyte solution in 1:1 w/w ethylene carbonate:diethyl carbonate (Novolyte) was used. A potentiostat (VMP3, BioLogic Science Instruments) was used to perform the electrochemical measurements.

Cell cycling. All cycling (MACCOR cycler except at NREL) was performed at room temperature. All cells were cycled between 2-4.7 V at 10 mA/g for the first cycle, and then between 2-4.7 V (vs. Li^+/Li) at 20 mA/g for the following cycles. The cells were cycled between 2 and 4.7 V for a minimum of 20 and a maximum of 50 times. While cycling, current interrupt measurements were carried out at 3.5, 3.9, 4.3, and 4.7 V during charge; and 4.0, 3.6, 3.2, and 2.0 V during discharge. Estimates of cell resistance were calculated from the values of cell voltage and current at times t_0 and t_1, as shown in Figure 1 using Eq. 1.

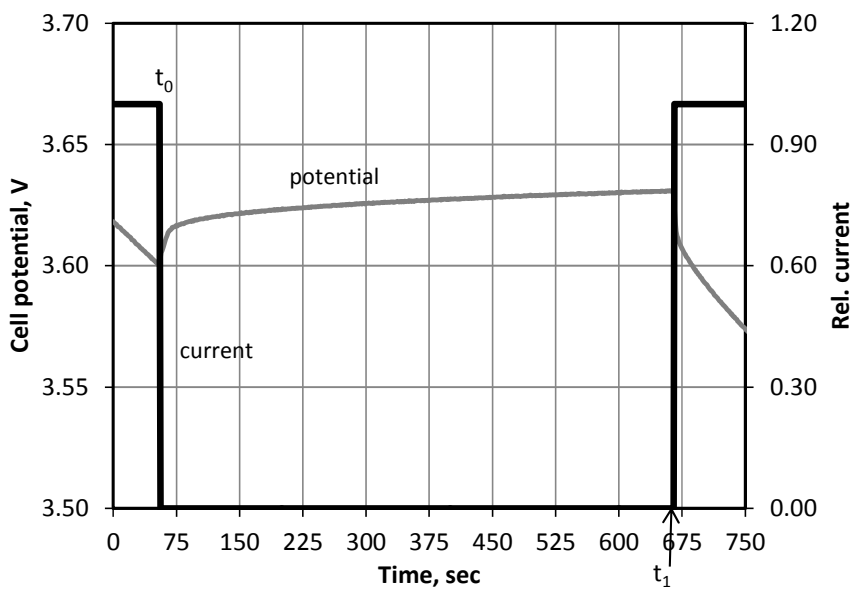

Fig. 1. Cell potential and relative current vs. time for a typical current interrupt, showing the measurement points, t_0 and t_1, which were used to calculate cell resistance. The current is indicated by the heavy black line and the voltage response of the cell, the gray curve. t_0 was just before the current was turned off and t_1 was just before the current was turned on.

Results

Examples of the data collected are shown in figure 2. Overall the data (table 1) indicates that no statically significant improvements in voltage fade were obtained by any coatings, surface treatment or additive.

Table 1. Relative change in average voltage in cells containing electrolyte additives or a coated cathode.

Coating/additive	Rel. change in average voltage after 20 cycles (s.e.)
Discharge	
Baseline	3.14×10^{-2} (9.99×10^{-4})
3-hexylthiophene	2.88×10^{-2}
LiDFOB	3.38×10^{-2}
Al_2O_3 (5 ALD cycles)	3.40×10^{-2}
Al_2O_3 (100 ALD cycles)	3.22×10^{-2}
AlF_3	2.67×10^{-2}
$AlPO_4$	3.68×10^{-2}
$LiAlO_x$	3.32×10^{-2} (7.28×10^{-4})
TiO_2 (100°C)	3.14×10^{-2} (3.90×10^{-4})
TiO_2 (150°C)	3.20×10^{-2} (7.30×10^{-4})
ZrO_2 (100°C)	3.17×10^{-2} (6.07×10^{-5})
ZrO_2 (150°C)	3.26×10^{-2} (3.08×10^{-4})
LiPON	
Charge	
Baseline	3.97×10^{-2} (4.92×10^{-3})
3-hexylthiophene	3.16×10^{-2}
LiDFOB	4.89×10^{-2}
Al_2O_3 (5 ALD cycles)	3.52×10^{-2}
Al_2O_3 (100 ALD cycles)	3.14×10^{-2}
AlF_3	4.20×10^{-2}
$AlPO_4$	3.66×10^{-2}
$LiAlO_x$	5.21×10^{-2} (4.97×10^{-4})

TiO_2 (100°C)	4.39×10^{-2} (1.36×10^{-3})
TiO_2 (150°C)	4.60×10^{-2} (1.28×10^{-3})
ZrO_2 (100°C)	4.62×10^{-2} (2.03×10^{-4})
ZrO_2 (150°C)	4.85×10^{-2} (2.93×10^{-4})
LiPON	

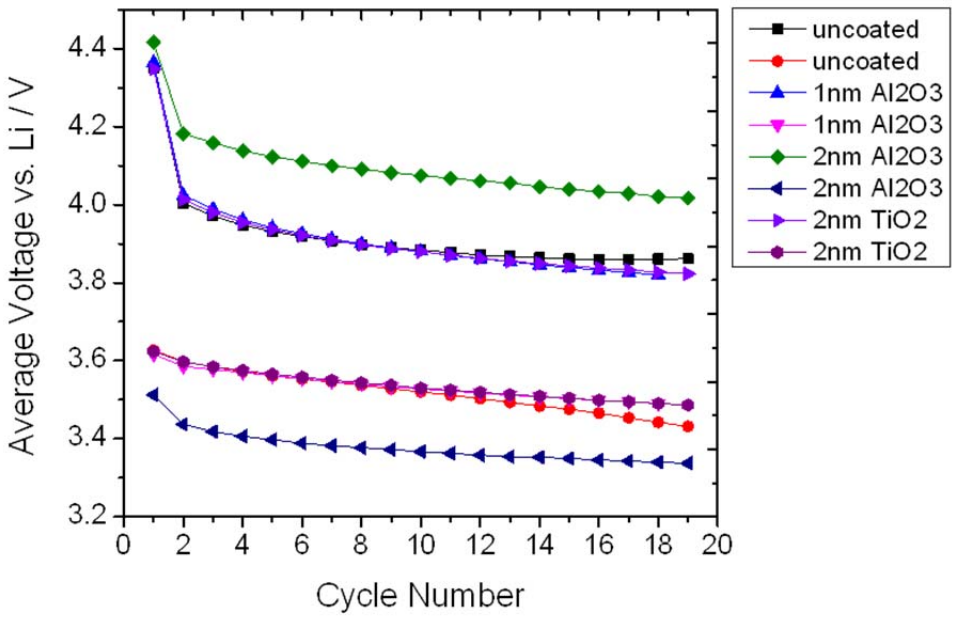

Fig. 2 Mean voltage vs. cycles of the ALD coated HE5050 powders

Conclusions

The effect of the coatings, Al_2O_3, $LiAlO_x$, ZrO_2, TiO_2, $AlPO_4$, LiPON and AlF_3, and of the electrolyte additives, 3-hexylthiophene and LiDFOB, on the voltage fade phenomenon in LMR-NMC cathodes was investigated. Cells containing these materials were cycled according to a standard protocol at room temperature. As expected, the cells containing either an additive or a coated cathode displayed less capacity loss than that in cells containing an uncoated cathode and no additive. The voltage fade phenomenon was quantified in terms of change in a resistance-corrected, average cell voltage. The results indicate that, within experimental error, there was little-to-no effect from the coatings and additives on voltage fade, pointing to voltage fade being tied to the intrinsic nature of the material.

(b) Summary of work in the past quarter related to milestone (b)

Determining the origin of the high capacity in the LMR-NMC materials has two clear advantages. First we will have an understanding of the "starting material" for voltage fade. In the past 10 years significant work to understand the pre-activated LMR-NMC material has led to a wealth of data. Unfortunately the activation step in the LMR-NMC materials results in significant structural changes that are not yet fully understood. Our contention is that an understanding of these changes will lead to a solution to voltage fade. We have implement several research directions to understand the nature of the activation.

We have been using solid state NMR techniques for characterization of Li environments and local order present in Li-rich transition metal oxide cathode materials, correlating the lithium local environments observed with the electrochemical performance in association with voltage fade team. With completion of the installation of our new low field magnet and spectrometer setup with high spinning speed capability, we are now able to obtain high resolution ^{6}Li MAS NMR data on different compositions of pristine and cycled baseline Li rich NMC materials and electrodes before and after activation. Our preliminary experiments with the new system have been focused on pristine Li-rich NMC type of materials. Figure 3 highlights high resolution ^{6}Li MAS NMR data for the TODA HE5050 cathode material. Two groups of resonances were observed for the Li species present in the lattice; Li in Li layers around 500-800 ppm region and Li in transition metal layers around 1300-1500 ppm region. The deconvolution of the peaks observed for lithium in Li layers reveals at least five different lithium environments indicating different local ordering/ domains and domain boundaries from Fermi-contact shifts of neighboring Ni, Co and Mn. For the lithium in transition metal layers, two resonances at 1371 and 1475 ppm were observed. The true origin of all the resonances and the corresponding Fermi-contact shifts are not clear and collaboration within ANL with computational groups is currently in progress to aid in this regard. The study is going to focus on generating a rule set to calculate NMR chemical shifts and perform peak fitting from domain models proving the nature of the different lithium sites observed by ^{6}Li NMR. In addition, comparison of the intensities of the peaks and nature of the lithium environments observed, will provide information on the sizes of the different domains/ local orderings.

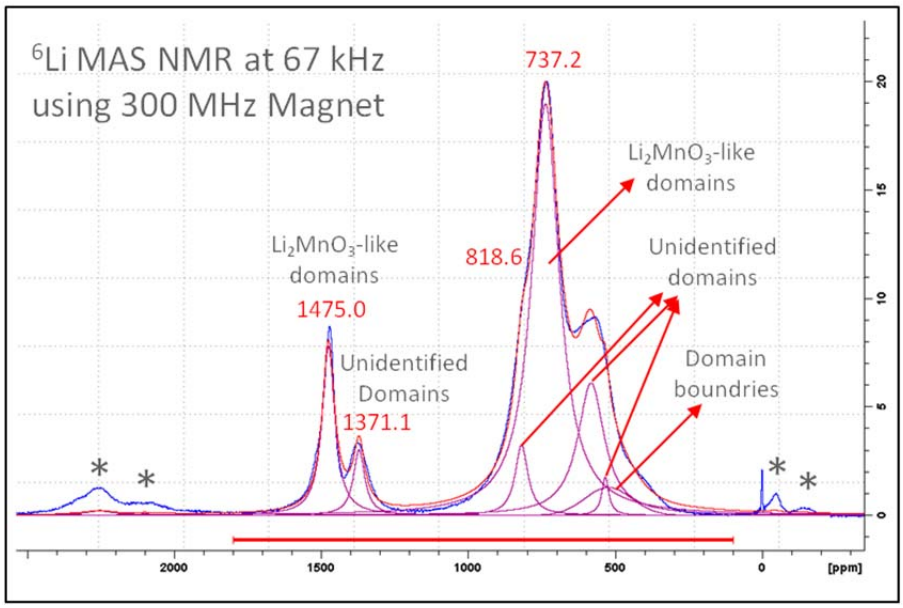

Fig. 3. ^{6}Li MAS NMR of pristine TODA HE5050 composite ($0.5Li_2MnO_3.0.5LiNi_{0.375}Mn_{0.375}Co_{0.25}O_2$ or $Li_{1.0}[Li_{0.2}Ni_{0.15}Mn_{0.55}Co_{0.10}]O_2$). * indicates spinning sidebands.

For the future characterization effort, we will initiate preparation of LRNMC type cathode materials with fully lithium-6 enriched cells (electrolyte, metal and cathode) and perform a quantitative study with high resolution ^{6}Li MAS NMR spectroscopy on the enriched cycled materials. The results will allow us to measure as a state of charge/discharge, Li domain evolution and how it corresponds to electrochemical hysteresis and rate of voltage fade in the related materials.

An electrochemical quartz crystal microbalance (EQCM) has been established in an inert glove box atmosphere. The instrument consists of the electrochemistry module and baseline QCM (E1) from Q-Sense. Aluminum-coated quartz crystals (5 MHz), mimicking aluminum current collectors in laminate composite cathodes, are used as the sensors/working electrodes. We aim to measure the mass changes on voltage fade cathodes and correlate the changes to SEI formation, gas loss from the cathode/cathode surface, and lithium addition and subtraction. For this study the EQCM response of bare aluminum, carbon additive, binder, and cathode material will all be measured. Toward this goal we have initiated spin coating of thin slurries onto Al foils.

The coating should be very thin and of uniform density and thickness (preferably less than one micrometer thick), and firmly attached to the underlying surface. Different overtones, from fundamental to higher frequencies, give information about the homogeneity of applied layers. The resonance frequency is extremely sensitive to the mass loading on the sensor. We can increase the accuracy of measurements by using higher frequencies in the data analysis. Higher frequency (higher overtones) requires even thinner coating.

Approach

A thin cathode slurry was made out of homemade LMR-NMC cathode material with particle sizes of ~0.5-3 µm (estimate). See Figure 4. The weight ratios of cathode to binder to nanocarbon was 80:12:8. NMP was used to adjust the slurry thickness. The slurries were spin-coated onto highly pure aluminum, dried overnight at 75 degrees C, and analyzed via SEM. See Figure 5.

Results

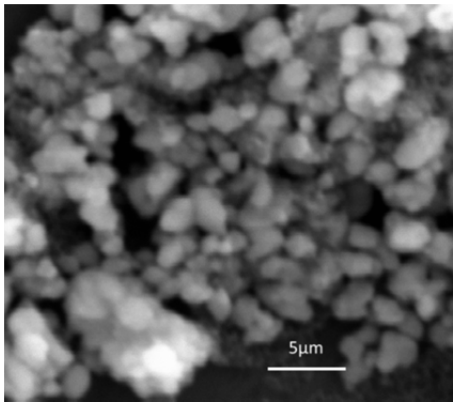

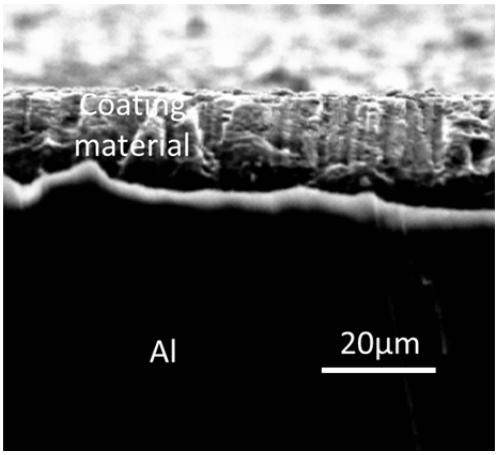

Fig. 4. Small LMR-NMC particles for attempts at EQCM sensor coating.
Fig. 5. Cross section of ~14 µm coating.

Coatings conditions that give uniform films were determined, yet film thickness still needs to be reduced. We are working to optimize the spin-coating technique and are considering other options for attachment, such as Langmuir-Blodgett.
Successful cathode films will be characterized electrochemically in coin cells and on Al-coated EQCM sensors. We intend to first fully understand the response of bare aluminum and aluminum with carbon and binder coatings in the EQCM.

High resolution XRD

The activation process of HE5050 in a fresh pouch cell has been studied by in-situ HR-XRD experiment. The results are quite different from the ex-situ study. A pouch cell after 100 cycles was also studied by in-situ HR-XRD, which show very different structural evolution of the HE5050 cathode materials, in comparison with that right after the activation.

Figure 6 shows the experimental setup for 2 pouch cells for in-situ HR-XRD experiments.
Figure 7 shows the diffraction patterns of HE5050 in a fresh cell during and right after the activation process (upper panel), and the diffraction patterns of HE5050 in a pouch cell after 100 cycles (lower panel). The structure of HE5050 has a drastic change at the beginning of the activation at 4.4 in the full cell. It is interesting to note that the

superreflection peaks due to the cation ordering do not disappear during the activation, while their positions change during cycling. The superreflection peaks exist even after the first cycle. In the pouch cell after 100 cycles, the superreflection peaks of HE5050 cathode materials totally disappear. The (003) reflection exhibits a behavior similar to a layered cathode materials, namely the inter-layer distance increases and then decreases during delithiation (charging).
Due to a large amount of dataset, detailed structural analysis is still on progress.

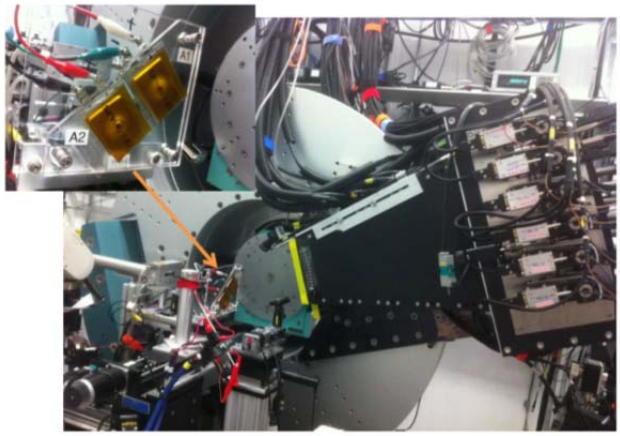

Fig. 6. Experimental setup for in-situ high-resolution X-ray diffraction measurements of pouch cell batteries at 11-BM-B.

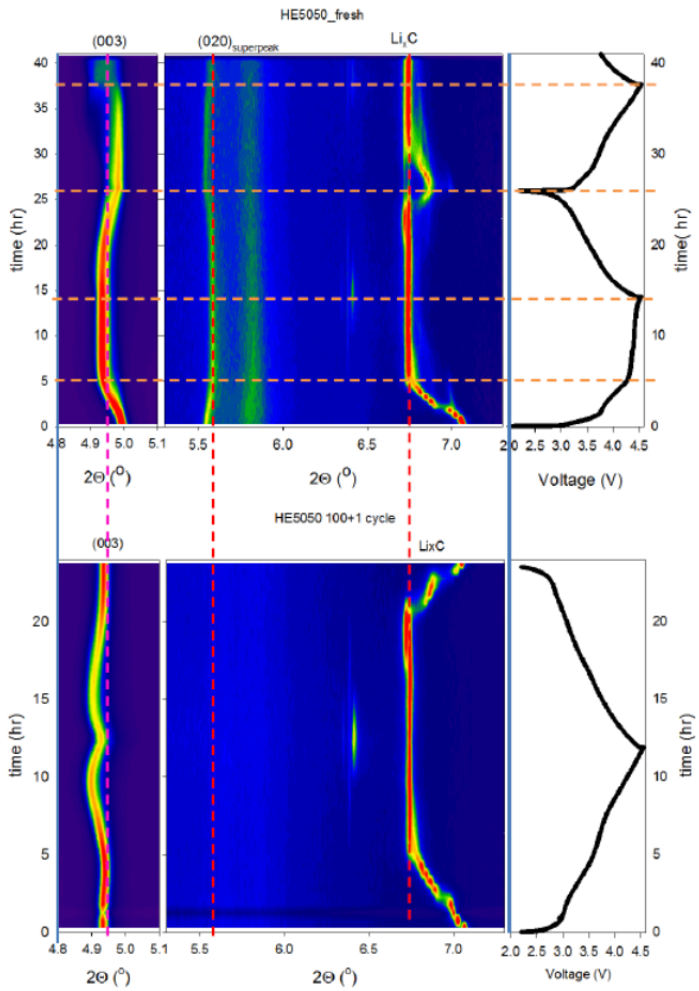

Fig. 7. Comparison of the HR-XRD diffraction patterns of a fresh cell during activation and a cell after 100 cycles. The left panel shows the reflection (003), the middle panel shows the superreflection regions together with graphite (002) reflections, and right panel shows the voltage curve during charge/discharge process.

Work on analyzing the data collected during these experiments will continue during the next quarter.

(c) Summary of work in the past quarter related to milestone (c)

One of the hypothesis in the community related to voltage fade is the nature of the material, based upon morphology and or possible synthetic route. We have established a sub-group to look into these issues with respect to a go-no/go for this FY.

We have prepared samples of LMR-NMC of similar composition which are prepared using sol-gel, carbonate, hydroxide and oxalate methods, shown in figure 8.

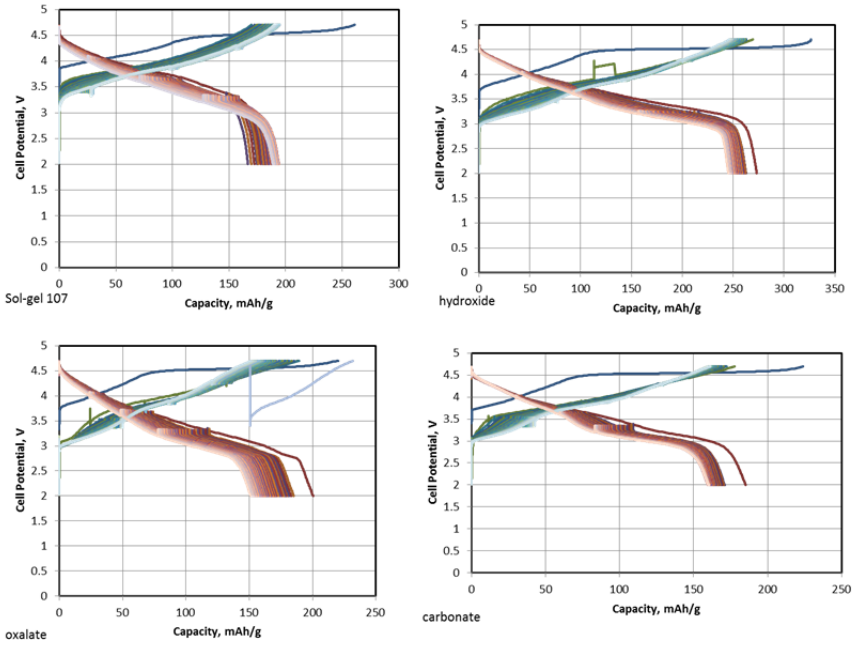

Fig. 8. Data collected using the voltage fade protocols for a single composition of LMR-NMC prepared using 4 different methods.

We are using this data to determine the "equivalent" material for comparison. We will determent the protocols for comparing materials and develop a go-no/go for synthesis method. In addition Guoying Chen (LBNL) is going to supply data on different morphologies, using the voltage fade protocols, for this milestone.

(d) Summary of work in the past quarter related to milestone (d).

The concept of embedding a spinel component in composite xLi_2MnO_3•$(1-x)LiMO_2$ (M=Mn, Ni, Co) 'layered-layered' structures is being explored to fully realize the advantages of high manganese content cathode materials. The spinel component is embedded by lowering the Li content in the xLi_2MnO_3•$(1-x)LiMO_2$ formula. We have recently shown that 'layered-layered-spinel' cathodes containing 5-10% spinel can deliver a high-capacity (~250 mAh/g) with a high, first-cycle efficiency [Kim et. al. *J. Electrochem. Soc.* 2013]; in this previous study, particular attention was paid to the system with end members xLi_2MnO_3•$(1-x)LiMn_{0.5}Ni_{0.5}O_2$ and $LiMn_{1.5}Ni_{0.5}O_4$ because both 'layered-layered' and spinel end members have a Mn:Ni ratio of 3:1. We have extended this approach by investigating substituted electrode materials in which Ni is partially replaced by Co, while maintaining a Mn:(Ni+Co) ratio of 3:1. During the past quarter, emphasis was placed on the preparation of baseline LiM_2O_4 spinel electrodes synthesized using oxalate precursors and annealing temperatures of either 450°C or 750°C. $LiMn_{1.5}Ni_{0.5}O_4$, $LiMn_{1.5}Co_{0.5}O_4$, and $LiMn_{1.5}Ni_{0.25}Co_{0.25}O_4$ spinels were successfully synthesized and characterized by powder X-ray diffraction (XRD). Figure 9 shows the XRD patterns of the three materials as well as the results of Rietveld refinements using space group symmetry Fd3m. An excellent fit between the experimental and calculated data was obtained with R_{wp} values all below 3%.

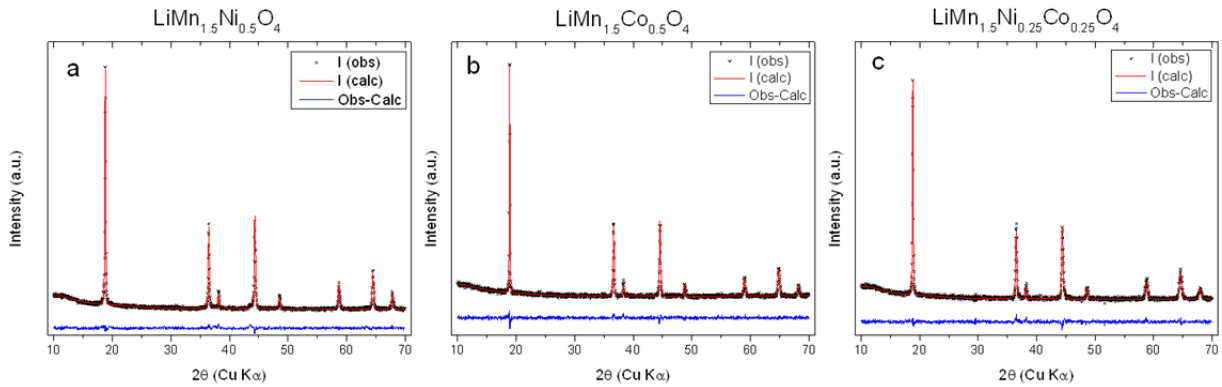

Fig. 9**.** XRD patterns and Rietveld refinements for spinel materials annealed for 12 hours at 450°C then 12 hours at 750°C: a) $LiMn_{1.5}Ni_{0.5}O_4$; b) $LiMn_{1.5}Co_{0.5}O_4$; c) $LiMn_{1.5}Ni_{0.25}Co_{0.25}O_4$. The blue line shows the difference between experimental and calculated patterns.

Electrochemistry of the spinel electrodes was performed against Li using various voltage ranges. Figures 10a and 10b highlight how substitution of Ni by Co in the spinel framework dramatically alters the charge and discharge voltage profiles, respectively, when lithium cells are cycled between 5.0 – 2.0 V. Included in the data are the voltage profiles of a $0.5Li_2MnO_3$•$0.5LiMn_{0.5}Ni_{0.25}Co_{0.25}O_2$ electrode after Li had been chemically removed to the spinel stoichiometry, and then annealed at 750°C, prior to cell assembly; the voltage response of this electrode strongly mimics that of the standard $LiMn_{1.5}Ni_{0.25}Co_{0.25}O_4$ spinel sample. The $LiMn_{1.5}Ni_{0.5}O_4$ electrode exhibits the highest charge and discharge capacity due to the Ni redox activity at 4.7 V, in good agreement with literature. The $LiMn_{1.5}Co_{0.5}O_4$ electrode exhibits the lowest capacity and shows Mn/Co redox activity below 4.0 V. The evaluation of compositional variations, coatings (e.g., AlF_3) and cycling stability of pure spinel electrode structures, and when embedded in 'layered-layered-spinel' composite electrode materials, is on-going.

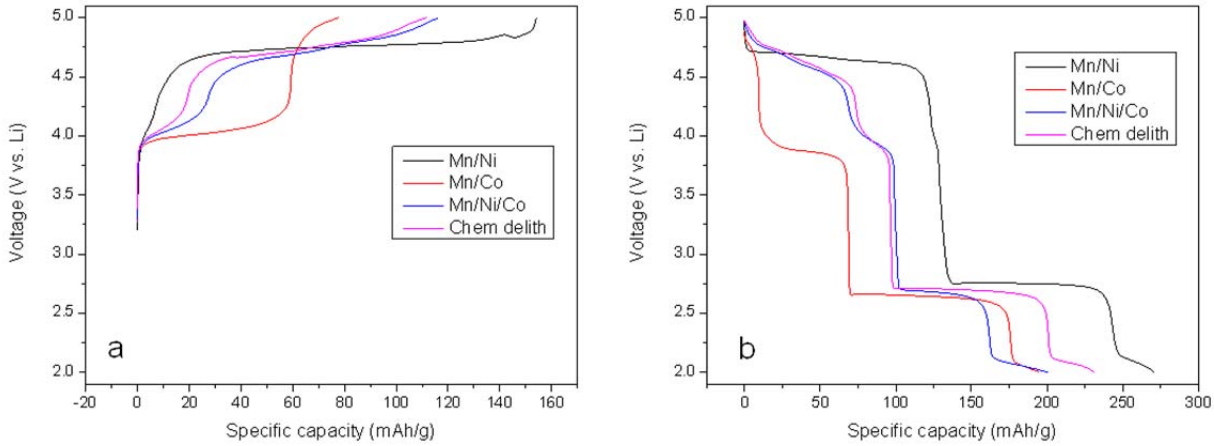

Fig. 10. First charge (a) and discharge (b) cycle of $LiMn_{1.5}Ni_{0.5}O_4$ (black), $LiMn_{1.5}Co_{0.5}O_4$ (red), and $LiMn_{1.5}Ni_{0.25}Co_{0.25}O_4$ (blue) spinel electrodes. Pink lines show profiles of a lithium cell with a 'layered-layered' $0.5Li_2MnO_3$•$0.5LiMn_{0.5}Ni_{0.25}Co_{0.25}O_2$

electrode after Li was chemically removed to the spinel stoichiometry, and then annealed at 750°C, prior to cell assembly.

(e) Summary of work in the past quarter related to milestone (e).

We have been modeling LMR-NMC cathode materials at the atomic scale to characterize the structure of the starting material and the mechanism of VF in cycled materials. We also identify and evaluate strategies for the design of high capacity, high energy-density VF-free materials. To do this we perform first-principles density functional theory (DFT) at the GGA+U level. Computational cells including up to two hundred atoms in the periodic unit are employed. Extensions of DFT are being employed, such as cluster-expansion techniques (collaboration with J. Bhattacharya, C. Wolverton, NU), which enable calculation of temperature dependent properties. This work is being coordinated with experimental efforts, including particularly the synthesis and NMR groups.

We had previously calculated properties of dilute levels of polyvalent (mostly transition) metal substitutions for Mn in Li_2MnO_3 and in $LiMO_2$ (with M=Co, $Ni_{0.5}Mn_{0.5}$, $Ni_{1/3}Mn_{1/3}Co_{1/3}$). More recently, we calculated properties of pure $Li_2M'O_3$ for several polyvalent elements M'. To establish benchmarks for stoichiometric Li_2MnO_3, calculations were performed for the R-3m, C2/m and C2/c structures. The total energies of Li_2MnO_3 in the R-3m and C2/m structures were essentially identical, whereas C2/c was lower in energy. Moreover, all elements of the stress tensor for C2/c could be reduced to zero in the C2/c structure, which could not be achieved for the other two structures. It is concluded that C2/c is likely a more realistic representation of the monoclinic structure of this material than C2/m, although the simpler C2/m is also a reasonable approximation. (This is a tentative result, since k-point convergence remains to be checked). C2/m was employed in the following calculations for $Li_2M'O_3$. As a measure of the cohesiveness of $Li_2M'O_3$ in (hypothetical) $Li_2M'O_3$• $LiNi_{0.5}Mn_{0.5}O_2$ composites, we consider the formation energy of a defect in which a single Mn ion in $LiNi_{0.5}Mn_{0.5}O_2$ and an M' ion in $Li_2M'O_3$ are exchanged, which can be viewed as a type of dissolution process (another elementary process is the dissolution of a single formula unit of $Li_2M'O_3$ into $LiMO_2$, which will be addressed in future work). The results indicate show the single ion Mn- M' exchange energy is small or exothermic for M'= Ru, Cr, Fe, and Mo, whereas positive energies of the order of 0.2 eV are found for V and Ti. Li_2VO_3 and Li_2TiO_3 "domains" in $Li_2M'O_3$•$LiNi_{0.5}Mn_{0.5}O_2$ composites are therefore expected to be more stable than the other M' choices, based on this criterion. In addition to domain cohesion, another property of interest is the cell voltage for Li extraction from $Li_2M'O_3$. We predict that voltages for M'= Ru and Mo are in the vicinity of 3 eV, whereas those for Fe, Cr, and V are 3.5 or higher. The practical usefulness of Fe, Cr and V as replacement (partial or full) for Mn in the Li_2MnO_3 component of LMRNMC systems, however, will depend on their ability to form $(LiM'_2)_n$ domains in the transition metal layers, and their stability against migration to tetrahedral sites in the Li layer during cycling, which will be investigated in future work.

There is considerable interest in the process whereby the transition metal M in $LiMO_2$ (or Mn in $Li_2M'O_3$) migrates from an octahedral site in the M layer to a tetrahedral site in the

Li layer (in a partially delithiated material). Simulations have begun of the migration of Cr ions in the model system $Li_{1-y}Co_{1-x}Cr_xO_2$, where y=1/16 (a trivacancy is introduced directly "above" a Cr ion) and x=1/48 (which corresponds to a single Cr ion), in a supercell that contains 48 formula units. We find that the energy for migration of a substitutional Cr ion from octahedral to tetrahedral site in $Li_{1-y}CoO_2$ is positive, however, the energy for such a migration in pure $LiCrO_2$ (x=1) is negative (so that the migration is favored thermodynamically). Tetrahedral Cr has been observed in Cr-doped $LiCr_{0.1}Ni_{0.45}Mn_{0.45}O_2$, where local environments similar to $LiCrO_2$ may occur in the presence of Cr clustering. The simulations of $Li_{1-y}CrO_2$, however, show three tetravalent Cr ions (for y=1/16), rather than a single hexavalent Cr ion (in a background of trivalent Cr), as found experimentally. This feature may indicate that the calculation is sensitive to the choice of on-site coulomb parameter U. Calculations have also been performed for the migration of Mn in $Li_{2-y}MnO_{3-z}$. For y=1/16 and z=0, the energy increases after migration of Mn from an octahedral to a tetrahedral site. In the presence of two oxygen vacancies (z=1/24) coordinated an octahedral Mn ion, the structure is destabilized and the migration to a tetrahedral site becomes energetically favorable. Oxygen vacancies are introduced at the electrode surface during the first (and perhaps subsequent) charges of LMRNMC materials. The oxygen vacancies may be driven into the interior of the material by their electrostatic attraction to cation (i.e., Li) vacancies, and thereby promote octahedral-Mn instability, even, perhaps, in a tetravalent oxidation state.

(f) Summary of work in the past quarter related to milestone (f).

As this synthesis project is directed by theory, we are making materials that, from DFT calculations suggest are useful compositions that can possibly retard voltage fade or VF. First, in this quarter we developed a consistent sol-gel synthesis route to make TodaHE5050 composition: ($0.5Li_2MnO_3 \cdot 0.5Li[Ni_{0.375}Mn_{0.375}Co_{0.25}]O_2$) and that which would facilitate the bulk incorporation of dopant or substitution. The Fe-doped $Li[(NMC)_{0.87}(Fe)_{0.013})]O_2$, was synthesized. The undoped and a Fe-doped (1.3%) materials show, by XRD, a pure layered phase, and the cycling resulted in approximately 265 mAh/g capacity. The Fe-doping did not change the VF result. We compared the VF in a carbonate co-precipitated precursor reactant with the target Toda HE5050 product composition to that of the aforementioned sol-gel derived product with the same composition, with the goal being to see if the synthesis route changes the voltage fade. As is shown in Fig. 11, the synthesis method used did not change the result – VF is about the same with the results similarly fitted to a paralinear function (Ira Bloom model). In the second part, we instead compare the O2 stacked ion-exchange derived sample with a Co-free composition VF to that of the conventionally synthesized O3 stacked materials.

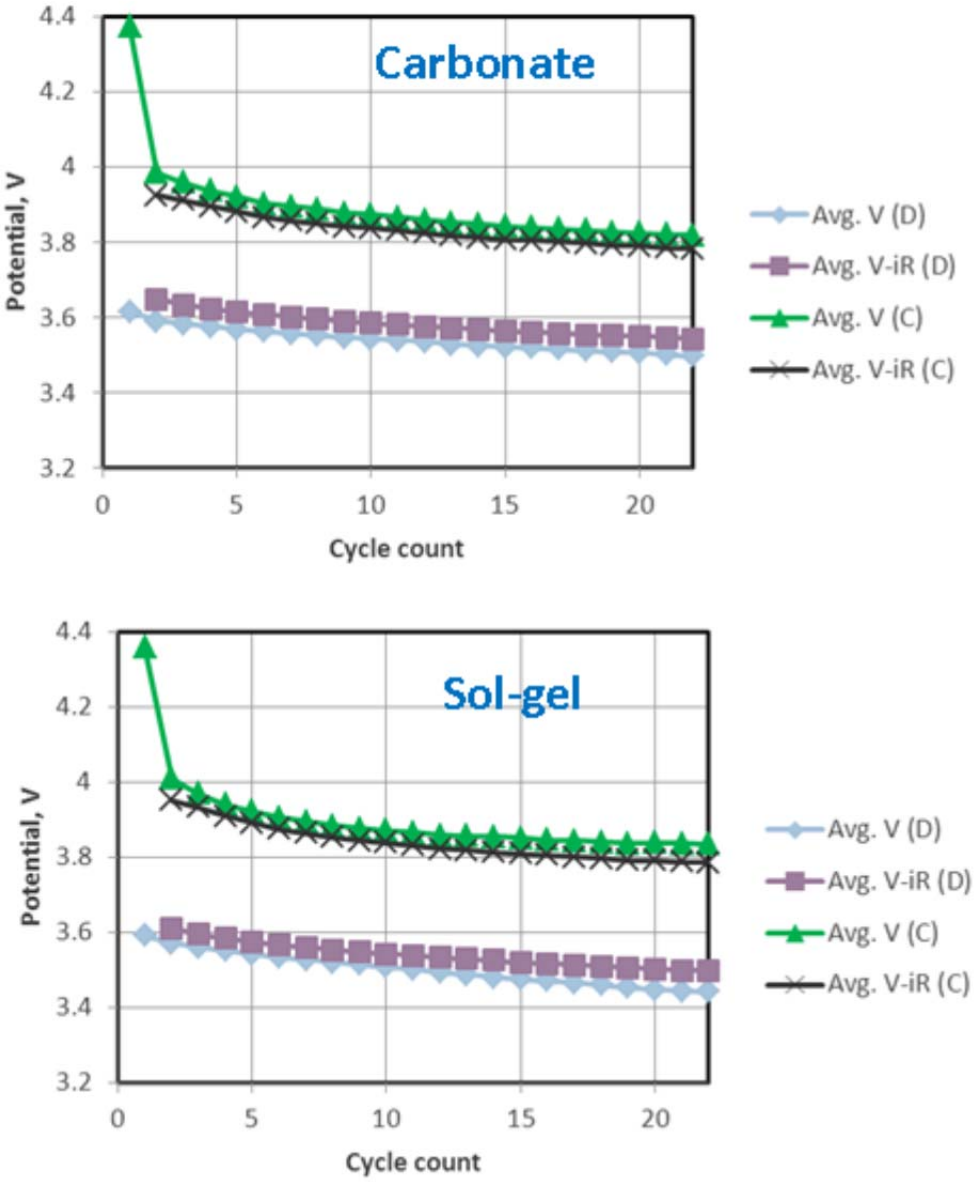

Fig. 11. Voltage Fade of $0.5Li_2MnO_3.0.5Li[Ni_{0.375}Mn_{0.375}Co_{0.25}]$

The VF result is shown in Fig. 12: the ion-exchanged sample does not fade as much as Toda HE5050 (sol gel) and the mechanism of fade appears to be different. Future studies will continue with sol-gel synthesis to make homogeneous composite materials which will enable us to compare and evaluate the role of dopants and substitutions to theory predictions.

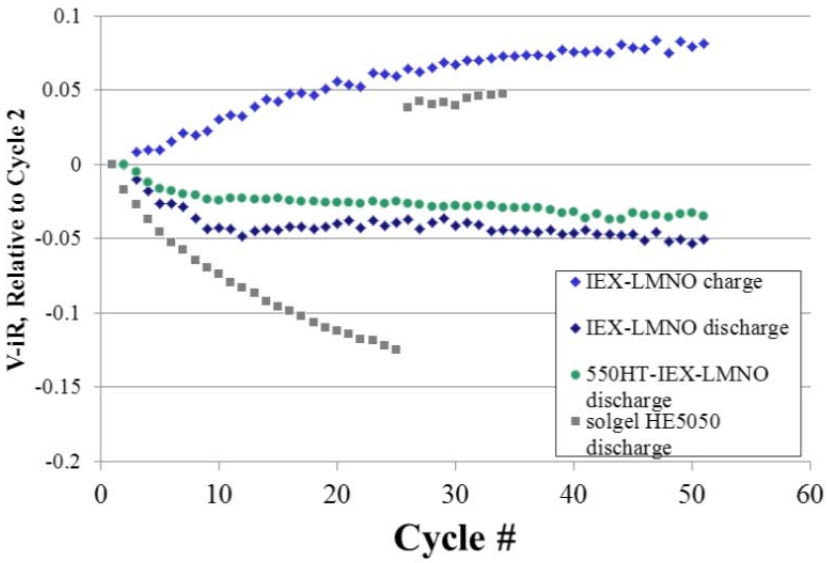

Fig 12. VF of various cathode materials.

Cathode active materials of nominal composition $^{6}Li_{1.2}Mn_{0.55}Co_{0.1}Ni_{0.15}O_2$ (6-Li enriched for NMR) were synthesized via a sol-gel process, which involves gel formation, decomposition of the gel at ~ 450 °C, followed by grinding of the intermediate, and a second firing at the "synthesis temperature," typically ca. 850 °C. The initial attempt to prepare a 6Li labeled HE5050 analogue, incorporating all metals in the gel stage, produced a material with significant spinel content, similar to "layered-layered-spinel" (LLS) cathodes, as evidenced by a secondary peak at lower angle of the R-3m (101) reflection near 37° 2Θ (see Figure 3).

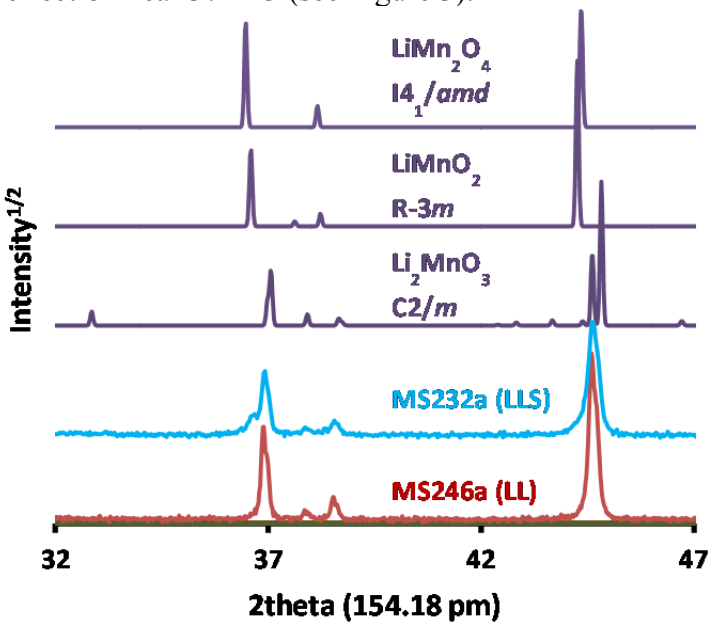

Fig. 13. Powder XRD of sol-gel process cathode materials. LLS = layered-layered-spinel, LL=layered-layered. Reference patterns from ICSD are in purple.

A second attempt at the synthesis withheld Li until the high temperature "synthesis" firing and resulted in the pure "layered-layered" (LL) material. One possible explanation for the difference is altered kinetics of the reaction: having the Li present in the gel formation and decomposition allows early formation of Li_2MnO_3-like (charge ordered) domains which leaves the rest of the system lithium poor, thus leading to spinel formation. Another possibility is that differences in material handling alter the stoichiometry, favoring the strictly LL product in the latter procedure.
The electrochemical performance of the two materials, using the VF protocol, is shown in Figure 14 Relative to the LL polymorph, the LLS material has a relatively longer activation plateau (capacity above 4.3 V) during charge as compared to capacity below 4.3 V, suggesting that it contains more Li_2MnO_3. On discharge, the specific capacities are similar with the LLS material showing some additional capacity characteristic of Li insertion in the spinel phase below 2.7 V.

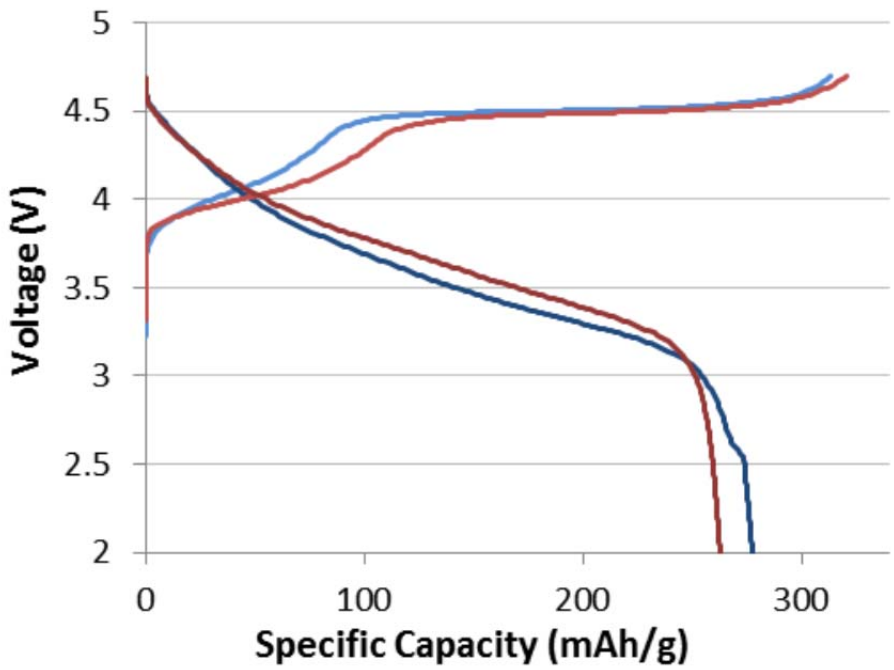

Fig. 14. First cycle profile comparison of $^{6}Li_{1.2}Mn_{0.55}Co_{0.1}Ni_{0.15}O_2$ for LLS (blue curves) and LL (red curves) polymorphs.

The voltage fade behavior of the two materials is shown in Figure 15. The faster rate of fade in the LL system during the first few cycles is possibly due to more extensive spinel formation, while the LLS material has taken these losses up-front. Elemental analysis, NMR, and more rigorous XRD are still required to fully characterize these materials and make correlations between structure and synthetic procedure.

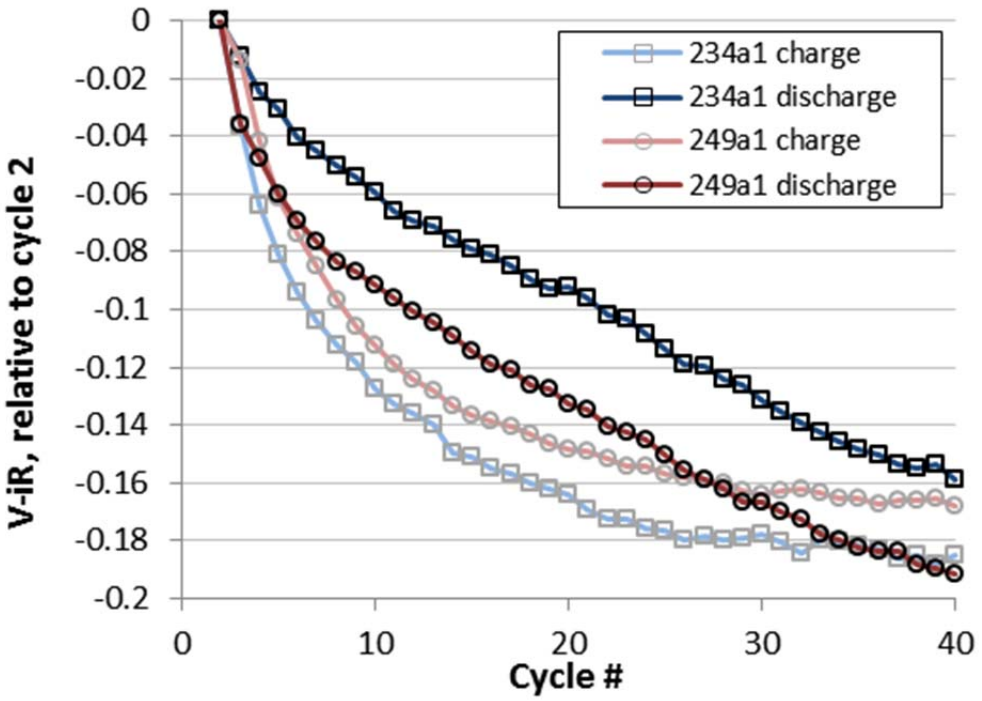

Fig. 15. Voltage fade behavior of LL (red curves) vs. LLS (blue curves) polymorphs of $^{6}Li_{1.2}Mn_{0.55}Co_{0.1}Ni_{0.15}O_2$.

TASK 1
Battery Cell Materials Development

Project Number: IV.E.1.1 (ES167) **2013 Q2 update**

Project Title: Process Development and Scale up of Advanced Cathode Materials

Project PI, Institution: Gregory Krumdick, Argonne National Laboratory

Collaborators (include industry):
Youngho Shin, Argonne National Laboratory
Ozgenur Kahvecioglu Feridun, Argonne National Laboratory
Gerald Jeka, Argonne National Laboratory (analytical)
Mike Kras, Argonne National Laboratory (analytical)

Project Start/End Dates: start: 10/1/2012; end: 9/30/2013

Objectives: Next generation cathode materials have been developed at the bench scale by a number of researchers focusing on developing advanced lithium ion battery materials. Process engineers will work with these researchers to gain an understanding of the materials and bench-scale processes used to make these materials and then scale–up and optimize the processes.

The objective of this task is to conduct process engineering research for scale-up of Argonne's next generation high energy cathode materials. These materials will be based on NMC chemistries and may include lithium rich technology, layered–layered and layered–spinel classes of cathode materials. The current bench scale processes, using a 4L reactor capable of generating 100-200 grams of precursors per hour (carbonate method) will be optimized and scaled up. Scaling up the process involves modification of the bench-scale process chemistry to allow for the semi–continuous production of material, development of a process engineering flow diagram, design of a pre-pilot scale system layout, construction of the experimental system and experimental validation of the optimized process. The design basis for the pre-pilot scale will be based on a 20L reactor, capable of generating 1 kilogram of precursors per hour (carbonate method). The electrochemical properties of the material will be validated by the Materials Screening group to confirm a performance match to the original materials. Synthesized materials will then be made available to industry for evaluation or to researchers for experimentation.

Approach: Much of FY12 was spent on the scale-up and process optimization of the synthesis of $Li_{1.14}Mn_{0.57}Ni_{0.29}O_2$ using the carbonate process. After several engineering issues were resolved and an optimization study completed, high quality cathode material was produced with a tap density of 1.89 with a C/3 held 210mAh/g and 1C rate of 195mAh/g by coin cell testing. However, when this material was calendared it cracked, yielding unpredictable results. This particle fracturing issue seems to be an inherent problem with the carbonate process as it has also been reported from bench scale

researchers. We took a look at the calendaring process and at the relation between electrode porosity and electrochemical performance. We also investigated smaller particles and investigated the relation between particle morphology, size and tap density to minimize particle fracturing.

Schedule and Deliverables: Deliverables will include scaled materials for independent testing, publications and a topical report.

Financial data:
Total project duration: 12 mo.
Staff and M&S: $1.3M

Progress towards deliverables: Effect of particle fracturing on electrode and its porosity on electrochemical performance was investigated (Figure 1). We tried to minimize particle fracturing by the decrease of particle size and to understand the relation between particle morphology, size and tap density for higher particle density.

We prepared four electrodes with different porosities and compared their performances and found that the rate performance and cycle life decrease as electrode porosity is reduced (Figure 1). Particle cracking is one reason for these undesirable behaviors. To minimize cracking, we tried smaller particles (7.8μm and 4.0μm) to see the effect of particle size on cracking and there is a tendency that the smaller particles results in less cracking (Figure 2). However, they also resulted in lower tap density. So we took a look at the relation between particle size, morphology and tap density. The 1st, 2nd and 3rd cathode materials of figure 3 have similar tap density even though their average particle sizes are quite different because they are spherical. But the SEM images of 4 through 7 of Figure 3 clearly show that if the morphology becomes less spherical, the tap density decreases even though the average particle sizes are similar. Therefore, particle morphology has a greater effect on tap density than particle size.

These results have prompted us to revisit carbonate process to make small, spherical secondary particles with increased particle density and to try a few techniques to attempt to minimize the particle fracturing. We also plan to continue to optimize pre pilot scale cobalt free material synthesized by the hydroxide process in an attempt to increase capacity and tap density.

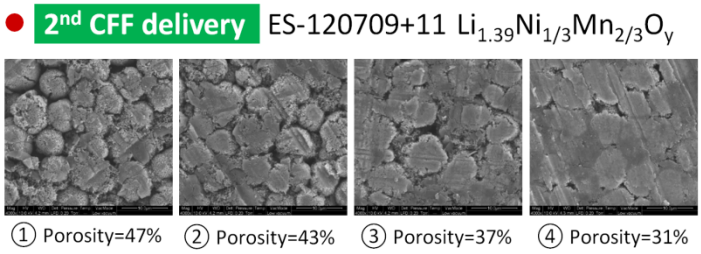

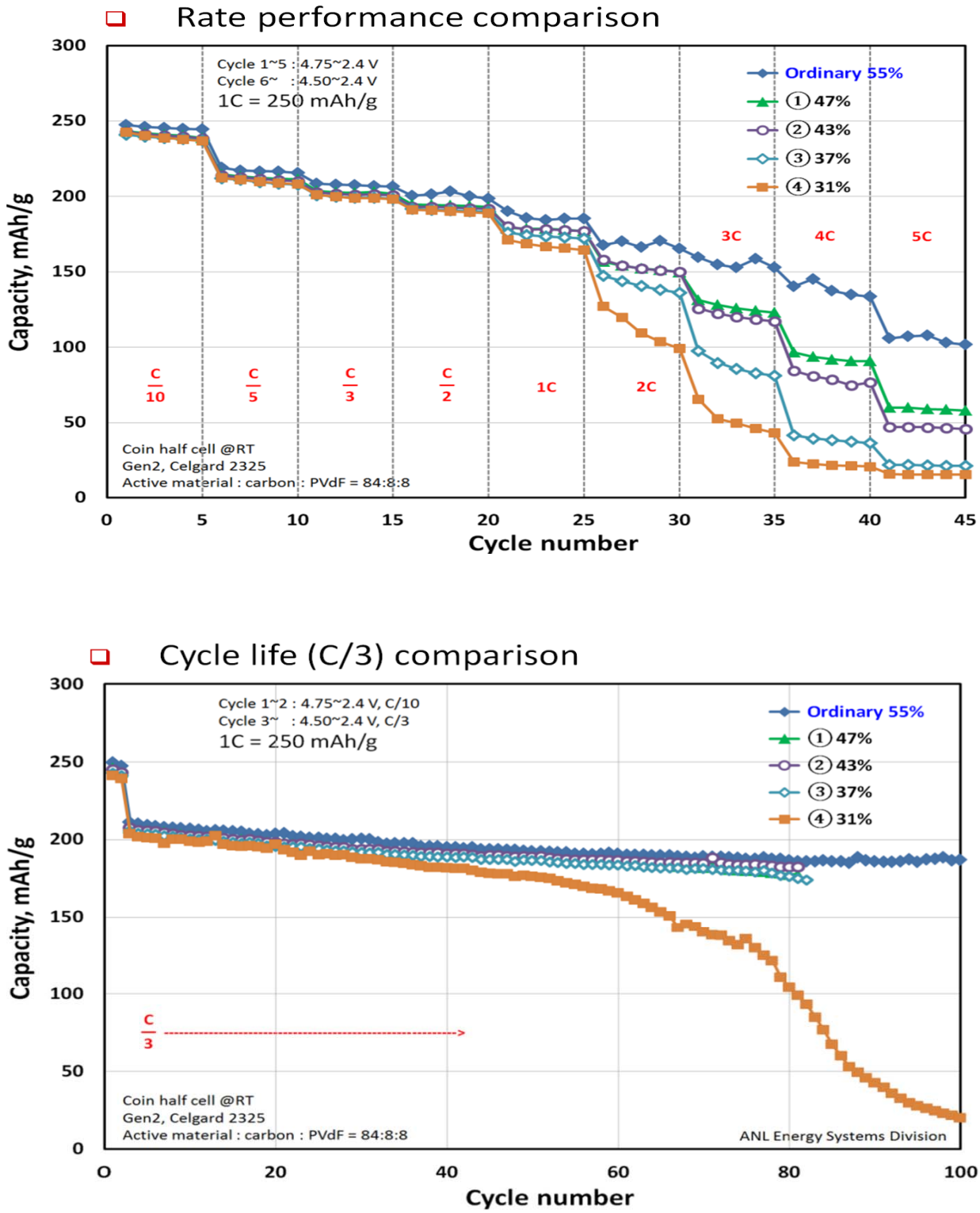

Figure 1. Effect of electrode porosity on electrochemical performance.

	Without calendaring	With calendaring			
Porosity	62 %	47 %	43 %	37 %	31 %
Coating layer w/o Al foil	84 μm (100%)	47 μm (72%)	44 μm (67%)	40 μm (59%)	36 μm (55%)
SEM x500	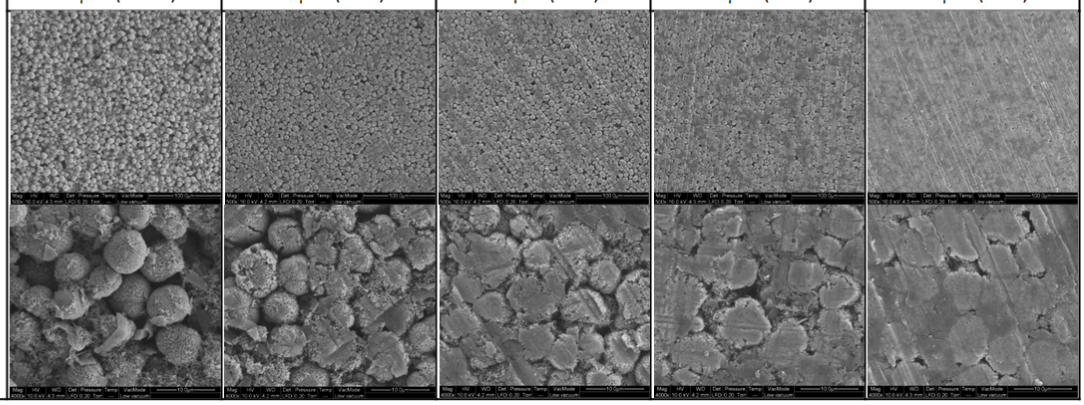				
2nd CFF delivery ES-120709+11 D50=7.8μm TD=1.49g/cc SEM x4000					
ES-130211-4 D50=4.0μm TD=1.12g/cc SEM x4000	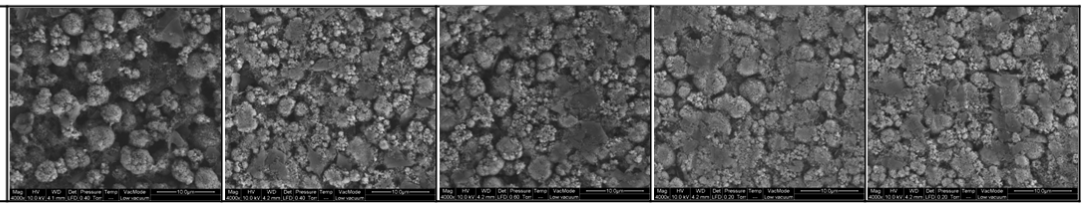				

Figure 2. Particle cracking issue during calendaring.

Same composition ($Li_{1.39}Ni_{1/3}Mn_{2/3}O_y$) by carbonate process (20L CSTR)

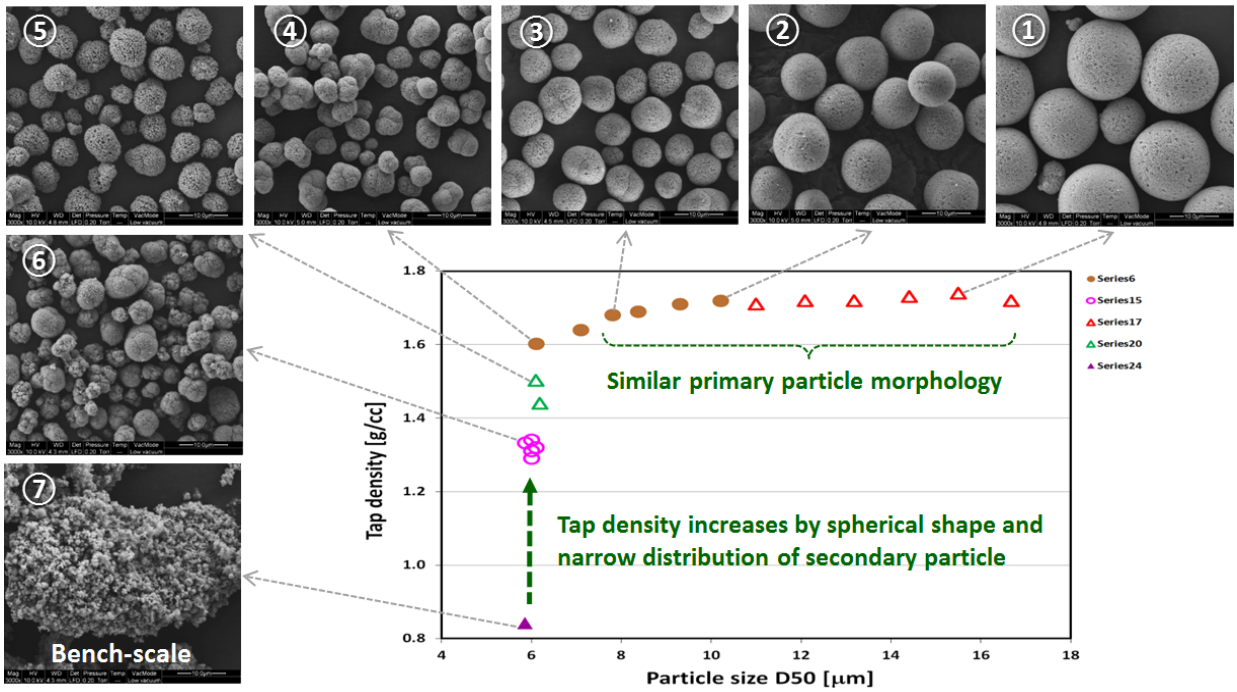

Figure 3. Comparison between particle morphology, size and tap density.

TASK 1
Battery Cell Materials Development

Project Number: IV.E.1.2 (ES168) **2013 Q2 update**

Project Title: Process Development and Scale up of Advanced Electrolyte Materials

Project PI, Institution: Gregory Krumdick, Argonne National Laboratory

Collaborators (include industry):
Krzysztof Pupek, Argonne National Laboratory
Trevor Dzwiniel, Argonne National Laboratory
Wenquan Lu, Argonne National Laboratory
Kang Xu, Army Research Lab

Project Start/End Dates: start: 10/1/2012; end: 9/30/2013

Objectives: The objective of this task is to conduct process engineering research for the scale-up of next generation electrolyte solvents and additive materials. Advanced electrolytes materials are being developed to improve battery safety and to stabilize the interface of lithium ion batteries by forming a very stable passivation film at the carbon anode. Stabilizing the interface has proven to be key in significantly improving the cycle and calendar life of lithium ion batteries for HEV and PHEV applications. Scaling up the process involves modification of the bench-scale procedure and selection of the optimized chemical route that allows for the semi–continuous production of materials, development of a process engineering flow diagram, design of a mini-scale system layout, construction of the experimental system and experimental validation of the optimized process. Electrolyte materials will be produced at the kilogram scale and will be analyzed to confirm material properties and for quality assurance. The electrochemical properties of the material will be validated to confirm a performance match to the original materials. Synthesized materials will then be made available to industry for evaluation or to researchers for experimentation.

Approach: A formal approach for the scale-up of electrolyte materials has been defined. This approach starts with the initial discovery of a new electrolyte material and an initial electrochemical evaluation. This determines if the material is to be added to the inventory spreadsheet, ranked and prioritized. At this point, the scale-up process begins with the initial feasibility study, proof of concept testing, 1st stage scale-up and 2nd scale scale-up. Go/No go decisions are located after feasibility determination and electrochemical validation testing. Scaled materials distributed to industry or to collaborating researchers are tracked in a materials distribution spreadsheet which includes intended use and results obtained.

Schedule and Deliverables: The schedule of electrolyte materials to scale is determined by the prioritized ranking of the scale-up spreadsheet. Materials currently being scaled

are reflected in the project milestones. Deliverables will include scaled materials for evaluation or experimentation and a technology transfer package of information on each material scaled. We expect to complete the scale-up of 3-5 electrolyte materials in FY13.

Financial data:
Total project duration: 12 mo.
Staff and M&S: $1.2 M

Progress towards deliverables: Work on the scale-up of the electrolyte additive PFTBP (perfluoro-*tert*-butyl phosphate), for the Army Research Lab has been initiated. The procedure provided by ARL was not reproducible. Several attempts to synthetize the material failed to provide the desired compound. Thorough literature search revealed that the compound although described in the literature cannot be synthetized by the method provided. Analysis (multinuclear NMR, FTIR, MS) of the authentic sample provided by ARL revealed that the material is lithium perfluoro-*tert*-butoxide (LiPFTB) not the intended perfluoro-*tert*-butyl phosphate (PFTBP). A new process for the synthesis of LiPFTB was developed and the synthesis was scaled up to 1.2 kg of the material. The material is available for sampling.

Since the start of the electrolyte materials scale-up program, 10 materials have been scaled, over 24,000 g of battery grade materials was produced, 40 samples have been provided to industry and various national labs for evaluation and experimentation (total 6,700 g, 4 samples in FY11, 25 samples in FY12 and 11 samples in FY13-Q2).

Table 1 – Electrolyte Materials FY13 Milestones

MILESTONE	DATE	STATUS	COMMENTS
ANL-1NM2			
Assess scalability of disclosed process	7/20/12	Completed	
WP&C documentation approved	8/1/12	Completed	
Develop and validate scalable process chemistry (10g scale)	8/20/12	Completed	
First process scale-up (100g bench scale)	9/17/12	Completed	
Second process scale-up (1000g pilot scale)	10/09/12	Completed	9,715g produced in single batch
ANL- RS21			
Assess scalability of disclosed process	9/28/12	Completed	
WP&C documentation approved	9/28/12	Completed	
Develop and validate scalable process chemistry (10g scale)	10/30/12	Completed	
First process scale-up (100g bench scale)	11/30/12	Completed	
Second process scale-up (1000g pilot scale)	01/10/13	Completed	2,320 g produced in single batch

ARL-~~PFTBP~~-LiPFTB			
Assess scalability of disclosed process	11/21/12	Completed	
WP&C documentation approved	9/28/12	Completed	Covered under existing WP&C document
Develop and validate scalable process chemistry (10g scale)	12/21/12	Completed 2/14/2013	This task took longer than anticipated due to an issue with the target material, which will be detailed in the FY13-Q2 report
First process scale-up (100g bench scale)	2/28/13	Completed	Date revised due to material issue
Second process scale-up (1000g pilot scale)	3/15/13	Completed 3/3/2013	Date revised due to material issue. 1.2 kg of the material was produced, >99%

Table 2 – Analytical Data Sheet for ARL-LiPFTB

Argonne NATIONAL LABORATORY

ARL-LiPFTB

Description	Lithium perfluoro-tert-butoxide
CAS #	29646-14-8
Formula	C_4F_9LiO
FW	241.97
LOT #	KP02083
Purity	>99%[1]
Quantity	1,203g
Manufactured	3/03/2013
Other	

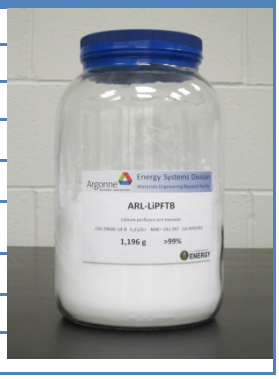

Analysis	Instrument/Method	Results	Analysis By:
GC/MSD	Agilent 7890A/5975C Triple-Axis Agilent DB-5MS, 0.25 um, 30m x 0.250 mm, 40 to 300 °C, 30 °C/min	>99%	K. Pupek
Melting Point	Buchi M-565 Automatic, range method	143-144 °C	K. Pupek
FTIR	Bruker Vertex 70 Attenuated Total Reflection	Consistent with Structure	K. Pupek
NMR	Bruker 500 MHz ^{13}C, ^{7}Li, ^{19}F observed in CD_3CN	Consistent with Structure	T. Dzwiniel

Figure 1 – ATR-FTIR of lithium perfluoro-*tert*-butoxide, MERF's lot KP02083

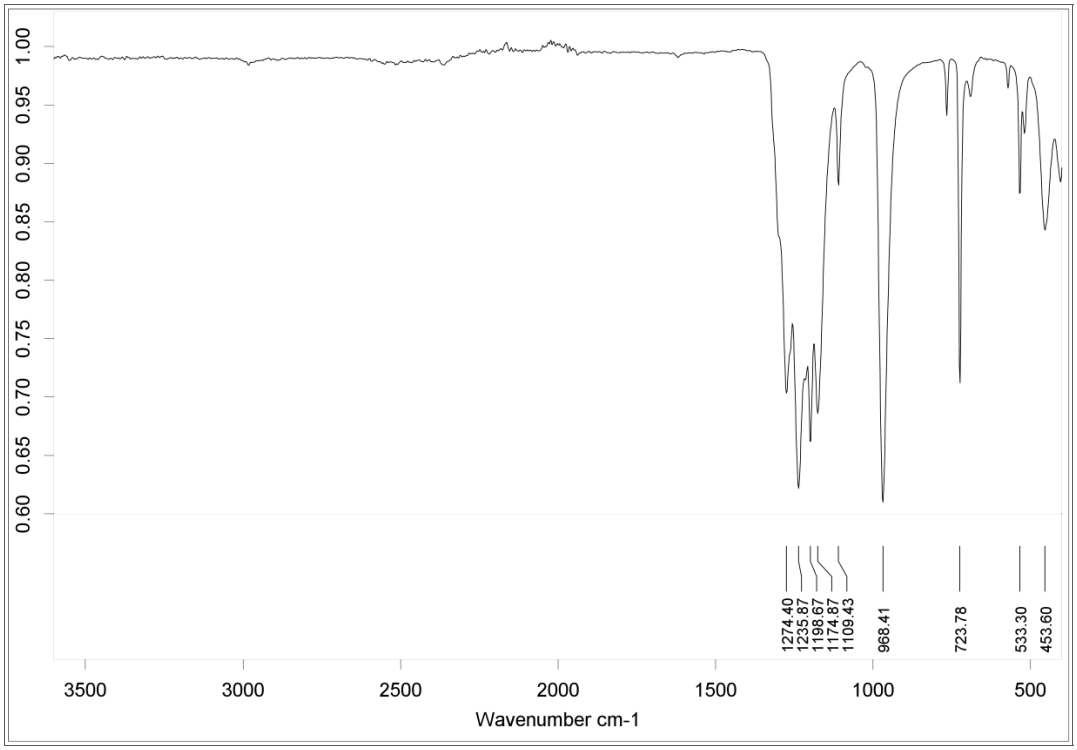

Figure 2 – ^{7}Li NMR of lithium perfluoro-*tert*-butoxide, MERF's lot KP02083

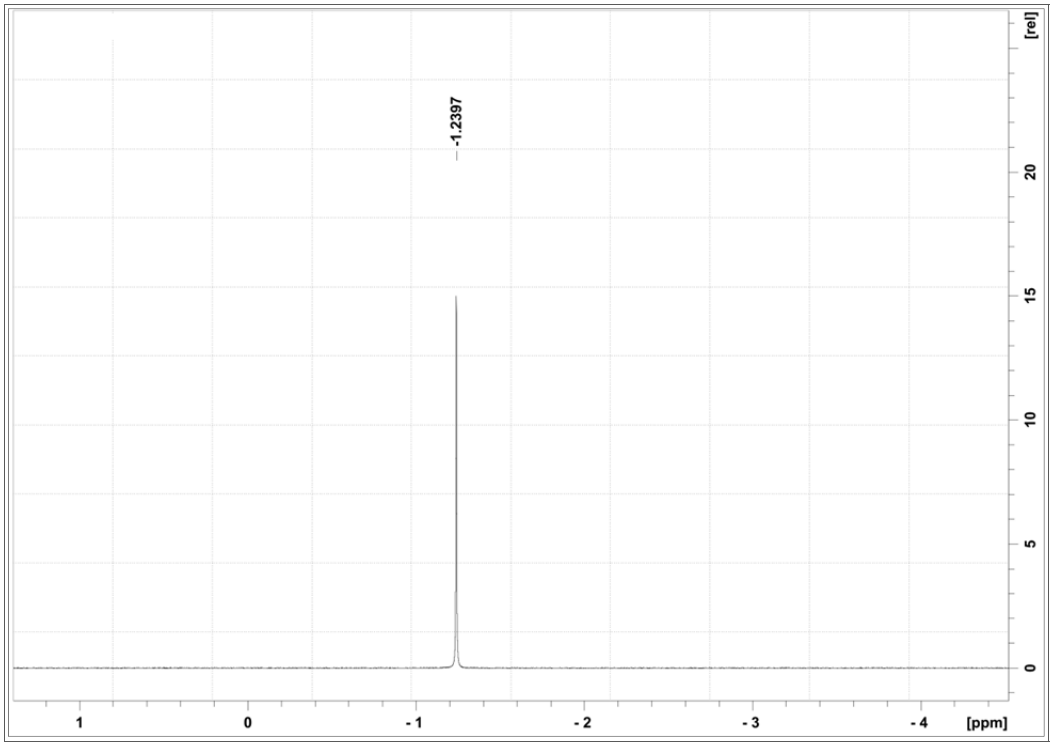

TASK 1
Battery Cell Materials Development

Project Number: ES024

Project Title: High Voltage Electrolytes for Li-ion Batteries

Project PI, Institution: Arthur Cresce, Kang Xu, Jan Allen, Oleg Borodin, Samuel Delp, T. Richard Jow, U.S. Army Research Laboratory

Collaborators (include industry): K. Gaskell (U. of Maryland); K. Amine, D. Dees, G. Krumdick (ANL); X. Yu and X. Yang (BNL)

Project Start/End Dates: June 2011 / May 2014

Objectives: Develop high voltage electrolytes that enable the operation of 5 V Li Ion Chemistry. With a 5-V high voltage electrode materials and a capacity similar to that of the state-of-the-art cathode, the energy density will be increased more than 25% than that of the-state-of-the-art Li-ion batteries for HEV/PHEV. Our other objective is to understand the surface chemistry at the high voltage cathode and electrolyte interface through surface characterization and computational effort. With better understanding, better electrolyte components and cathode materials can be developed.

Approach: Three approaches were taken.

1. **Design and Synthesis of New Additives**
   a. Rationale of electron deficient center
   b. Synthesis, purification and structural characterization by NMR and FTIR
2. **Electrochemical Evaluation**
   a. CC and CC-CV cycling in half and full cells at various temperatures
   b. Impedance analysis
3. **Characterize Interfacial Chemistry at the Elecrode/electrolyte Interface**
   a. Use high resolution XPS, NMR and AFM
4. **Computational Evaluation**
   a. Understand oxidative stability of solvents/electrolytes
   b. Understand reactive pathways of additives and electrolytes
   c. Understand how electron-deficiency would impact on the oxidation stability of additives

Milestones:

(a) Continued testing of new additives (June 2013)
(b) Postmortem diagnostic studies: surface characterization and SEI chemistry (Oct 2013)
(c) Erratum and re-characterization of additive structure (Dec 2012)
(d) Test and evaluate electrolytes with additives in LNMO/graphite, doped-LCP/graphite and other cell couples (Oct 2013)

Financial data: $250,000/year

PROGRESS TOWARD MILESTONES

(a) Additives Design and Synthesis Rationale (Arthur Cresce, Kang Xu)

It has been realized in the past reports that fluorinated alkyl groups may play the main role of passivating the oxidizing sites on cathode. Starting this quarter, syntheses were conducted to make a few favored structures that can deliver the effective ingredient of the additives onto cathode surface, especially the Ni^{2+}/Ni^{4+} sites.

Two such compounds were already synthesized, and structural characterization is under way.

(b) Impact of Additives on Cycling of LNMO/A12 at 55°C (Samuel Delp, Jan Allen, Richard Jow)

The cycling of LNMO at 55°C remains challenging. The LNMO/A12 full cells were tested at at 25°C and 55°C to study the effectiveness of various additives including HFiP, VC and A2 on capacity retention. Both LNMO ($LiNi_{0.5}Mn_{1.5}O_4$) and A12 (graphite) were provided by ANL. The baseline electrolyte is 1.2 M $LiPF_6$ in EC:EMC (3:7).

The effectiveness of additives such as HFiP and VC in retaining capacity at 55°C was not shown as good as A2. The figure below shows the cell capacity versus cycling number for the LNMO/A12 full cells cycled at 55°C between 3.5 and 4.9 V at a rate of C/3 in the baseline electrolyte with and without A2, respectively. The capacity loss was only 11% at the 25th cycle relative to the original capacity for the cells cycled in the baseline electrolyte containing A2. Comparatively, the capacity loss was 43% at the 25th cycle for the cells in the baseline electrolyte. The coulombic efficiencies (CE) were 98% and 96% for the cells in the base electrolyte with and without A2.

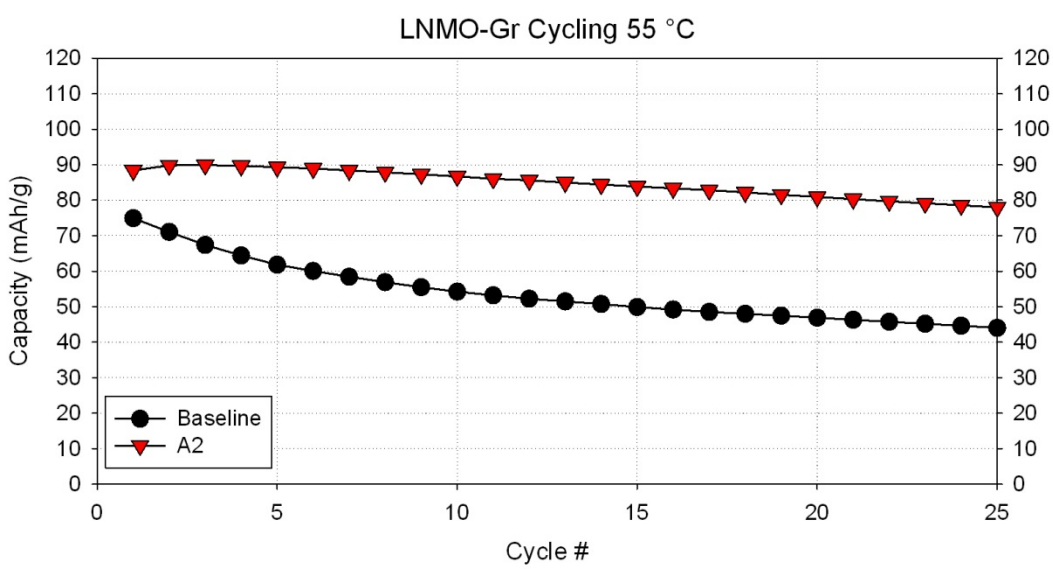

Publications

(1) "Architecturing Hierarchical Function Layers on Self-Assembled Viral Templates as 3D Nano-Electrode Arrays for Integrated Li ion Microbatteries", Y. Liu, W. Zhang, Y. Zhu, Y. Luo, A. Brown, J. N. Culver, K. Xu, C. A. Lundgren, Y. Wang, and C. S. Wang, *Nano Lett.*,**2013,** *13,* 293

(2) "3D Sn nanoforest template on viral scaffolds as high capacity anodes for Na ion chemistry", Yihang Liu, Yunhua Xu, Yujie Zhu, Adam Brown, James N. Culver, Cynthia A. Lundgren, Kang Xu, and Chunsheng Wang, in press at *ACS Nano*

(3) "Understanding Li+-carbonate interaction with 17O-NMR", X. Bogle, S. Greenbaum, and K. Xu, to be submitted

(4) "Direct Observation of SEI Formation on Graphitic Electrodes", D. Baker, S. Russell, A. v. Cresce, and K. Xu, to be submitted

Presentations

(1) "Additive Impacts on the Electrochemical Behavior of High Voltage Li-ion Batteries", S. A. Delp, T. R. Jow, 223rd ECS Meeting, May 12-16, 2013, Toronto, ON, Canada.

(2) "High Voltage Electrolytes and Their Interphases", K. Xu, **invited speech** at the 2013 Advanced Automotive Battery Conference, Pasadena, Ca (Feb 4~8, 2013)

(3) "Interfacing Electrolytes with Electrodes in Li Ion Batteries", K. Xu, Seminar at Department of Materials Sciences, University of Washington (Feb 11, 2013)

TASK 1
Battery Cell Materials Development

Project Number: ES026

Project Title: Electrolytes for Use in High Energy Li-Ion Batteries with Wide Operating Temperature Range

Project PI, Institution: Marshall Smart, Jet Propulsion Laboratory, California Institute of Technology

Collaborators (include industry): (1) University of Rhode Island (Prof. Brett Lucht) (Analysis of harvested electrodes, on-going collaborator), (2) Argonne Nat. Lab (Khalil Amine) (Source of electrodes, on-going collaborator), (3) LBNL (John Kerr, Li Yang) (Evaluation of novel salts), (4) Loker Hydrocarbon Institute, USC (Prof. Surya Prakash) (Fluorinated Solvents and novel salts), (5) A123 Systems, Inc. (Electrolyte development, on-going collaborator), (6) Quallion, LCC. (Electrolyte development, on-going collaborator), (7) Yardney Technical Products (Electrolyte development, on-going collaborator), (8) Saft America, Inc. (Collaborator, industrial partner under NASA program), (9) NREL (Smith/Pesaran)(Supporting NREL in model development by supplying data), (10) Sandia National Laboratory (Safety testing of low flammability electrolyte and supplier of electrode materials), (11) Hunter College (Prof. Greenbaum) (Ex-situ NMR measurements), and (12) North Carolina State University (Prof. Wesley Henderson) (Evaluation of novel salts).

Project Start/End Dates: Start Date: Oct 1, 2009, Projected End Date: September 30, 2014

Objectives:

- Develop a number of advanced Li-ion battery electrolytes with improved performance over a wide range of temperatures (-30 to +60°C) and demonstrate long-life characteristics (5,000 cycles over 10-yr life span).
- Improve the high voltage stability of these candidate electrolyte systems to enable operation up to 5V with high specific energy cathode materials.
- Define the performance limitations at low and high temperature extremes, as well as, identify life limiting processes.
- Demonstrate the performance of advanced electrolytes in large capacity prototype cells.

Approach: The development of electrolytes that enable operation over a wide temperature range, while still providing the desired life characteristics and resilience to high temperature (and voltage) remains a technical challenge. To meet the proposed objectives, the electrolyte development will include the following general approaches: (1) optimization of carbonate solvent blends, (2) use of low viscosity, low melting ester-based co-solvents, (3) use of fluorinated esters and fluorinated carbonates as co-solvents, (4) use of novel "SEI promoting"

and thermal stabilizing additives, (5) use of alternate lithium based salts (with USC, LBNL, and NCSU). Many of these approaches will be used in conjunction in multi-component electrolyte formulations (i.e., such as the use of low viscosity solvents and novel additives and salts), which will be targeted at improved operating temperature ranges while still providing good life characteristics.

The candidate electrolytes are characterized using a number of approaches, including performing ionic conductivity and cyclic voltammetry measurements, and evaluating the performance characteristics in experimental ~ 200-400 mAh three-electrode cells. In addition to evaluating candidate electrolytes in spirally-wound experimental cells, studies will be performed in coin cells, most notably in conjunction with high voltage cathode materials. Cells will be fabricated using a number of electrode couples: (a) MCMB/$LiNi_{0.8}Co_{0.2}O_2$, (b) graphite/$LiNi_{0.8}Co_{0.15}Al_{0.05}O_2$, (c) graphite/$LiNi_{1/3}Co_{1/3}Mn_{1/3}O_2$, (d) $Li_4Ti_5O_{12}$ (LTO)/$LiNi_{0.5}Mn_{1.5}O_2$ (LMNO), and (e) graphite/$LiNiCoMnO_2$ (lithium excess, layered-layered composite). Other chemistries can be evaluated depending upon availability from collaborators. In addition to performing charge/discharge characterization over a wide range of temperatures and rates on these cells, a number of electrochemical characterization techniques will be employed, including: (1) Electrochemical Impedance Spectroscopy (EIS), (2) DC linear (micro) polarization, and (3) Tafel polarization measurements. The electrochemical evaluation in proven three-electrode test cells enables electrochemical characterization of each electrode (and interface) individually and the identification of performance limiting mechanisms for each electrode and for the cell. Electrodes are easily harvested from these test cells and samples will be delivered to collaborators (i.e., URI and Hunter College).

Performance testing of prototype cells containing candidate advanced electrolytes will be performed and evaluated under a number of conditions, i.e., assessment of wide operating temperature capability and life characteristics. JPL has on-going collaborations with several battery vendors and also has the capabilities to perform extensive testing. Typical prototype cell designs that will be considered include (i) Yardney 7 Ah prismatic cells, (ii) Quallion prismatic cells (0.250Ah size and 12 Ah size), and (iii) A123 2.2 Ah cylindrical cells. Cells will be procured and/or obtained through on-going collaborations

Milestones:

Month/Year	**Milestone**
Sept. 2013	Milestone A: Prepare and characterize experimental laboratory cells containing advanced electrolytes, designed to operate over a wide temperature range in high-voltage systems (i.e., $LiNiMnCoO_2$), and identify performance-limiting characteristics. (Sept. 13)
Sept. 2013	Milestone B: Demonstrate improved performance of experimental and prototype cells with next generation electrolytes over a wide temperature range (-30° to $+60^oC$) compared with baseline electrolytes. (Sept. 13)

Financial data:

Total project funding:

- 875K total (~ 175K/year)
- Contractor share = 0K

Funding received:

FY'10 = 175K (Start Date = Oct 1, 2009)
FY'11 = 175K
FY'12 = 170K
FY'13 = 170K

Accomplishments and Progress toward Milestones:

We have continued the performance testing of a number of large capacity 12 Ah cells (MCMB Carbon/$LiNiCoAlO_2$) manufactured by Quallion, LCC that contain JPL methyl propionate (MP)-based wide operating temperature range electrolytes. The current testing is being performed to determine their life characteristics, and to evaluate the degree to which the low temperature capability degrades with time. These cells contain electrolytes that have been reported and demonstrated to have excellent low temperature capabilities, namely (i) 1.20M $LiPF_6$ in EC+EMC+MP (20:20:60 v/v %) and (ii) 1.20M $LiPF_6$ in EC+EMC+MP (20:20:60 v/v %) + 4% FEC. In addition to JPL developed electrolytes, the group of cells contain a Quallion developed wide operating temperature range electrolyte and the DOE baseline electrolyte (i.e., 1.2M $LiPF_6$ in EC+EMC (30:70 v/v %). The cycle life testing consists of partial depth of discharge cycling (approximately 50% DOD), where one cycle is performed each day using a variable load profile with low to moderate rates, as shown in Fig. 1A. After completing increments of 100 cycles (i.e., 100 days of testing), the cells have been re-characterized to determine the capacity, impedance, and low temperature discharge rate capability. As illustrated in Fig. 1B, good capacity retention was observed for all of the cells after completing low temperature testing and 300 cycles, representing approximately 1.75 years of testing. The best capacity retention observed was with the cell containing the methyl propionate-based electrolyte that contains FEC as an additive (4%), slightly outperforming the baseline electrolytes, suggesting that the additive has produced a desirable, protective SEI layer. The cells were also periodically subjected to discharge rate testing at low temperature (-20° to -50°C) over a range of rates (C/10 to 2C) to determine the extent to which the low temperature capability has degraded. For example, as shown in Fig. 2A and Fig. 2B, good retention of low temperature capability was observed at -40° when evaluated at a 2C rate and at -50° when evaluated at a C/5 rate after competing 300 cycles, with the cells containing the methyl propionate-based cells delivering the highest capacity. It should be noted that the cell containing the electrolyte with the 1.20M $LiPF_6$ in EC+EMC+MP (20:20:60 v/v %) + 4% FEC electrolyte displayed the best retention of the initial low temperature capability, suggesting that the additive does function to minimize impedance growth. However, it should be mentioned that under certain conditions higher capacity at low temperatures was observed after life testing. This is attributed to the increased impedance leading to enhanced internal cell heating during discharge.

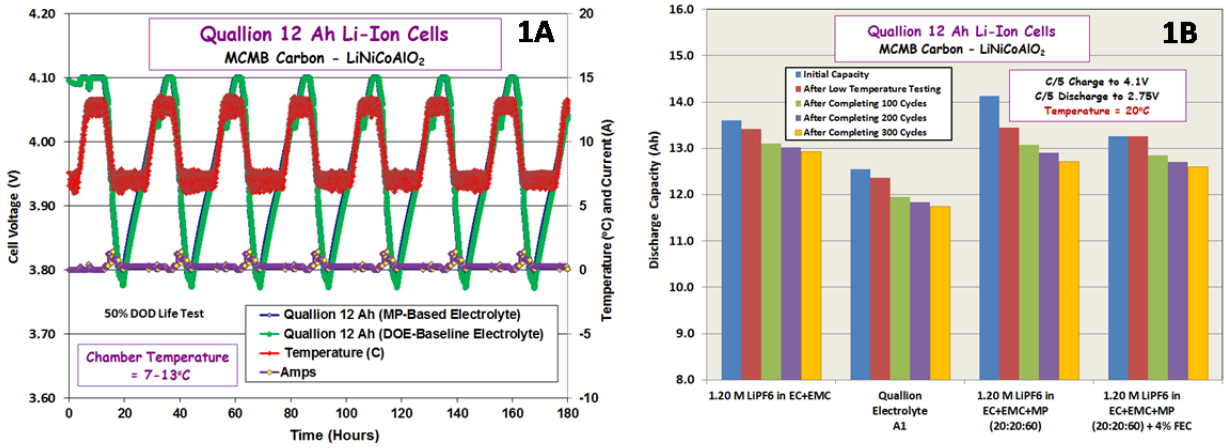

Figure 1: Partial depth of discharge (DOD) variable load profile (1A) subjected to the Quallion 12 Ah cells containing various electrolytes and the 100% DOD capacity determination (1B) performed throughout the life testing, using C/5 rates over a voltage range of 2.75V to 4.10V.

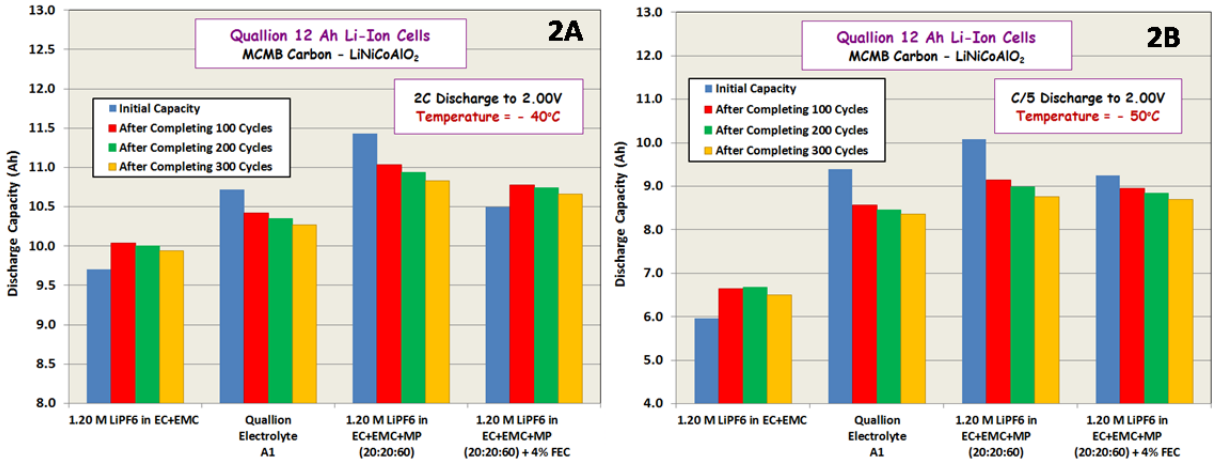

Figure 2: Discharge rate testing of 12Ah MCMB-$LiNiCoAlO_2$ cells (Quallion, LCC) using a 2C discharge rate containing various electrolytes at -40°C using a 2C discharge rate (2A) and -50°C using a C/5 discharge rate (2A) after low temperature characterization and partial DOD cycle life testing (cells were charged at 20°C prior to low temperature discharging).

In the recent quarter, we have continued to investigate electrolytes that are permutations of the approach described above, which consist of methyl propionate with varying amount of mono-fluoroethylene carbonate (FEC) (i.e., 4, 10, and 20%), with the intent of improving the high temperature resilience. In one permutation, we have entirely replaced ethylene carbonate (EC) with FEC. We have also continued the study of using

LiBOB as an additive to methyl propionate-based electrolytes, based upon previous findings from three electrode cell results that it improves the cathode kinetics significantly. As reported previously, we have incorporated these electrolytes in prototype cells (0.25Ah MCMB/$LiNiCoAlO_2$ cells manufactured by Quallion, LCC), and we continue to assess their performance characteristics. Recently, we have subjected a number of these cells to high rate discharge (i.e., 10C to 20C rates) at low temperature (-20°C to -40°C). As illustrated in Fig. 3A, of the MP-based electrolytes displayed dramatically improved power capability compared with the DoE baseline all carbonate electrolyte. The cell containing the electrolyte with methyl propionate and LiBOB has displayed very high power capability at -20°C, being able to provide over 60 Wh/kg at a 20C discharge rate. Under these conditions, the cell containing the MP-based electrolyte delivered over 11 times greater discharge energy (i.e., 62.2 Wh/kg compared to only 5.5 Wh/kg for the baseline). As shown in Fig. 3B, very comparable energy was obtained when the cell containing 1.20M $LiPF_6$ + 0.10M LiBOB in EC+EMC+MP (20:20:60 v/v %) was evaluated at 10C, 15C, and 20C discharge rates. Although lower voltage was observed during the initial portion of the discharge at higher rates, internal cell heating during discharge led to higher discharge capacities and comparable discharge energies. Further enhanced performance is anticipated upon utilizing higher capacity cells and/or battery designs in which the internal cell heating can heat neighboring cells. Future effort will be devoted to evaluating the performance using lower discharge voltages at these high rates, to mitigate the initial voltage drop early in the discharge and allow the cells to heat up sufficiently to deliver high capacity.

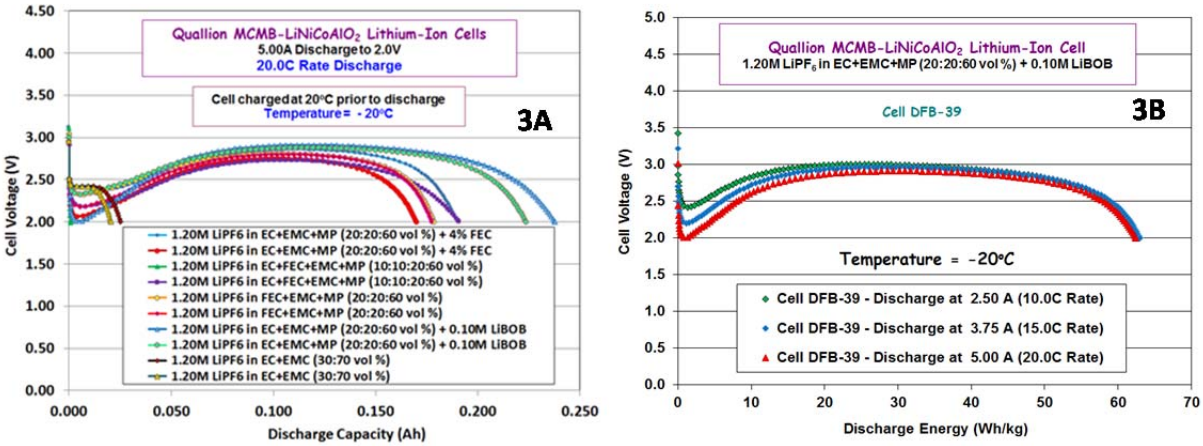

Figure 3: Discharge performance of 0.25Ah MCMB-$LiNiCoAlO_2$ cells (Quallion, LCC) containing methyl propionate-based electrolytes at -20°C using a 20C discharge rate (3A) and the discharge energy (Wh/Kg) delivered by a cell containing 1.20M $LiPF_6$ + 0.10M LiBOB in EC+EMC+MP (20:20:60 v/v %) (3B) at various rates.
(Cells were charged at room temperature prior to low temperature discharging).

We have also continued the on-going cycle life testing of these prototype cells under a number of conditions, including 100% DOD cycling at 20°C, 40°C, and 50°C, as

well as variable temperature cycling between temperature extremes (i.e., -20° and +40°C). As illustrated in Fig. 4, excellent performance has been obtained with many of the formulations when subjected to 100% DOD cycle life testing at 20°C, with over 2,100 cycles completed to-date on some of the cells. A trend of lower capacity fade is observed with increasing FEC content in the electrolyte, although high FEC content was observed to led to somewhat lower initial capacity. For example, the cell containing 1.20M $LiPF_6$ in FEC+EMC+MP (20:20:60 v/v %) displays excellent cycle life characteristics delivering 229 mAh after completing 2,200 cycles (i.e., 94.8% of the initial capacity). In terms of the capacity fade observed, the cell containing the electrolyte with 10% FEC and 10% EC also outperforms the all carbonate baseline. Although the electrolyte with LiBOB resulted in cells with the best low temperature discharge rate capability, the cycle life performance was inferior to that of the baseline and the cells containing FEC in high proportion.

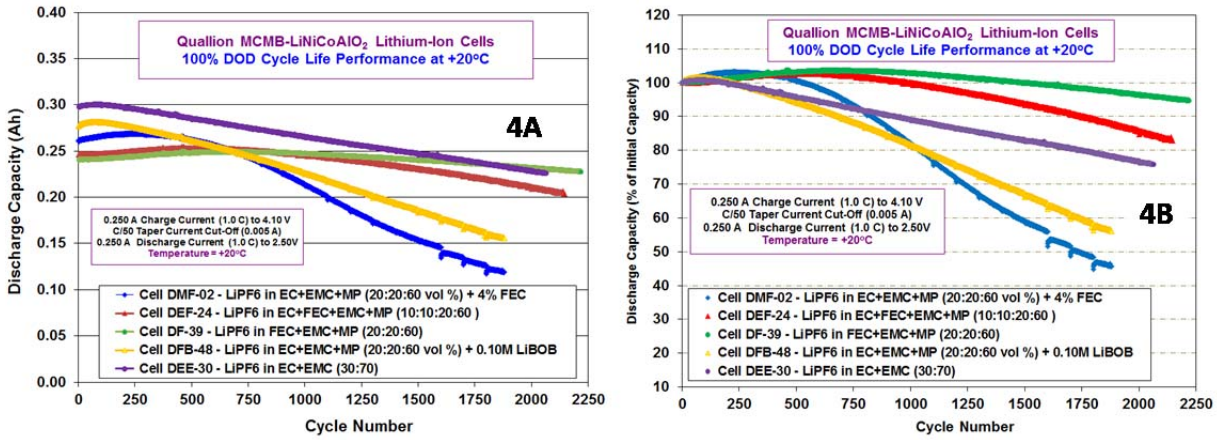

Figure 4: Cycle life performance 0.25Ah MCMB-$LiNiCoAlO_2$ cells (Quallion, LCC) containing methyl propionate-based electrolytes at 20°C using C rate charge and discharge.

In the previous quarter, we continued to evaluate the life characteristics of a number of A123 cells that possess methyl butyrate-based electrolytes previously investigated and reported under this program (i.e., specifically 1.20M $LiPF_6$ in EC+EMC+MB (20:20:60 vol %) + 4% FEC and 1.20M $LiPF_6$ in EC+EMC+MB (20:20:60 vol %) + 2% VC). As illustrated in Fig. 5A, excellent cycle life has been obtained with these cells containing wide operating temperature range electrolytes, and have completed over 8,800 cycles to-date (on test for over 2.75 years) and have displayed comparable performance to the baseline electrolyte (over 79% of the initial capacity). As previously reported, these cells (i) have exhibited excellent rate capability over a wide temperature range (down to -60°C), (ii) were demonstrated to have dramatically improved power capability compared with the baseline (at -30 and -40°C), and (iii) have been shown to have good cycle life performance up to +60°C. Under this program, we have continued the evaluation of commercial-of-the-shelf (COTS) A123 cells which are being subjected to partial depth of discharge (DOD) cycling, ranging from 30% to 60%

DOD. This testing was originally initiated under a NASA-IPP program in collaboration with A123 Systems, Inc. Under the current program, we have continued the testing and have provided data to NREL in support of their in-house modeling program. As illustrated in Fig. 5B, cells subjected to 30-50% DOD cycling have completed over 25,000 cycles, representing over 5 years of testing (each cycle consists of a one hour charge period and a 30 minute discharge period). Periodically, the cells have been subjected to 100% DOD cycles and current-interrupt impedance measurements to determine the health of the cells.

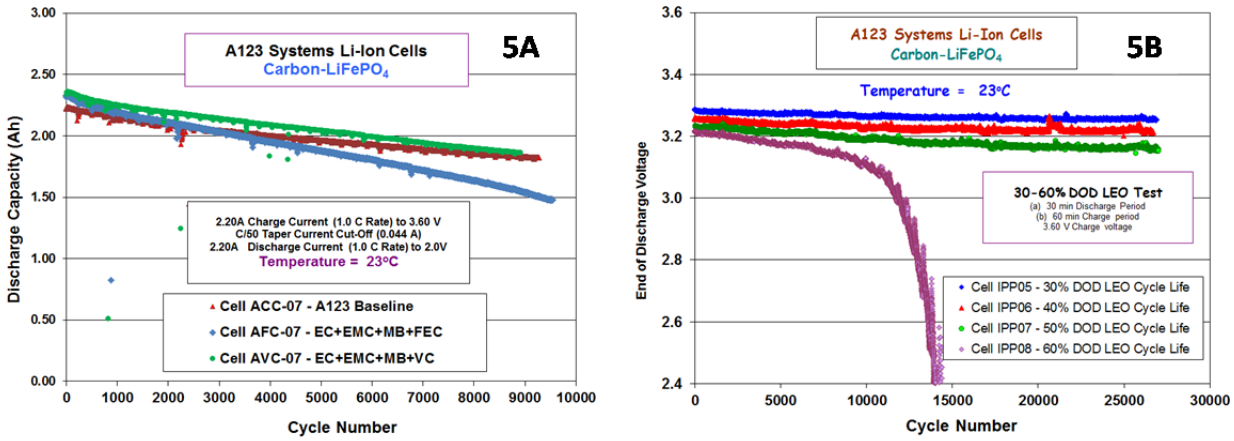

Figure 5: Cycle life performance of $LiFePO_4$-based A123 cells containing various wide operating temperature range electrolytes at +23°C (Fig. 3A) and partial DOD cycle life performance of COTS A123 cells (Fig. 3B), expressed in terms of the end of discharge voltage (V).

We also continue to investigate methyl butyrate-based formulations in cells consisting of Conoco graphite anodes and NMC cathodes (HE5050) supplied by Argonne National Labs, in an extension of our previous studies with this system. This study is being performed in both coin cells as well as larger experimental three electrode cells equipped with lithium reference electrodes. In an attempt to develop advanced electrolytes which will improve the low temperature performance and enhance the high temperature resilience, a number of electrolyte additives have been investigated, including (i) LiBOB, (ii) lithium difluoro(oxalato)borate (LiDFOB), (iii) lithium tetrafluoroborate ($LiBF_4$), (iv) lithium 4,5-dicyano-2-(trifluoromethyl) imidazole (LiTDI), (v) vinylene carbonate (VC), and (vi) lithium oxalate. The LiDFOB and LiTDI were synthesized and provided by Prof. Wesley Henderson's group at North Carolina State University (NCSU). After the formation cycles of the three-electrode cells were completed, electrochemical measurements were performed at a number of temperatures, including Electrochemical Impedance Spectroscopy (EIS), Tafel polarization, and linear micro-polarization measurements. For example, as shown in Fig. 6, Tafel polarization measurements were performed on three-electrode cells containing various electrolytes at -20°C on both the graphite anodes (6A) and the NMC cathodes (6B). As illustrated, the most favorable kinetics at the anode was observed with the cells containing lithium oxalate and VC. Whereas, the most facile kinetics observed at the cathode was observed with the cell containing LiBOB as an additive, suggesting that it participates

beneficially in the formation of the cathode electrolyte interface (CEI). It should also be noted that at -20oC, the kinetics of the cathode are much poorer than that of the anode for all of the samples (by nearly an order of magnitude), suggesting that the low temperature rate capability will be dictated by the cathode kinetics. We are currently evaluating the discharge performance of these systems as a function of temperature in both the three-electrode cells, as well as in coin cells.

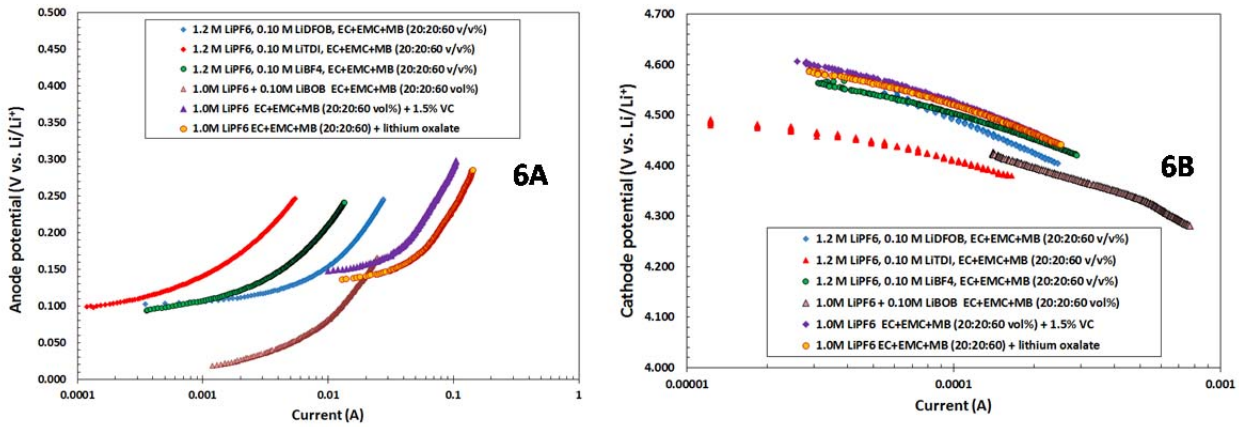

Figure 6: Tafel polarization measurements performed on Conoco graphite anodes (6A) and NMC cathodes (HE5050) (6B) in three electrode cells at -20°C after completing the formation cycling**.** Cells were fully charged at room temperature prior to performing the measurements.

Publications:

1. M. C. Smart, M. R. Tomcsi, L. D. Whitcanack, B. V. Ratnakumar, M. Nagata, and V. Visco, "The Use of Methyl Propionate-Based Electrolytes with Additives to Improve the Low Temperature Performance of $LiNiCoAlO_2$-Based Li-Ion Cells, 224th Meeting of the Electrochemical Society, San Francisco, October 2013.
2. F. C. Krause, C. Hwang, B. V. Ratnakumar, M. C. Smart, D. W. McOwen and W. A. Henderson, "The Use of Methyl Butyrate-Based Electrolytes with Additives to Enable the Operation of Li-Ion Cells with High Voltage Cathodes over a Wide Temperature Range", 224th Meeting of the Electrochemical Society, San Francisco, October 2013.
3. M. C. Smart, B. V. Ratnakumar, and L. D. Whitcanack, "Development of Low Temperature Electrolytes for Lithium-Ion Batteries", Advanced Automotive Batteries Conference, Pasadena, CA, February 5, 2013.
4. M. C. Smart, C. Hwang, F. C. Krause, J. Soler, W. C. West, B. V. Ratnakumar, and K. Amine, "Wide Operating Temperature Range Electrolytes for High Voltage and High Specific Energy Li-Ion Cells", ECS Transactions, accepted.
5. M. Jun, K. Smith, E. Wood, and M. C. Smart, "Battery Capacity Estimation of Low-Earth Orbit Satellite Application", *International Journal of Prognostics and Health Management*, ISSN2153-2648, 2012 009.

6. M. C. Smart, B. L. Lucht, S. Dalavi, F. C. Krause, and B. V. Ratnakumar, "The Effect of Additives upon the Performance of MCMB/$LiNiCoO_2$ Li-Ion Cells Containing Methyl Butyrate-Based Wide Operating Temperature Range Electrolytes", *J. Electrochem. Soc.*, **159 (6)**, A739-A751 (2012).

The work described here was carried out at the Jet Propulsion Laboratory, California Institute of Technology, under contract with the National Aeronautics and Space Administration (NASA).

TASK 1
Battery Cell Materials Development

Project Number: ES027 **Reporting Period:** FY 2013 Q2

Project Title: Novel Phosphazene Compounds for Enhancing Electrolyte Stability and Safety of Lithium-ion Cells

Project PI, Institution: Kevin L. Gering, INL

Collaborators (include industry): Michael T. Benson (INL), Mason K. Harrup (INL), Harry W. Rollins (INL), Sergiy V. Sazhin (INL), Khalil Amine (ANL), Chris Orendorff (SNL), Princess Energy Systems, Dow Chemical

Project Start/End Dates: Jan. 2009/Ongoing

Objectives: Our focus is to understand stability of our new classes of phosphazene materials and to establish viability for their use in lithium-ion cell electrolytes, considering both conventional voltage ranges (4.2V) and higher voltage electrode couples (4.5-5V). Comprising this overall work are the following focus areas:

- Synthesize novel solvents for Li-ion cells that are safer alternatives to volatile organics.
- Gain understanding of molecular-scale interactions between phosphazenes and other electrolyte components.
- Determine what phosphazene structures are more tolerant to high and low voltage, and to high temperatures.
- Determine the effect of phosphazenes on SEI films, cell performance, and cell aging in general, using ABR-relevant electrode couples.
- Synthesize and engineer novel phosphazene polymers that would serve as safe and robust alternatives to carbon-based anodes. Linked with our electrolyte research, this enhances overall compatibility of cell chemistry.

This collective effort will enable us to engineer advanced materials for more robust lithium-ion cells and move us closer to the overall goal of a carbon-reduced cell chemistry.

Approach: The INL is leveraging this work based on interdepartmental synergy between a well-established battery testing program and its foremost experts in phosphazene chemistry that are producing new classes of novel compounds for use in lithium-ion batteries. As such, the INL is strongly positioned to approach primary targets for ABR electrolyte development while maintaining historical knowledge of phosphazene chemistry and related applications.

This work is split under four primary tasks: solvent synthesis, characterization, DFT modeling, and lithium-ion cell testing. Upfront issues are

- voltage stability (CV)
- temperature stability

- ♦ flammability (flash point)
- ♦ lithium salt solubility
- ♦ transport properties (viscosity, conductivity)
- ♦ chemical compatibility with the cell environment
- ♦ molecular interactions (solvent-ion)

Coin cell testing covers issues of formation, interfacial impedance, polarization testing, and aging, using our compounds as electrolyte additives (1-10%). In previous quarters we investigated our electrolytes with ABR electrode couples LNMO/LTO, NMC(3M)/Carbon, and HE5050/Carbon. We test our novel polymeric anodes against ABR-relevant cathodes such as NMC. For most coin cell testing the general protocol is: formation cycling (C/10 @ 3), EIS, followed by a matrix of C/10, C/3, C/1, and 3C, all at 30 °C. Testing concludes with 3C cycling at 45-55 °C to determine electrolyte effect on high temperature tolerance. Final EIS is optional.

Milestones (cumulative over FY 2011-2013):

	= Activity completed in reporting period

Milestone	**Status**	**Date**
a. Synthesis of Fluorinated Phosphazene series (FM1,2,3)	completed	March 2011
b. Synthesis of Gen1 Ionic Liquid Phosphazene (PhIL-1)	completed	Feb. 2011
c. Synthesis of newer SM series (SM 5,6,7)	completed	October 2010
d. Development of improved voltammetry techniques for SEI characterization.	completed	December 2010
e. DFT simulations of selected phosphazenes regarding interaction with lithium ions	completed	Feb./March 2011
f. Thermal stability testing of blends with SM6 and SM7	completed	March 2011
g. Cell testing using LNMO/LTO and NMC/Carbon* couples: characterization of capacity and impedance attributes	completed	March 2011
h. Cell testing using LNMO/LTO and NMC/Carbon* couples: aging studies	completed	October 2011
i. Phase 1 concept validation for alternative anode materials	completed	October 2011
j. Cell testing using HE5050/Carbon couple: characterization of capacity and impedance attributes	completed	December 2011
k. DFT study on complete FM Series (fluorinated cyclics)	completed	February 2012
l. Cell testing using HE5050/Carbon couple: aging studies	completed	March 2012
m. Phase 2 concept validation for alternative anode materials	completed	March 2012

n. Initial PALS measurements of alternative anode materials	completed	March 2012
o. Synthesis of newer FM series and second-generation Ionic Liquid Phosphazenes	In Progress	
p. Abuse testing of INL electrolyte additives at SNL, Phase 1	Completed	November 2012
q. Collaboration with ANL regarding scale-up of INL electrolyte compounds	In Progress	
r. Cell testing using NCA (Toda)/Carbon couple: characterization of capacity and impedance attributes	Completed	January 2013
s. Phase 3 Alternative Anode materials with improved electronic conductivity and capacity	In Progress	
t. NMR evaluation of electrolyte fate at elevated temperatures (Washington State Univ.)	In Progress	
u. Abuse testing of INL electrolyte additives at SNL, Phase 2 (10-20% additives in electrolyte)	In Progress	

Financial data: Funding Received: FY 10: $ 400K; FY 11: $ 400K ; FY 12: $500K (under subcontract, a small portion of this might go to Washington State University for specialized NMR measurements).

PROGRESS TOWARD MILESTONES

(a, b) Completed 2011 Q2.

(c) Completed 2011 Q1.

(d) Completed 2011Q1.

(e) Completed 2011 Q2.

(f) Completed 2011 Q2.

(g) Completed 2011 Q2.

(h) Completed 2012 Q1.

(i) Completed 2012 Q1.

(j) Completed 2012 Q1.

(k) Completed 2012 Q2.

(l) Completed 2012 Q2.

(m) Completed 2012 Q2.

(n) Completed 2012 Q2.

(o) *A key driver of our work is to move toward an "inorganic cell chemistry" that has a common chemical basis throughout the cell. The next step in this progression is to test phosphazene-containing electrolytes against an electrode couple comprised of a phosphazene-based anode and a high voltage cathode.* Our synthesis targets during this quarter are newer generations of FM and phosphazene-based ionic liquid (PhIL) compounds. We are reviewing synthesis routes to arrive at a streamlined, economical, and high-purity path toward production of these unique compounds. In previous quarters our voltammetry studies clearly showed that our phosphazene compounds can triple the voltage window of the baseline electrolyte while at moderate levels (20%), and small amounts of phosphazenes (1%) can dramatically improved the temperature stability of the electrolyte. These compounds will be tested against ABR-relevant higher-voltage cathode materials and our novel electrode materials in (m) and (s) to further enhance cell voltage stability at 5V. Work for Q2 2013 centered around final synthesis and characterization of FM series compounds, each having different arrangement of fluorinated pendant groups. In addition, another ionic liquid additive was synthesized during this period. Selected compounds will be forwarded to SNL for final abuse testing, as specified in Task (q).

(p) Phase 1 abuse testing of INL Phosphazene compounds at SNL concluded November 2012, using 18650 cells containing the NMC (3M)/carbon (A10) couple. INL additives included FM-2, SM-6, and PhIL-2 at one and three percent levels. The focus of this work was to determine how INL additives help mitigate (delay) the onset of thermal runaway. Initial results from this work indicate overall benefit of INL phosphazene additives in terms of thermal stability, in the order of {SM-6 > PhIL-2 > FM-2}. For example, at 3% levels SM-6 decreases the peak heating rate by over 100 degrees C per minute, while PhIL-2 cuts the gas evolution to one-third that of the baseline system. Flammability testing at SNL established that the PhIL-2 additive provides significant benefit. The baseline, SM-6, and FM-2 cells all exhibited similar burn times (100-300s) and relatively short ignition times. However, the PhIL-2 electrolyte showed a significantly shorter burn time (<20 s) and longer ignition times. This suggests reduced flammability for the PhIL-2 electrolyte relative to the baseline and other electrolytes. Phase 2 work under Task (u) to be completed Q3 2013 will perform abuse testing for electrolytes having selected INL additives from task (p) up to 20% by mass.

(q) We have continued our efforts to collaborate with ANL regarding the synthesis of INL phosphazene electrolyte compounds in the ANL materials scale-up facilities. The top candidate for scale-up will be the best compound(s) is emerging from the results of the SNL abuse testing, as mentioned in Tasks (p) and (u). FM2 appears as a likely candidate for scale-up.

(r) Completed 2013 Q2. Cell testing using NCA (Toda)/Carbon couple continued, covering a large matrix of INL additives from the FM series. Characterization of capacity and impedance attributes was accomplished for coin cells made with phosphazene-doped

electrolytes and the NCA (Toda)/Carbon couple provided by ANL. Electrolyte performance was on par with that seen for earlier testing with LNMO/LTO, HE5050/Carbon, and NMC/Carbon couples. In some cases the electrolytes with FM-1 and FM-2 performed better than the baseline system. These results clearly suggest that the INL additives are compatible with the NCA (Toda)/Carbon couple. With the chosen electrode couple, acceptable performance is seen up to a C/1 rate for FM-2 levels up to 12.4 percent. Polarization effects diminish transport performance at the 24.7 percent level at cycling rates C/1 and greater.

(s) Our work on alternative anode materials seeks to improve electronic conductivity, as well as energy storage and safety beyond the carbon anode baseline. We are nearing completion on a third phase matrix of our alternative anode materials investigation, using a composite polymeric approach toward engineering new carbon-reduced anode materials. Phase 1 and 2 studies showed cycling to 5V (full cell) was achieved, yet we determined that the observed capacity was being impacted by low electronic conductivity and limited porosity of the 3D polymer framework. Capacities of Phase 1 and 2 materials approached that of conventional carbon systems, and we concluded that enhancing the electronic conductivity and optimizing porosity of these materials will allow us to improve capacity to achieve competitive levels. Lastly, these alternative anodes will enhance cell safety, since the presence of the phosphorus in the phosphazene electrode polymer matrix adds to the overall flame resistance and safety of the cell chemistry under conditions of thermal runaway.

In Q2 2013 *our newer materials showed improved performance, achieving high gravimetric capacities* in several formulations in our "B22" series (no Si in formulations). Electrode laminate resistivities have been correlated with electrochemical performance, and we have seen a strong correlation between BET surface area and discharge capacity (**Fig. 1**). Post-formation electrochemical efficiencies meet or exceed 95% in most cases (**Fig. 2**). We are also seeing correlations between polymer type/composition and lithium uptake, indicating further information regarding the 3D molecular framework of these materials. **Table 1** documents the C/25 discharge capacities for the B22 formulations to date cycled against HE5050 between 4.25 and 3.4V, with most values *at or above 300 mAh/g laminate mass*. **Figure 3** shows the C/25 discharge capacity curves for cycling from 4.7V for these same cells, wherein the equivalent gravimetric capacities *exceed 400 mAh/g in most cases*. Differential capacity plots for the B22 series is shown in **Fig. 4**. We are currently investigating extended cycle-life testing of these novel systems to understand aging mechanisms and to determine appropriate conditions that would minimize capacity losses over time. Optimization of polymer properties in terms of cross-linking, porosity, conductivity, etc. will further enhance stability and performance of these novel anode materials. In Q3 2013 we will complete this investigation, followed by a plan to publish a set of papers on our findings.

(t) NMR evaluation of electrolyte fate at elevated temperatures (Washington State Univ.). Sub-contracted work with WSU (contact: Prof. Bill Hiscox) performs advanced NMR studies in two areas of our new materials development. The first area employs

high resolution multi-dimensional solution NMR. The thrust here is to identify early degradation fragments from conventional electrolytes and determine the primary mechanisms of thermal degradation. Then electrolyte formulations containing INL phosphazene additives are being studied using the same techniques in an attempt to elucidate the mechanisms by which the phosphazene additives prevent the organic carbonate degradation. The value added in using WSU instead of INL facilities is their NMR center has more NMRs at various field strengths and a greater instrumental capability than currently possessed at INL. Further, their resident NMR experts have greater concentrated expertise in these types of complex multi-dimensional analyses.

From initial WSU findings, the baseline sample, having no protection from the phosphazene, formed a gel at the bottom of the tube as time progressed at 60˚C. The sample has become much more viscous overall than Sample 1 (having the protective cyclic phosphazene), which has not undergone a perceptible viscosity increase. The evidence of phosphorus-proton coupling in the reaction products of the baseline sample suggest that phosphorus is reacting with the solvent, which is a mixture of ethyl and methyl carbonates. These NMR-observable product species may be intermediates in polymerization of the carbonates, leading to a polycarbonate formation. This would account for the viscosity change in the baseline sample. However, formation of dimers, trimers, etc. of solvent molecules containing PF2 linking units, may explain why the new PF2 signals have continued to increase in intensity with respect to PF_6^- signals, and why they appear to be stable products in the mixture. However, the final fate of these species is not known from the present preliminary aging study. Continued monitoring of the two samples, and further studies of starting materials and products will be necessary to sort this out. The complexity of this system (5+ observable nuclei with spin-spin coupling interactions among at least 4 of them) will require a number of approaches to fully elucidate the mechanisms of degradation in the unprotected system, and the mode of protection of the cyclic phosphazenes. The second area employs solid-state 1- and 2-dimensional analyses of the phosphazene anode materials under development.

(u) Phase 2 of abuse testing of INL electrolyte additives at SNL will investigate the impact of having 10-20 percent INL additives in the baseline electrolyte, using 18650 cells containing the NMC (3M)/carbon (A10) couple. We leverage the knowledge gained in Phase 1 (Task p) to target best candidates that would promote significant benefit in thermal resilience and safety while allowing cells to achieve satisfactory cycling performance for the intended application. This will also allow a fair assessment of TRL values of INL materials for commercial battery applications. This task will be completed Q3 or Q4 2013.

Publications, Reports, Intellectual property

- "Lithium binding in fluorinated cyclic triphosphazenes" M. T. Benson, M. K. Harrup, K. L. Gering, *Computational and Theoretical Chemistry*, 1005 (2013) 25–34.
- Intellectual Property relating to novel materials is being documented case-by-case as needed.

Fig. 1

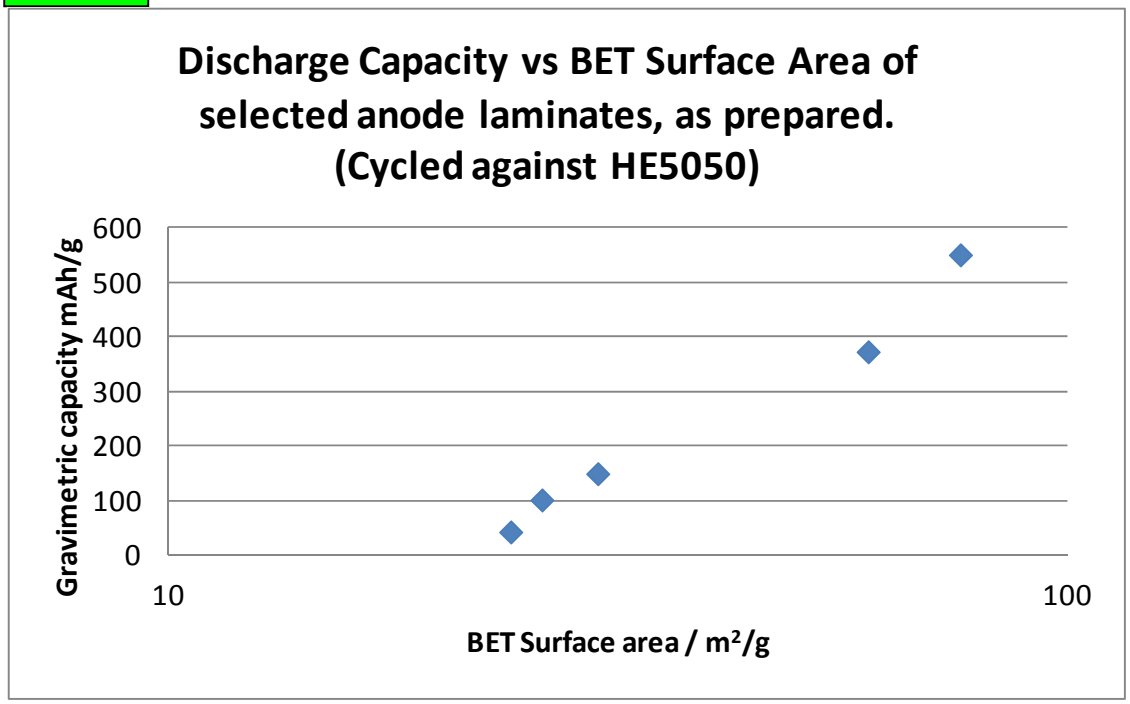
Discharge Capacity vs BET Surface Area of selected anode laminates, as prepared. (Cycled against HE5050)
Gravimetric capacity mAh/g
600
500
400
300
200
100
0
10
100
BET Surface area / m²/g

Fig. 2

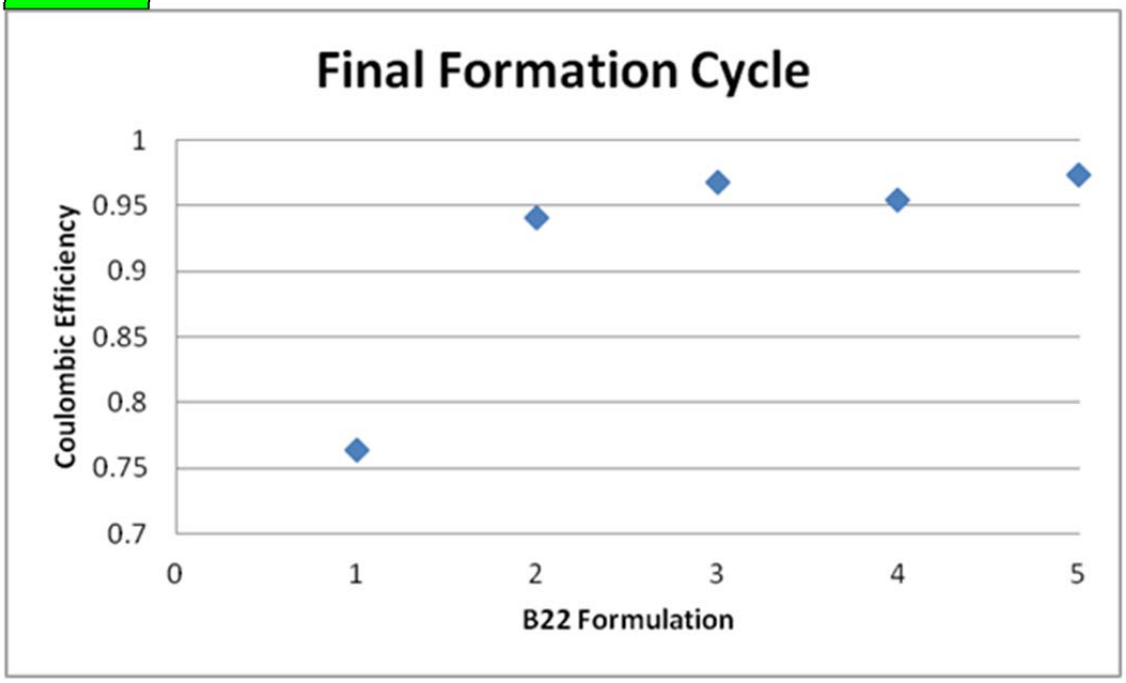
Final Formation Cycle
Coulombic Efficiency
1
0.95
0.9
0.85
0.8
0.75
0.7
0
1
2
3
4
5
B22 Formulation

Table 1. Discharge capacities assessed by C/25 cycling from 4.25 to 3.4 V for recent INL composite polymer anodes cycled against HE5050.

Sample	Discharge Capacity at **4.25 V** (gravimetric, mAh/g laminate)
B22-01	138.8
B22-02	296.8
B22-03	358.4
B22-04	681.4
B22-05	346.6

Fig. 3

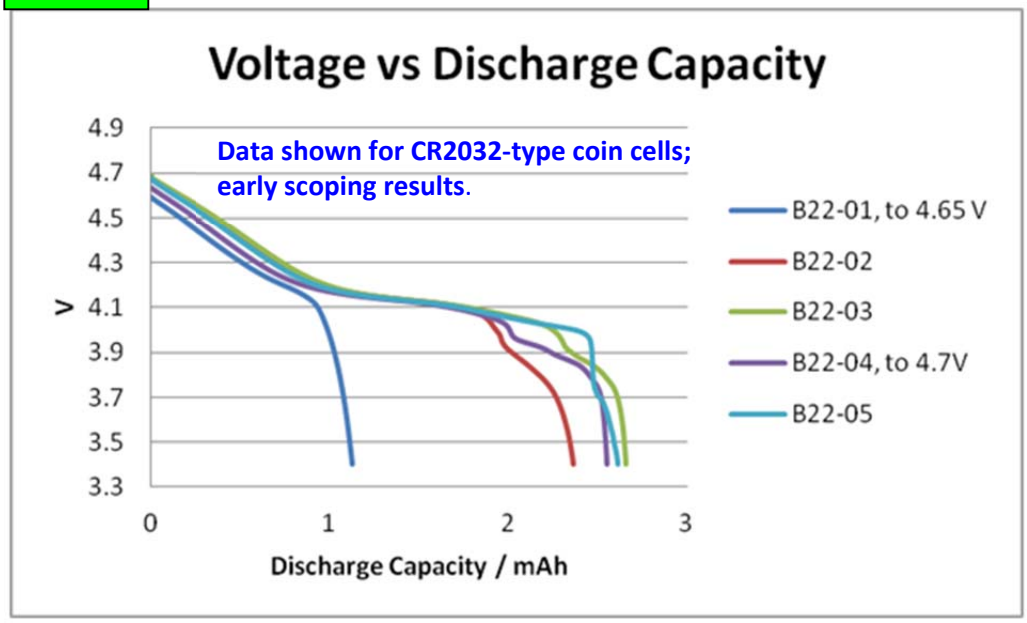

Fig. 4

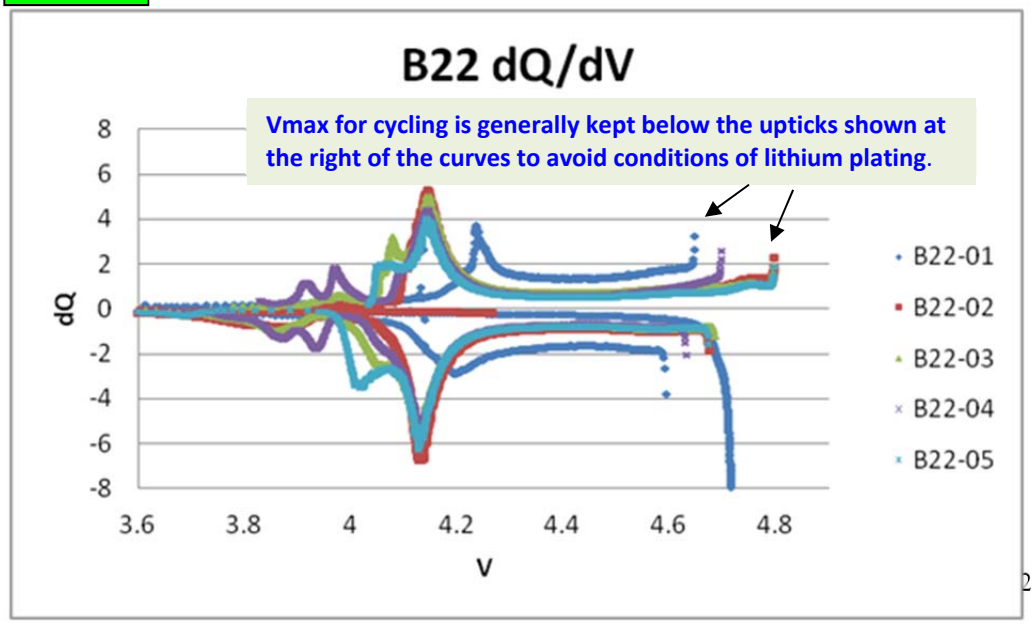

TASK 1
Battery Cell Materials Development

Project Number: 1.2.2 (ES029)

Project Title: Scale-up and Testing of Advanced Materials from the BATT Program

Lead PI and Institution: Vince Battaglia, Lawrence Berkeley National Laboratory

Barrier: Cost is too high (energy density needs to be increased); life is short of 15 year target.

Specific Objectives: (*i*) Identify materials in the BATT Program that are ready for enhanced screening diagnostics, (*ii*) provide feedback on cell performance attributes to BATT researchers so that they may improve their materials, and (*iii*) provide information to the ABR Program about materials that provide significant improvements over the baseline chemistry, ABR_1.

General Approach: Work with BATT PIs in deciding what materials are ready for scale-up and enhanced testing and diagnostic evaluation in full cells. Once materials are identified, decide on the best approach for increasing the quantity of the material to approximately 10 g (1 ml if it is electrolyte). Prepare laminates of the material and test in coin cells against Li. Based on initial test results, decide on best vehicle application for the material, design the electrodes for that application, and perform long-term cycling tests. Provide comparisons to ABR Program baseline materials and cells.

Current Status as of October 1, 2012: Five Ni-spinel materials, including three from MIT and UT, were tested for rate capability to the same cut-off voltages in half- and full-cells. All but one of the materials consisted of cations in a disordered state. The one ordered material showed the lowest rate capability when tested against Li metal. When the materials were tested against graphite, the cells displayed worse rate performance than against Li. Four electrolytes were tested in graphite/Ni-spinel cells. The electrolyte with FEC showed the best rate capability. Electrolytes from CWRU and URI were tested in graphite/NCM cells. All of the electrolytes showed improved cycling performance when compared with 1 M $LiPF_6$ in EC:DEC 1:2.

Expected Improvement by September 30, 2013: Will have identified at least five more BATT Program materials that should or should not undergo further testing. There will be an emphasis on electrolytes and anodes as these projects have been running for four and three years, respectively. Results of this analysis will help guide BATT PIs and BATT management with regard to their approach to future RFPs

Schedule and Deliverables: Attend review meetings and present interim results on the scale-up of BATT Program materials (November 2011, February 2012, August 2012) and in Quarterly Reports.

Milestone:
Battery design, performance, and cycling characteristics of multiple materials from the BATT Program and for the $LiNi_{1/2}Mn_{3/2}O_4$ system will be reported on at the DOE Annual Merit Review (May 2012).

PLAN TO ACHIEVE DELIVERABLES

During the second quarter of this fiscal year, amongst the testing of baseline materials for the Ni-spinel system and some salts from HQ, two $LiNi_{1/2}Mn_{3/2}O_4$ (NMO) materials from the University of Texas produced by Prof. Manthiram's Group in the BATT Program were evaluated. From the BATT Focus Group on NMO, it was discovered that particle morphology and the level of transition metal disorder of the active material were critical parameters with regard to cathode performance. Specifically, Dr Chen showed that octahedron demonstrated better performance than platelets and Dr. Cabana showed that disordered material provided better rate performance than ordered material. With this in mind, Dr. Manthiram synthesized two NMO materials with polyhedron shape and disordered configurations, one with and one without fluorine doping, referred to as NMFO and NMO, respectively. The fluorine is meant to improve cycling stability.

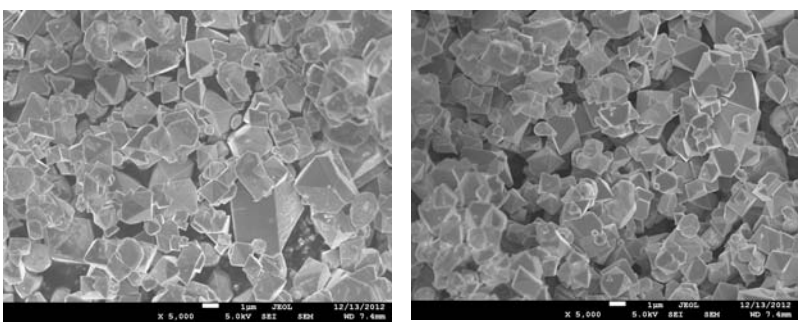

Figure 1. Left, SEM of NMO; right, SEM of NMFO. Materials appear nearly identical.

In figure 1 is provided the SEMS of both materials. The images are nearly identical. The particles are between one half micron to 3 microns in size and polygonal in shape. Electrodes were made of each with the same active and inactive material fractions, thicknesses, and porosity. The laminates were punched to circular electrodes and tested in coin cells with a standard electrolyte of 1 M $LiPF_6$ in EC:DEC 1:2. The counter electrode was either lithium metal or graphite. As seen for NMO in our lab, cycling against Li is stable. Most of the capacity is available with very little fade over 100 cycles before Li dendrites short the cells. Cycling with a graphite anode is slightly different. In that case, only half of the

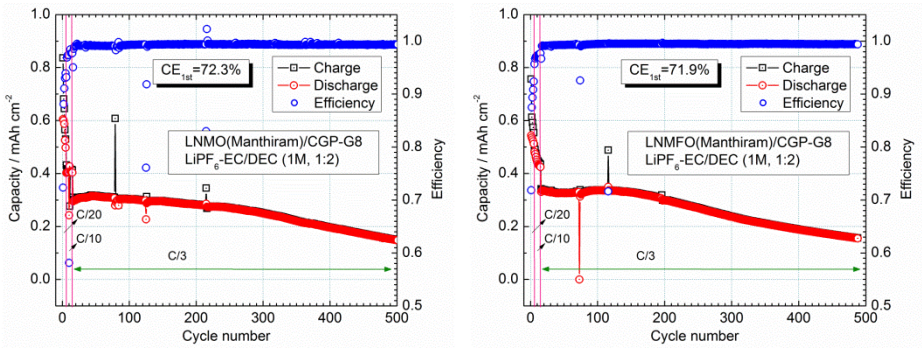

Figure 2. Left, capacity *versus* cycle number for a full cell of graphite/NMO; right capacity *versus* cycle number for graphite/NMFO. Note the large capacity decline in the early cycles for both cells.

capacity of the cathode is accessible after formation. However, once formation is completed, the loss of capacity for the next 200 cycles is minimal. This is the same for the baseline chemistry as it is for the materials Prof. Manthiram produced, see figure 2. The source of capacity fade for the first five formation cycles is still under investigation. Half of the loss can be attributed the poor first cycle coulombic efficiency, seen for nearly all chemistries tested. Another 20% of the capacity loss occurs during the first five C/20 formation cycles, and another 15% of the capacity is lost when the cycling current is increased to C/3. Much of the loss can be attributed to SEI formation on the anode and impedance rise in the cell.

TASK 1
Battery Cell Materials Development

Project Number: CPS Project 18502, CPS Agreement 23060, ORNL FWP CEVT110 (ES164)

Project Title: Overcoming Processing Cost Barriers of High Performance Lithium Ion Battery Electrodes

Project PI, Institution: David Wood, Oak Ridge National Laboratory

Collaborators by Category:

- National Laboratories: Argonne National Laboratory, Sandia National Laboratories
- Battery Manufacturers: Dow Kokam, A123 Systems, Navitas Systems
- Material Suppliers: ConocoPhillips, Phostech Lithium, TODA America, Timcal, JSR Micro, Solvay Specialty Polymers, Arkema
- Equipment Manufacturer: Frontier Industrial Technology

Project Start/End Dates: 10/1/11 to 9/30/14

Objectives: Electrode suspensions for lithium ion batteries are currently formulated using expensive polyvinylidine fluoride (PVDF) binder and toxic, flammable n-methylpyrrolidone (NMP) solvent. It is desirable to replace these components with water and water-soluble binders, but methods of mass production of these suspensions are currently underdeveloped. The major problems with aqueous electrode dispersions are: 1) agglomeration of active phase particles and conductive carbon additive; 2) poor wetting of the dispersion to the current collector substrate; and 3) cracking of the electrode coating during drying. NMP based processing also has the inherent disadvantages of high solvent cost and the requirement that the solvent be recovered or recycled. Initial projections of the minimum cost savings associated with changing to water and water-soluble binder are 70-75%, or a reduction from $0.210/Ah to $0.055/Ah. The objective of this project is to transform lithium ion battery electrode manufacturing with the reduction or elimination of costly, toxic organic-solvents.

Approach: Fabrication of composite electrodes via organic (baseline) and aqueous suspensions will be completed. A focus will be placed on the effect of processing parameters and agglomerate size on the aqueous route cell performance and microstructure of the composite electrode. Several active anode graphite and cathode (NMC, $LiFePO_4$, etc.) materials will be selected with various water-soluble binders. The conductive carbon additive will be held constant. Rheological (viscosity) and colloidal (zeta potential) properties of the suspensions with and without dispersant will be measured with a focus on minimization of agglomerate size. These measurements will show the effects of agglomerate size and mixing methodology on suspension rheology and help determine the stability (i.e. ion exchange processes across the surfaces of various crystal structures) of active materials in the presence of water. Composite

electrodes will be made by tape casting and slot-die coating, and the drying kinetics of the electrodes will be measured by monitoring the weight loss as a function of time and temperature. Solvent transport during drying will also be monitored as a method to control electrode morphology, porosity, and tortuosity. Electrode microstructure and surface chemistry will be characterized and correlated with cell performance. Electrochemical performance of electrode coatings made from the various suspensions will be supplied to ORNL's strategic industrial partners for external validation in large cell formats.
Improved cell performance with reduced processing and raw material cost will be demonstrated using pilot-scale coatings. At ORNL coin cells will be tested and evaluated for irreversible capacity loss, AC impedance, capacity vs. charge and discharge rates, and long-term behavior through at least 500 charge-discharge cycles. Half cells, coin cells, and pouch cells will be constructed and evaluated. The coin cells will be used for screening and coarse evaluation of different suspension chemistries and coating methodologies. A fine tuning of these research areas will be completed using ORNL pouch cells and large format cells with ORNL's industrial partners. Electrode coatings will be produced on the ORNL slot-die coater and supplied in roll form to the industrial partners for assembly into large format cells.

Electrode morphology will be characterized by scanning electron microscopy (SEM) and TEM. The bulk structure and surface of the active materials will be characterized using XRD and XPS, respectively.

FY13 Milestones:

1) Complete half-cell, full coin cell, and pouch cell round robin testing with ANL and SNL with CP A10/A12 and Toda NCM 523 electrochemical couple for NMP/PVDF based dispersion chemistry (Complete).
2) Match full coin cell performance through 100 cycles (0.2C/-0.2C) of aqueous suspension and water-soluble binder to NMP/PVDF based suspensions for CP A10/A12 and Toda NCM 523 electrochemical couple (June 2013 – delayed to August 2013).
3) Match pouch cell (≥3 Ah capacity) performance through 100 cycles (0.2C/-0.2C) of aqueous suspension and water-soluble binder to NMP/PVDF based suspensions for CP A10/A12 and Toda NCM 523 electrochemical couple (September 2013).

Financial data: $300k/year (FY12-FY13)

PROGRESS TOWARD MILESTONES
Summary of work in the past quarter related to milestones (1)-(3)

1. Completed round robin testing with Argonne National Laboratory (ANL) and Sandia National Laboratories (SNL) on VTO Applied Battery Research (ABR) baseline TODA NMC 532 cathode and ConocoPhillips (CP) A12 graphite anode:

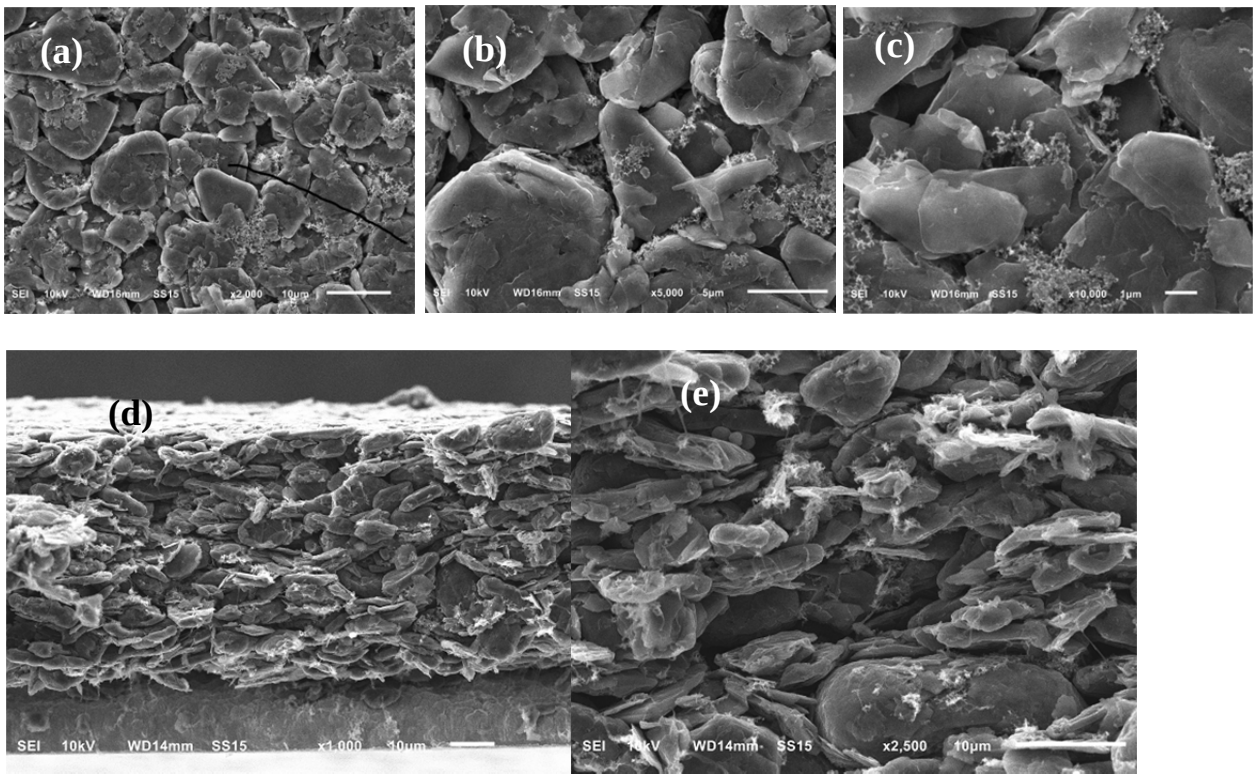

Figure 1. Morphology of CP A12 anodes; (a)-(c) surface morphology at different magnifications and (d)-(e) cross-section morphology at different magnifications.

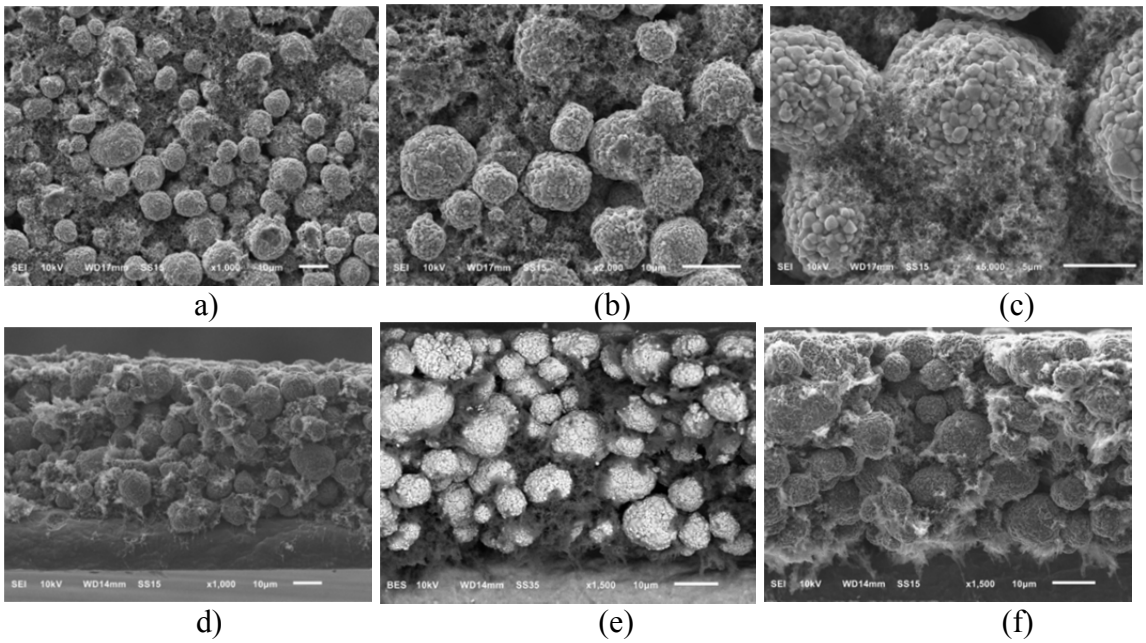

Figure 2. Morphology of NMC 532 cathodes (a)-(c) surface morphology at different magnifications and (d)-(f) cross-section morphology at different magnifications.

CP A12 anode (A12/super P Li carbon/Kureha 9300 PVDF=92/2/6 wt fraction) and NMC 532 (NCM 523/Denka carbon black/Solvay 5130 PVDF=90/5/5 wt fraction) were fabricated at the ORNL BMF and sent to ANL for round robin testing. Figures 1 and 2 show the morphologies of the electrodes, which indicate uniform distribution of constituents. Physical properties of the NMC532 and A12 electrodes after calendaring are listed in Table 1.

Table 1 Physical property of NMC532 and A12 electrodes.

	Areal loading (mg/cm^2)	Coating thickness (μm)	Electrode porosity (%)	Electrode balance
NMC532 cathode	12.57	65.3	37.8	A12/NMC532: 1.27-1.36
A12 anode	7.51	66.3	37.6	

The rate performance of NMC 532 and A12 half cells (with Li as the counter electrode) and NMC 532/A12 full cells is shown in Figure 3. C-rate was calculated based on 1C = 320 mA/g for the NMC 532 half-cell, 380 mA/g for the CP A12 half-cell, and 300 mA/g for the full cell. Both half and full cells demonstrated excellent capacity at low C-rate. The capacity of the NMC 532 half cells dropped considerably at 1C and above, which is most likely due to the higher thickness of the electrode and solid loading when electrode performance suffers from slow lithium ion diffusion and low electronic conductivity. The ANL reference performance test (RPT) was carried out to characterize capacity fade. As shown in Figure 4, the NMC 532/A12 full cells show good-to-excellent cycle life, with 12-36% capacity fade through ~400 cycles.

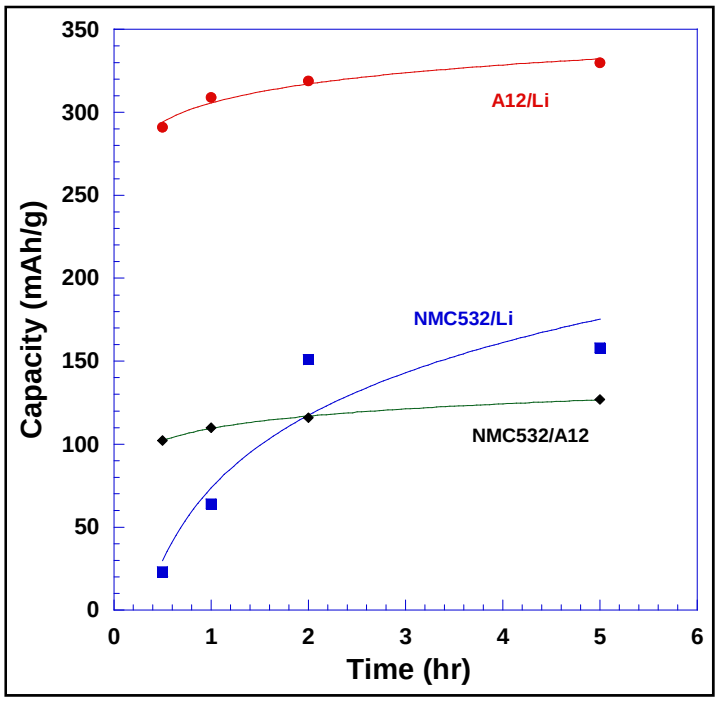

Figure 3. Rate performance of NMC 532 and A12 half cells and NMC 532/A12 full cells.

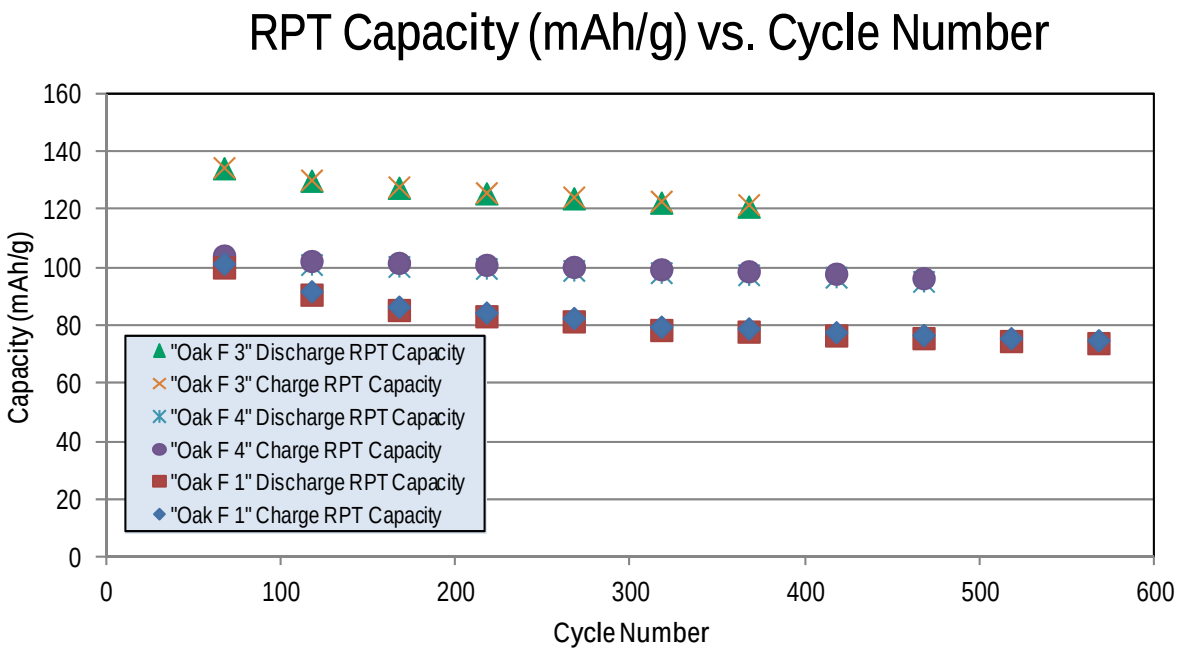

Figure 4. Full cell capacities from ANL reference performance test (RPT); capacity fade ranged from 12-36% through 400 charge-discharge cycles.

2. Full coin cell results:

Performance of full coin cells using a $LiFePO_4$ cathode and the ABR baseline CP A12 graphite anode was recorded with $LiFePO_4$ electrodes from both NMP-based and water-based processing. The electrode balance was between 1.0 and 1.2 (negative electrode/positive electrode), and the cells were cycled between 2.5 V and 4.2 V. Each cell underwent rate performance evaluation with 5 cycles at each rate followed by 100 cycled at 0.2C/-0.2C (1C=170 mA/g). During rate performance, the cells were charged at 0.2C and discharged at various C-rates.

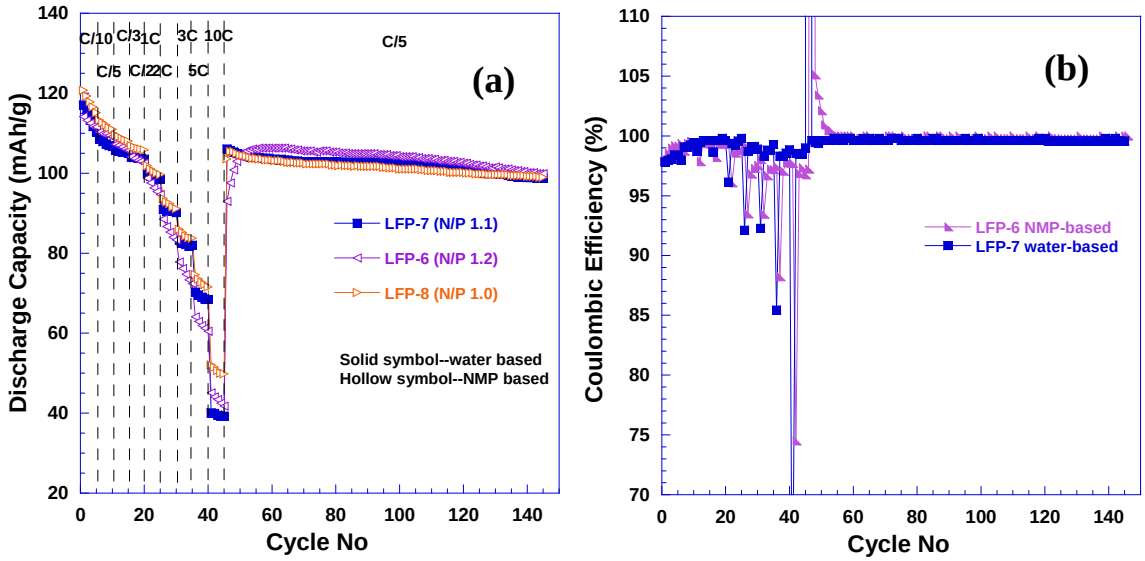

Figure 5. Performance comparison of $LiFePO_4$/A12 full cells; a) discharge capacity comparison of $LiFePO_4$ using NMP-based and water-based processing and b) comparison of Coulombic efficiency of $LiFePO_4$ from NMP-based and water-based processing.

As shown in Figure 5, both $LiFePO_4$ rate performance and capacity fade through 145 combined cycles with aqueous processing was identical to that with NMP-based processing. Discharge capacity retention was 93% and 94%, respectively after 100 total cycles at 0.2C/-0.2C. The Coulombic efficiency was also high, especially during the 100 cycles at 0.2C/-0.2C (> 99.5%). These full-cell results indicate cathodes from aqueous processing can deliver the same long-term performance as those from NMP based processing.

3. Water removal from electrode via water-based processing:

How to efficiently remove residual water from LIB electrodes has been one major problem for electrode manufactures with respect to aqueous processing. ORNL and its industrial partner have demonstrated extremely low capacity fade with large-format pouch cells over 1000 high-rate charge-discharge cycles when water was removed to below 500 ppm before cell assembly. To follow up on this study, water content was measured using a NMC 532 cathode, which was fabricated through water-based processing and pre-dried in seven convection-oven zones up to 90°C during electrode coating. Water content was characterized by Karl Fischer titration after the NMC 532 cathode had been further dried at 90°C for 2 hours under 68 kPa abs. As shown in Figure 6, the water content was 170 ppm (much lower than the 500 ppm industrial benchmark) indicating residual water can be effectively removed from electrodes, and its presence in low residual amounts should not contribute appreciably to capacity fade when aqueous electrode processing is implemented.

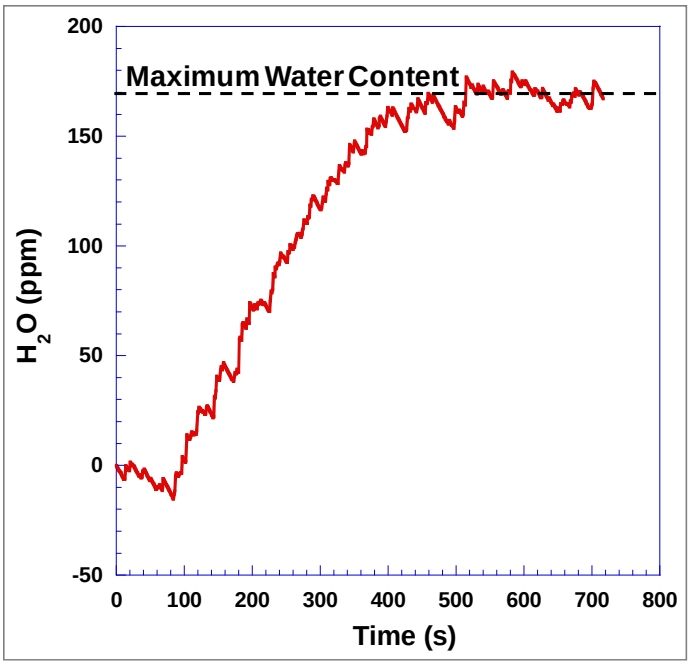

Figure 6. Residual water content of NMC 532 cathode after water-based electrode processing.

4. Preliminary results on NMC 532 via aqueous processing.

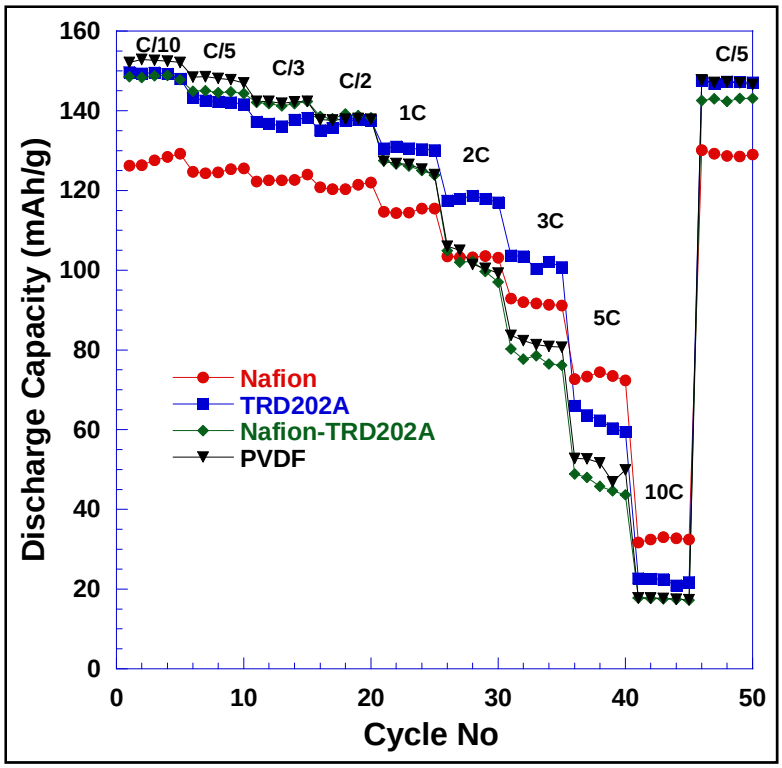

Figure 7. Comparison of NMC 532 cathode performance via NMP-based and water-based processing. The NMC 532 cathodes from water-based processing demonstrate comparable performance to that from NMP-based processing.

NMC 532 cathodes were coated with a doctor blade using aqueous electrode processing. Three water soluble binders, TRD-202A (JSR Corporation), DuPont Nafion® (Ion Power, Inc.) and a 50/50 wt% mixture of the two, were used as the cathode binders. All NMC 532 cathodes consisted of 90 wt% NMC 532, 5 wt% Denka carbon black and 5 wt% binder and had an areal loading of ~7.5 mg/cm^2. Rate performance in half coin cells is compared to that with PVDF binder via NMP-based processing in Figure 7. The NMC 532 cell with TRD-202A binder demonstrated almost identical performance to that with PVDF at low C-rate (< 1C) and outperformed it at higher C-rates. The cathode with Nafion® (only) exhibited somewhat lower capacity at <1C; however, it showed excellent high rate performance (the best performance at >5C). In this case, the Nafion® PFSA was not converted to the lithium form prior to making the cathode dispersions, so the hydronium ions (present when the PFSA is in the "acid form") could have exchanged with electrolyte lithium ions during the lower C-rate cycles. This exchange process would have lowered the lithium-ion concentration of the electrolyte, but the benefit of the improved interfacial lithium-ion conductivity (due to the lithium-exchanged PFSA film) at high C-rate more than offset this electrolyte conductivity loss.

Mixing TRD-202A with Nafion® increased capacity at low C-rate since less Nafion in the acid form resulted in less electrolyte lithium ions exchanging with inherent hydronium ions. A lower weight fraction of Nafion® could also have resulted in a discontinuous lithium-ion conducting phase, and the contribution to interfacial lithium-ion conductivity improvement was, therefore, limited. Consequently, improvement at high C-rate was negligible (see Figure 7). While TRD-202A and Nafion® did improve electrode performance at low and high C-rates, respectively, performance could be maximized across the entire C-rate range by optimizing the respective compositions.

5. Future work:

High quality NMC 532 cathodes will be fabricated using the ORNL slot-die coater through aqueous processing. Full cells with NMC 532 cathodes made from water-based processing and A12 anode from NMP-based processing will be tested and the performance matched to NMC532/A12 full cells made from NMP-based processing.

Publications, Reports, Intellectual Property or Patent Application filed this quarter.

1. J. Li, B. Armstrong, J. Kiggans, C. Daniel, and D. Wood, "Optimal Polyethyleneimine Concentration and Mixing Sequence for $LiFePO_4$ Aqueous Nanoparticle Dispersions", *Journal of Colloids and Interface Science*, Accepted, 2013.
2. D. Wood, J. Li, M. Debasish, C. Daniel, B. Armstrong, R. Dinwiddie, H. Wang, R. Trejo, N. Gallego, C. Contescu, J. Howe, R. Meisner, J. Kiggans, B. Brown, "Advanced Materials Processing and Novel Characterization Method for Low-Cost, High Energy-Density Lithium-Ion Batteries", Conference Proceedings of Advanced Automotive Battery Conference 2013, Pasadena, California, February 4-8, 2013 (Invited).

TASK 1
Battery Cell Materials Development

Project Number: ES162

Project Title: Development of Industrially Viable Battery Electrode Coatings

Project PI, Institution: Robert Tenent (PI), NREL

Collaborators (include industry): Chunmei Ban (NREL), Steven George and Robert Hall (University of Colorado, Boulder), Chris Orendorff (Sandia National Laboratory), Bryant Polzin (Argonne National Laboratory), Claus Daniel, David Wood and Jianlin Li (ORNL)

Project Start/End Dates: December, 2012 – September, 2013

Objectives: (1) Demonstration of Al_2O_3-based Atomic Layer Deposition coatings for improved cycling durability and abuse tolerance using standard electrode materials currently employed within the ABR program. (2) Design of an in-line atmospheric pressure atomic layer deposition (AP-ALD) system to demonstrate a process that may easily and inexpensively be integrated into the existing industrial Li-ion electrode fabrication lines.

Approach: Previously obtained results indicate that atomic layer deposition (ALD) can be used to form thin and conformal coatings on electrode materials that lead to both increased cycling lifetime, especially at high-rate, as well as abuse tolerance (e.g. stable cycling at high temperature and/or high voltage). This project will initially focus on using existing deposition capabilities to demonstrate an Al_2O_3-based ALD protective coating process for materials that are already commercially available at large-scale or are under advanced study within the VTP-EERE programs. This will include both anode and cathode materials in order to facilitate full cell testing and abuse studies. Initially, testing will be performed at the coin cell level to establish a stable baseline for comparison to existing data. In a later phase of the project larger format electrodes will be coated for testing in both pouch and 18650 cells. Coatings will be demonstrated on electrode materials produced at NREL as well as from outside parties. Finally, testing will be conducted both at NREL as well as within collaborating laboratories via a "round robin" process to ensure quality of data and the development of robust and transferrable processes.

In addition to small-scale exploratory research on various possible coating/electrode combinations, design work will be conducted for the development of a deposition system that will allow in-line coating at atmospheric pressure using an "ALD-

like" process. The ultimate goal is to demonstrate a process that can be inexpensively integrated into existing industrial Li-ion battery electrode fabrication lines.

Milestones:

a) Continued supply of ABR collaborators with alumina ALD coated electrodes and materials
   Due: On-Going
   Status: In Progress

b) Design and initiate construction of a deposition system capable of in-line AP-ALD on commercially relevant substrate sizes.
   Due: September 2013
   Status: On-Schedule

Financial data: Current Funding $150K/year

PROGRESS TOWARD MILESTONES

a) The NREL team has coated and tested HE5050 cathode materials as part of the voltage fade effort focused at Argonne. NREL performed coatings of three different thicknesses of aluminum oxide on coated HE5050 electrodes as provided by the Argonne Cell Fabrication Facility. These samples were then tested in a coin cell format. Recent testing was conducted using the Argonne Voltage Fade Testing Procedure and data was submitted to the Argonne team for final analysis and inclusion in their database.

   It was determined that while the alumina coating did reduce capacity fade for the HE5050 material, the surface treatment had no impact on the observed voltage fade phenomenon. The NREL team participated in discussions with the Argonne team regarding the impact of a wide variety of surface treatments on voltage fade. Based on data provided by Argonne, NREL and ORNL a unanimous decision was reached that regardless of coating method or material, no surface treatment appeared to have a significant effect on the voltage fade issue. The NREL team worked along with the Argonne and ORNL teams to compile a joint publication discussing these results and subsequent conclusions.

   In addition to the HE5050 work with Argonne, NREL has recently received and is processing samples of materials from both ORNL and Sandia for ALD alumina coating. The ORNL team will fabricate pouch cells in a preliminary experiment to assess performance of ALD coated electrodes in that format. Sandia will perform safety analysis with focus on the impact on thermal runaway effects.

b) Within the last quarter, NREL was able to hire a post-doctoral researcher under subcontract with the University of Colorado at Boulder to continue work on the design of a new "digital modular roll-to-roll ALD reactor". This improved design incorporates what we have designated as a "push/pull" system and is

demonstrated in **Figure 1**. The porous electrode coatings require that precursors be "pushed" into sample pores at an over pressure to ensure reaction with the entire available surface. To maintain the ALD reaction, unreacted precursor must be "pulled" out of the pores via a vacuum port before the porous electrode encounters the second reactant. If the ALD precursors encounter each other the reaction becomes CVD and the required controlled deposition is nullified.

Figure 1

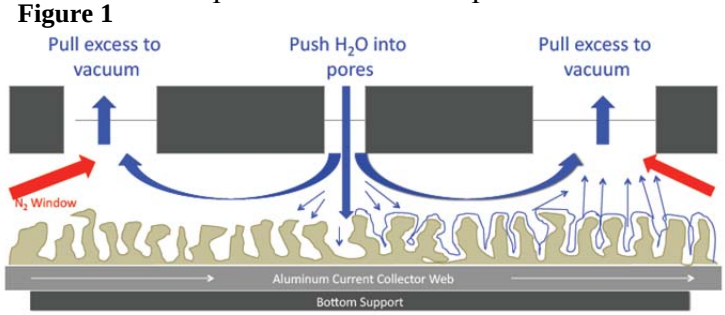

"Push-Pull" design for ALD in porous battery material on web.
High pressure H_2O reactant "pushed" into pores. Excess H_2O reactant and reaction product "pulled" out by vacuum region. N_2 used to separate reactants and provide entrainment.

As also shown in **Figure 1**, a linear translational roll-to-roll design was initially considered for the first design due to ease of manufacturing and modifications but the push/pull aspect employed with the linear reactor design was not able to adequately maintain tension on the web substrate. The best design when considering "push/pull" is a drum within a drum design as seen in **Figure 2**. The outer drum is fixed and contains the deposition source head. The inner drum rotates the web while maintaining the required tension. To ensure the precursors do not encounter each other during the deposition there is a vacuum port on each side of the reactant gas port. In between the different precursor ports is a nitrogen gas window that is pressured higher than the dosing precursors. This ensures no cross talk between the different reactants which leads to bulk CVD deposition. To allow the optimal amount of adaptability, a "digital modular" system has been designed for the deposition head. This means that the outer drum is fixed and allows the entrance or removal of gases through slots as shown in **Figure 3**. The slots are uniform in design and allow a variety of modules to be fitted. This will allow the spacing between dosing and vacuum to be increased or decreased allowing the maximum amount of variability. In addition, other modules can be added in the future without having to modify the main deposition head. Specifically, we are interested in the integration of on-board diagnostic equipment for detecting pressure, generation and identification of reaction products as well as film thickness all of which will

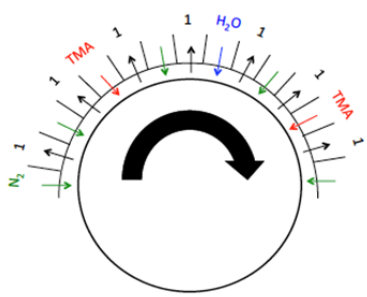

Figure 2

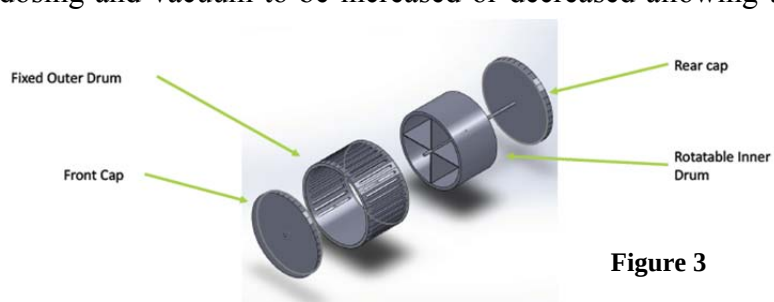

Figure 3

be monitored in-situ. Additional modules could be added to increase the reactivity of the precursors such as a plasma source.

Publications, Reports, Intellectual property or patent application filed this quarter. (Please be rigorous, include internal reports--invention records, etc.)

Recent results were presented at the Vehicles Technology Office Annual Merit Review. In addition, the NREL team collaborated with Argonne and Oak Ridge on the preparation of a manuscript detailing work conducted by all partners to assess the effect of various surface pre-treatments on the voltage fade phenomenon observed for the Toda HE5050 cathode material. The improved reactor design is currently under evaluation for potential intellectual property which will be filed shortly.

TASK 1
Battery Cell Materials Development

Project Number: 25194 (IV.B.2.5) (ES196)

Project Title: Evaluate ALD Coatings of LGCPI Cathode Materials and Electrodes

Project PI, Institution:
Shriram Santhanagopalan, National Renewable Energy Laboratory, Golden CO 80401

Collaborators (include industry):

Mohamed Alamgir, LG Chem Power Inc., Troy MI
Karen Buechler, David King, ALD Nanosolutions, Broomfield CO

Project Start/End Dates: June 2012 – June 2013

Objectives:

The objectives of this work are two-fold: i) to evaluate the scalability of the process to coat LG Chem Power Inc. (LGCPI) cathodes with alumina, using the Atomic Layer Deposition (ALD) technique, and ii) to demonstrate improvements in rate capability and life of ALDcoated LGCPI electrodes.

Approach:

LGCPI and NREL have collaborated to demonstrate the scalability of the ALD coating process over the last 6 months, and the benefits of ALD coatings for long term cycling and calendar life are being quantified.

- NREL received samples of baseline material to be coated from LGCPI.
- NREL carried out ALD coating of the samples with help from a subcontractor - ALD Nanosolutions.
- NREL fabricated cells from those samples for quick screening and feedback to ALD Nanosolutions.
- LGCPI is currently fabricating larger format cells for further evaluation.

Milestones: Project deliverables and decision points. Milestones should clearly show progress towards your project objectives, including overcoming issues, and should clearly support achieving a significant improvement in cell energy density, safety, and/or cost. If your material or couple has known issues, please address some or all of them in your milestones.

(a) Receipt and characterization of baseline material and electrodes, July 2012, Complete
(b) ALD coating and characterization of baseline cathode powder, Sept. 2012, Complete

(c) ALD coating of baseline electrodes, Dec. 2012, Complete
(d) Pouch cell fabrication and long term evaluation, June 2013, On Schedule

Financial data: 110k (2012), 50k Sub-contract to ALD Nanosolutions
$0 (2013)

Progress Towards Milestones:

The work in the previous quarter focused on coating electrodes directly using the Atomic Layer Deposition technique. The sub-contractor, ALD Nanosolutions, already had in place small volume traditional flat ALD reactors and roll to roll ALD coating capabilities. Under the current effort, these were extended to coat large size (6" x 6") sheet electrodes by installing a holder into the large volume ALD particle reactor. The modified reactor can accommodate the new electrode holder for up-to 25 electrodes per batch. Evaluation of the reactor performance included analysis of coating uniformity across the web and through the depth of the reaction chamber during several repeats.

The process steps for coating the sheet electrode samples are essentially the same as those for the fluidized bed reactors:

1) Load Reactor with Electrodes
2) Bring reactor to coating temperature and pressure
3) Sequentially introduce ALD precursors
4) Repeat 3 for desired number of cycles

Static dosing on the electrodes until after breakthrough in the residual gas analysis signals ensured the uniformity of the coating across the chamber dimensions.

Towards the final milestone, the coated samples were shipped back to LGCPI for fabrication of pouch format to quantify improvements to the cycling capability from the ALD coating process. The only pending item on this effort is the results from cell-evaluation of electrode-sheets directly coated using the ALD technique, currently being tested at LGCPI.

This project was not supported in FY13 - future work, pending support, will include optimizing the coating process for the electrodes based on the sheet-electrode coating results from this quarter, and improvements to the recipe to build the cathodes from the ALD coated powders.

Publications, Reports, Intellectual Property or Patent Application filed this quarter:

1. Shriram Santhanagopalan, *Impact of ALD Coating on Manganese Rich Cathode Materials*, Poster presented at the 2013 Annual Merit Review in Arlington, VA (May 2013).

TASK 2
Calendar & Cycle Life Studies

Project Number: 1.1 (ES030)

Project Title: Cell Fabrication Facility Team Production and Research Activities

Project PI, Institution: Andrew N. Jansen, Argonne National Laboratory

Collaborators (include industry): Dennis W. Dees, Daniel P. Abraham, Kevin G. Gallagher, Wenquan Lu, Bryant J. Polzin, Stephen E. Trask, Nancy L. Dietz-Rago, Javier Bareno, Qingliu Wu, Martin Bettge, Ye Zhu, Joseph J. Kubal, and Paul A. Nelson (Argonne National Laboratory)
Prof. Jai Prakash (Illinois Institute of Technology)
Prof. Ivan Petrov (University of Illinois)
Prof. Alex Wei (Purdue University)
Yan Li (University of Rochester)

Toda Kogyo
Phillips 66
JSR Micro
Zeon Chemicals
Materials Engineering Research Facility (MERF)
Post-Test Facility (PTF)
Electrochemical Analysis and Diagnostic Laboratory (EADL)

Project Start/End Dates: October 2012 / September 2014

Objectives: The overarching objective of this core-funded effort is to design, fabricate, and characterize high-quality prototype cells of at least 200-mAh capacity to enable a realistic and consistent evaluation of candidate chemistries in a time-effective manner. In order to achieve this main objective, it was necessary to divide this effort into interlinked sections designed to support the activities of the Cell Fabrication Facility (CFF). As with the CFF, each of these support sections (Materials Validation, Modeling, and Diagnostics) are designated specific goals and responsibilities. It is not the aim of this task to become a small battery manufacturer, but instead to become a laboratory research facility with cell production capabilities that adequately evaluate the merits and limitations of mid-to-long term lithium-ion chemistries in a close-to-realistic industrial format.

Approach: As new cell chemistries and systems progress, they may reach the point where they are considered for further development in larger prototype cells. When this happens, a limited quantity of these materials, along with their preliminary data, are transferred from the inventor or originator to the Materials Validation support section, where they will be evaluated to determine if they warrant production in prototype cells by

the CFF. The source of these materials (anodes, cathodes, electrolytes, additives, separators, and binders) may originate from the ABR and BATT Programs, as well as from other domestic and foreign organizations such as universities, national labs, and industrial vendors. Electrochemical couples with high power and energy density will be given extra priority.

Coin cells (2032 size) will be used for materials validation purposes with initial studies performed at room temperature or 30°C. After formation cycles, the coin cells will go through hybrid pulse power characterization (HPPC) testing, rate capability testing, and limited cycle life testing. Accelerated aging studies will also be performed at 45°C to 55°C for promising materials to give a preliminary indication of life. Where appropriate, the thermal abuse response will be studied using a differential scanning calorimeter. The key areas to monitor are the materials' influence on capacity, energy, power, and cycle/calendar life. The Materials Validation results will be used by the other support efforts, and if needed, by the Materials Engineering Research Facility (MERF) and the Post-Test Facility (PTF).

Once the materials' performance has been validated, promising cell chemistries will be recommended for further development by the CFF. Using the recommendations and results obtained by the Materials Validation, the CFF will initiate a prototype cell build that will include the generation of single-sided electrodes for the Diagnostics support effort. Diagnostics examines the new cell chemistries in detail using advanced electrochemical and analytical techniques, including the employment of micro-reference electrode cells. This information lays the foundation for the electrochemical Modeling support effort focused on correlating the electrochemical and analytical studies, in order to identify performance limitations and aging mechanisms. The Modeling effort supports the CFF through the development and utilization of efficient simulation and design tools for advanced lithium-ion battery technologies. These modeling tools cover a broad range of applications, from correlating analytical diagnostic results with electrochemical performance in small test cells to predicting the performance and cost of full size PHEV battery packs based on limited results.

If the results from Diagnostics still look promising, the CFF will begin fabrication of full cell builds using double-sided electrodes. The CFF at Argonne has the capability to make two prototype cell formats in their 45 m^2 dry room: pouch cells (xx3450 format, with capacity around 0.4 Ah) and 18650 cells. Pouch cells are anticipated to be easier to assemble, but they may suffer from bulging if gases are evolved during cell aging and cycling. 18650s, which are rigid containers, may be used if the pouch cell format is deemed unreliable due to gassing, or if higher capacity cells are needed (greater than 1 Ah). Central to this effort is a pilot-scale coating machine that operates with slurry sizes that range from 20 grams to a few kilograms. This is a key feature of the CFF that enables a professional evaluation of small quantities of novel materials. If needed, the MERF is available for scaling up materials for these prototype cell builds.

The main emphasis of the CFF will be to fabricate electrodes and prototype cells for calendar and cycle life studies. These cells will undergo rigorous electrochemical

evaluation and aging studies under the combined effort of the CFF and Argonne's Electrochemical Analysis and Diagnostic Laboratory (EADL). The Diagnostics effort will use advanced electrochemical and physicochemical diagnostic tools and techniques to identify factors that determine cell performance and performance degradation (capacity fade, impedance rise) on storage and on extensive deep-discharge cycling. The results of these tests are used to formulate data-driven recommendations to improve the electrochemical performance/life of materials and electrodes that will be incorporated in pouch– and 18650– type PHEV cells assembled in the CFF. After testing, the cells will be destructively examined by the Post-Test Facility that will interface with the Diagnostics effort to elucidate failure mechanisms in end-of-life cycled cells from CFF – the information generated will enable the design of cell chemistries that meet the performance, life and safety targets of PHEV cells. The CFF & Support effort will collect and share all results with other members of the ABR Program and to the materials origin. This information is then used to further improve the new chemistry, as well as future electrode and cell builds. The CFF may also provide this information and prototype cells to battery developers for their evaluation.

The general approach taken in the Modeling effort is twofold. First, spreadsheet based simulations are employed that determine the impedance behavior, available capacity, and thermal effects for general and specific cell, battery module, and battery pack designs. The design model calculates power and energy, weight and volume of materials and components, as well as their thermal performance. The model is also capable of performing simulations on multiple battery designs for comparison and optimization. The battery design model also includes a module that calculates battery costs by combining materials and components costs with manufacturing expenses based on a plant design.

The second part of the Modeling effort utilizes an electrochemical model that accurately describes all the pertinent physicochemical phenomena in the cell under study. Continuum based transport equations using concentrated solution theory describe the movement of salt in the electrolyte. Volume-averaging of the transport equations accounts for the composite electrode geometry. Electrode kinetics, thermodynamics, electronic migration, and diffusion of lithium in the active material particles are also included. Phase change in the active materials and detailed transport through the solid electrolyte interphase or SEI can also be included. Two versions of the electrochemical model have been developed (i.e. AC and DC) to describe the full range of electrochemical tests conducted on the advanced lithium-ion battery technologies.

Milestones:

(a.) Obtain viable supplier of battery grade silicon powder, March, 2013 (Delayed)

(b.) Assess influence of LiDFOB, LiBOB, and HFiP electrolyte additives for HE5050 cathode, May, 2013 (On schedule)

(c.) Evaluate MERF cathodes ($Li_{1.25}Ni_{0.3}Mn_{0.62}O_2$) based on hydroxide and carbonate precursors, July, 2013 (On schedule)

(d.) Add silicon-graphite, LiFePO4, LiCoO2, and hard carbon to electrode library, July, 2013 (On schedule)
(e.) Fabricate pouch cells based on silicon-graphite anodes and LMR-NMC cathodes, August, 2013 (On schedule)
(f.) Validate performance of advanced battery materials, September, 2013 (On schedule)
(g.) Determine sources of impedance rise and capacity fade during extensive cycling of cells containing various electrochemical couples, September, 2013 (On schedule)
(h.) Recommend solutions that can improve the life of high energy LMR-NCM electrodes and cells by 30% at 30°C and 15% at 55°C, September, 2013 (On schedule)
(i.) Enhance battery design and cost model concentrating on designs for advanced lithium-ion electrochemical couples, September, 2013 (On schedule)
(j.) Advance development of electrochemical models focusing on the impedance of LMR-NMC positive electrodes, September, 2013 (On schedule)

Financial data: $2500K / FY13 **(**subcontracted $30K to Purdue University, $70K to Illinois Institute of Technology, and $30K to University of Rochester)

PROGRESS TOWARD MILESTONES

(a) Summary of work in the past quarter related to milestone (a).

In addition to the two commercially available silicon materials obtained last quarter (Alfa Aesar, Shanghai Guan Jin), another silicon powder has been obtained from Nanostructured and Amorphous Materials Incorporated. This material is a 130 nm silicon powder (spherical with some nanowires mixed in). While validation of this material is in preliminary stages, this material shows some promise as a possible battery grade silicon source.

The binder systems are equally important to the performance of silicon and silicon/graphite based electrodes. PVDF has been generally shown to be an inferior binder with uncoated silicon-based electrodes, thus other binders are needed to be explored. Silicon undergoes major expansions and contractions during cycling. When PVDF is used as the binder, electrical contacts between particles are difficult to be maintained possibly due to the inability of PVDF to strongly adhere to the silicon particles. Repeated cycling of the electrode tends to fracture and isolate silicon particles from the conductive network, which diminishes the capacity. Using other binders such as CMC, Alginic Acid, or Polyacrylic acid (PAA) has been shown to increase cyclability by helping to minimize the loss of contacts between particles. In addition to the binders that have been tested, Polyethylene-co-acrylic acid (PEAA) has been considered a possible binder for silicon based electrodes. While electrodes made with only PEAA for a binder have shown poor electrochemical results, the electrode itself had better mechanical

properties than electrodes made only with PAA or CMC, meaning that PEAA could be a useful additive. Other two and three componant binder systems have begun to be examined. Some of the systems being evaluated are SBR : PAA, SBR : LiPAA, SBR : PAA : Xanthan Gum, and PEAA : Xanthan Gum.

In addition to testing silicon materials from various sources obtained thus far, collaborations are ongoing with companies to make improved silicon/graphite composite electrodes. In particular, work has begun with a material supplied by Electrochemical Materials (EM), who has put a proprietary organic coating on the silicon which allows it to cycle when using PVDF as a binder in a silicon/graphite composite electrode. Preliminary half-cell work with their material shows vast improvements over Si particles that have not been coated.

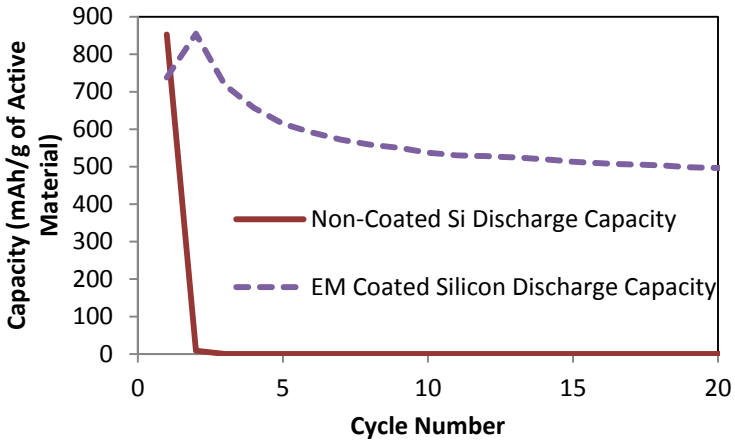

Figure 1. Comparison between Electrochemical Materials' (EM) surface-treated silicon against that of a silicon powder that has not been treated, both using PVDF as the binder. The EM electrode is able to maintain high capacities over extended cycling. The EM electrode has a composition of 9 wt.% EM-treated silicon, 51 wt.% graphite, 10 wt.% carbon black, and 30 wt.% PVDF.

Additionally, collaborations with binder manufacturer Zeon Chemical have produced useful insights into binder mechanisms. Zeon produces a poly styrene-butadiene rubber (SBR), which has been shown to improve the laminate's physical properties along with increased electrochemical performance. Zeon's binder has been tested in conjuction with mainly CMC at their recommendations. In addition to supplying their binder, they have loaned Argonne a Primix mixer, and with this mixer nine large scale slurries (all over 100 grams of solids) were made. Several graphite/SBR/CMC slurries were successfully coated on the large scale in the Cell Fabrication Facility, with these being the first aqueous-based slurries to have been coated in the dry room environment. No adverse effect on the humidity in the facility was noted.

Other sources of battery grade silicon are actively being pursued and a few promising sources have been identified. One of which is Dow Corning, which has provided a small sample of silicon & silicon composite powders to Argonne for evaluation purpose. This initial study will investigate three silicon/graphite blends with three different binders. The silicon/graphite blends consist of 0%, 10%, and 20% silicon,

and the three binder systems will be PVDF, CMC/SBR, and PAA (with and without SBR). In addition, silicon samples were received including a sample from an Argonne researcher (Dr. A. Abouimrane) and another sample from XG Sciences that is based on graphene. A silicon electrode sample was also received from LBNL (Dr. G. Liu). Electrochemical performance tests (materials validation) are being initiated on these samples and are discussed in section (f) below.

(b) Summary of work in the past quarter related to milestone (b)

Studies have continued in investigating the performance degradation observed using LiDFOB and LiDFOB + LiBOB additives in standard 1.2M $LiPF_6$ in EC:EMC 3:7 by wt.% electrolyte (Tomiyama) in larger format cell sizes (xx3450 pouch cells) for HE5050 versus A12 graphite. Previous diagnostic work has shown improved electrochemical performance using coin cells with the additives listed above. Recent work has been done to try to understand why the pouch cell electrochemical performance differs from the performance in coin cells.

There are several fundamental differences in cell design formats between coin cells and the larger pouch cells that could be the source of this discrepancy. First, the coin cell format is generally flooded with electrolyte which creates a high electrolyte to electrode area ratio. In a pouch cell format the design limits the amount of electrolyte that can be added. This lower ratio in the pouch cell format also correlates with there being less additive (mole basis) per area of electrode than there is in the coin cell format. The second factor is that in a coin cell, due to the larger electrolyte to electrode area ratio and the lower electrode thickness, coin cells do not usually undergo a special procedure to ensure that the electrode has been wetted fully. Whereas, the larger format cells have thicker electrode coatings and multiple electrodes that are stacked, which take longer to wet fully. The general procedure used in pouch cells to encourage proper wetting is to first perform a quick tap charge for five minutes to minimize copper corrosion, and then let the cell rest for 24 hours.

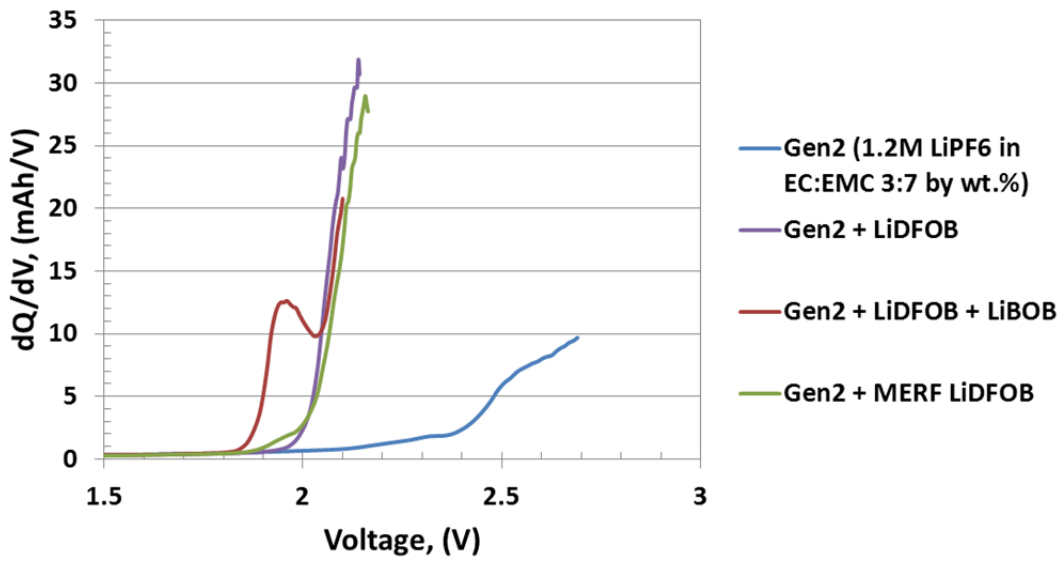

a)

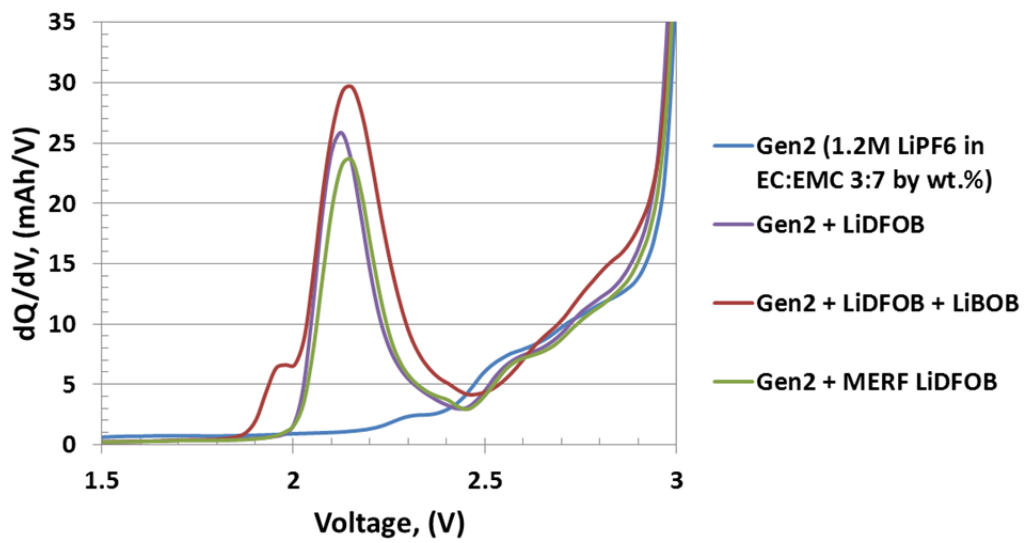

b)

Figure 2. Pouch cell data of the initial 5 minute C/10 tap charge (a) and the subsequent C/10 charge of the 1st cycle dQ/dV that occurs after the 24 hour rest step (b) using various additives. (All data above is from CFF-B9 "HE-5050 vs. A12", except for the series "Gen2 + MERF LiDFOB" which is CFF-B12 "NHE5050 vs. A12". "Gen2" electrolyte is 1.2 M $LiPF_6$ in EC:EMC 3:7 by wt.%. "Gen2 + LiDFOB" is Gen2 + 2 wt.% LiDFOB. "Gen2 + LiDFOB + LiBOB" is Gen2 + 2 wt.% LiDFOB + 1wt.% LiBOB. "Gen2 + MERF LiDFOB" is Gen2 + 2 wt.% MERF-made LiDFOB).

The LiDFOB & LiBOB additives are bifunctional, in that they react on both the cathode and anode. In order to achieve improved cell performance, the additive should ideally form passivation layers that minimize cathode reactions with the electrolyte. The dQ/dV plots show that the additives (LiBOB & LiDFOB) are mainly consumed on the anode during both the tap charge and the 1st cycle charge of the formation procedure. The peak at ~1.8 to 2.0 V is due to the LiBOB additive reduction, and the peak at ~2.0 to 2.4 V is due to the LiDFOB additive reduction at the anode based on results found in

diagnostic studies. Because of these reduction processes, there is insufficient additive leftover to form effective passivation layers at the cathode.

It is clear from the data shown in Figure 2 that the pouch cell formation protocol must be modified when using these additives. Suggested modifications include the following: (i) using elevated temperatures after the electrolyte fill to encourage electrode wetting; (ii) replacing the tap charge with a 1.5 V voltage hold for 24 h; (iii) applying a higher C rate (greater than C/10) to pass through the 1.8 V to 2.4 V window more quickly to minimize consumption of additives on the anode; (iv) using a higher additive concentration (3-4 wt.%, instead of 1-2 wt.%) in the Gen2 electrolyte. These modifications and other formation cycling protocols will be explored/validated first in coin cells before they are applied to the pouch cells.

(c) Summary of work in the past quarter related to milestone (c)

Half-cell coin cells with the composition of 84 wt.% LMR-NMC (Lot# 2012-07-09&11), 8 wt.% Timcal C-45 carbon black, and 8 wt.% Solvay 5130 PVDF were made by MERF staff. The cells performed well with good rate performance and C/3 cycling. The corresponding CFF pouch cell build using the same LMR-NMC original powder was made with the electrode composition of 90 wt.% LMR-NMC, 5 wt.% Timcal C-45 carbon black, and 5 wt.% Solvay PVDF versus a 91.8 wt.% A12 graphite anode. The pouch cell build showed good formation cycles but significant performance degradation during the high current rates of the rate study. The pouch cells did not recover after the high rates.

In an effort to understand and improve the performance of the MERF-made LMR-NMC ($Li_{1.25}Ni_{0.3}Mn_{0.62}O_2$) material, particle optimization and electrode composition was examined. Previous studies of the MERF-made LMR-NMC powder had shown that particle cracking occurred during the calendering process on the coated electrodes. The particle cracking has been hypothesized to be a significant factor in the poor performance at high current rates due to the particles having less of an electronic network because the particle fragments had been dislodged and isolated from the network. To troubleshoot the problem, staff at MERF milled the original LMR-NMC powder using the method of ball milling for 72 hours then drying the LMR-NMC material at 95°C for 48 hours. The dried material was then pulverized using a small-scale pulverizer for 3 minutes. The idea was to “pre-crack” the weaker particles before the calendering process to allow the binder and carbon black to coat the newly created particle surface areas during the slurry preparation for a thorough covering over all particles.

Thus electrodes were fabricated using both the original (un-milled) LMR-NMC powder and the milled LMR-NMC powder with the 84/8/8 composition and 90/5/5 (LMR-NMC/Timcal C45/Solvay PVDF) composition, respectively. The results indicated that the milling of the LMR-NMC powder was detrimental to the overall electrochemical performance of the coin cell half-cells, especially at higher discharge rates in the rate study shown below.

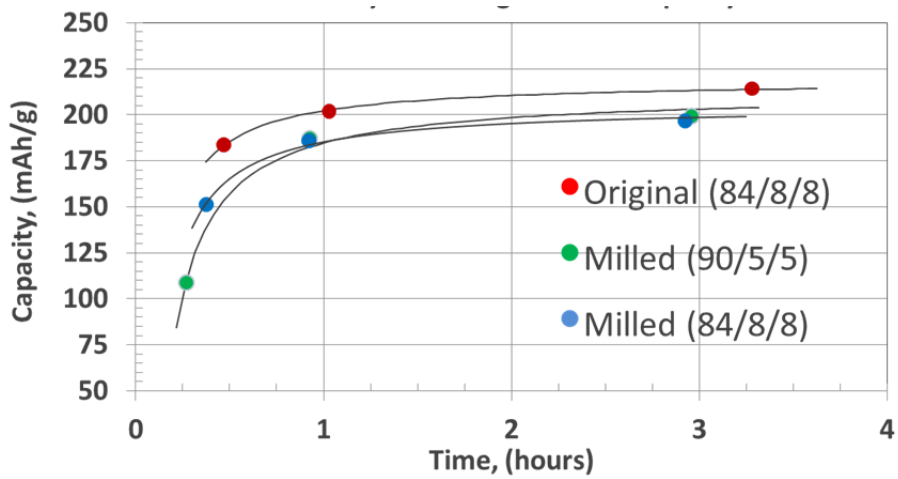

Figure 3. Discharge capacities for original (un-milled) and milled LMR-NMC powder from MERF versus lithium as a function of discharge time in 2032 coin cells. Voltage Window (2.0 - 4.6 V), charged and discharged at C/3 (11 mA/mg), 1C (33 mA/mg), and 2C (66 mA/mg) rates; 5 cycles at each rate. All electrodes were calendered to ~35% porosity.

Table 1. Rate data derived from Figure 3 for original and milled LMR-NMC powder from MERF.

Discharge Capacities	Original (84/8/8)			Milled (90/5/5)			Milled (84/8/8)		
C-rate	mAh	mAh/g	mAh/cm²	mAh	mAh/g	mAh/cm²	mAh	mAh/g	mAh/cm²
C/3	2.18	219	1.37	1.97	198	1.23	1.95	196	1.22
1C	2.06	207	1.29	1.85	186	1.16	1.84	185	1.15
2C	1.87	188	1.17	1.08	108	0.67	1.50	150	0.93

The original (un-milled) LMR-NMC powder in an electrode composition of (90/5/5) is still to be fabricated in order to complete the data set. Full cell testing vs. A12 graphite is also on queue for coin cell testing. Continued efforts by the CFF will be performed to evaluate future MERF cathode materials using pouch cells. The LMR-NMC powders will be made via carbonate and hydroxide processes.

(d) Summary of work in the past quarter related to milestone (d)

Several new materials are of interest to the CFF because requests have been made by various research groups for electrodes of these new materials as part of the Electrode Library service the CFF maintains. These electrodes will enable research in electrolyte development, additive development, silicon anode work, and modeling.

The following materials were received: $LiFePO_4$ powder from Hanwha, $LiCoO_2$ powder from BTR (Shenzhen, China), Hard Carbon powder (2 materials) from Kureha, 4 V Spinel powder from Toda, and an experimental high voltage cathode powder. Small electrode samples for all these materials have been fabricated and lithium half cells are

under test. Two additional graphite powders are on queue for materials validation process. These materials are M5 and G8 graphite powders produced by Phillips 66. A second batch of HE5050 powder from Toda (10 kg) along with NMC442 powder from Toda (5 kg) was ordered; these materials are yet to be delivered. Work on the hard carbon from Kureha and $LiFePO_4$ from Hanwha will be initiated next quarter.

<u>$LiCoO_2$ from BTR</u>

$LiCoO_2$ is one of the most used cathode materials in lithium ion batteries and serves as a valuable baseline for material researchers. An electrode was made with the $LiCoO_2$ from BTR (China), which was used as received. The electrode consisted of 94 wt.% $LiCoO_2$, 2 wt.% Super P-Li carbon black, and 4 wt.% PVDF binder. The punched electrode was fabricated into 2032 coin cells after calendaring with 1.2 M $LiPF_6$ in EC/EMC (3:7 by wt.) as the electrolyte. These lithium half cells were cycled between 4.1 V and 3.0 V at C/10 for three cycles. The voltage profile is shown in Figure 4. The reversible capacity after three cycles was 125 mAh/g with less than 10 % initial irreversible capacity loss during the 1st cycle.

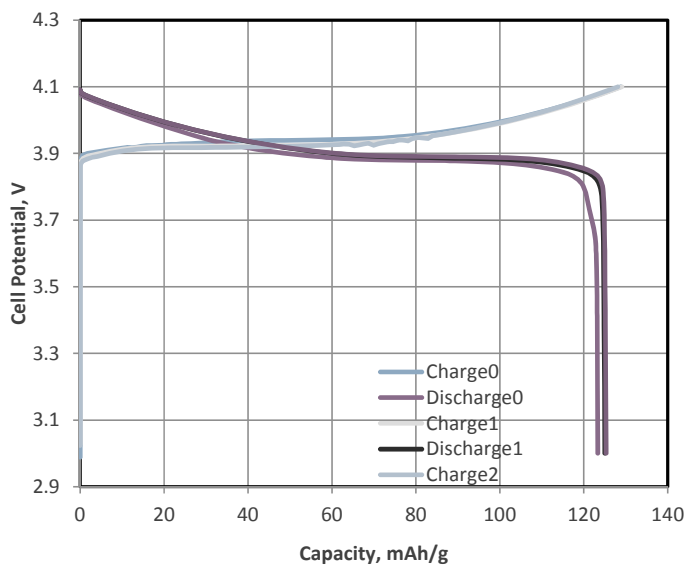

Figure 4. Voltage profile of Li/$LiCoO_2$ cell at C/10 rate.

After three formation cycles, the cells were subjected to a capacity rate study. These results are shown in Figure 5. It can be seen from the figure that this material can deliver over 110 mAh/g up to the 1C discharge rate. The cells were then cycled at a 0.3 C rate between 4.1 V and 3.0 V. More than 90% capacity retention was obtained after 50 cycles.

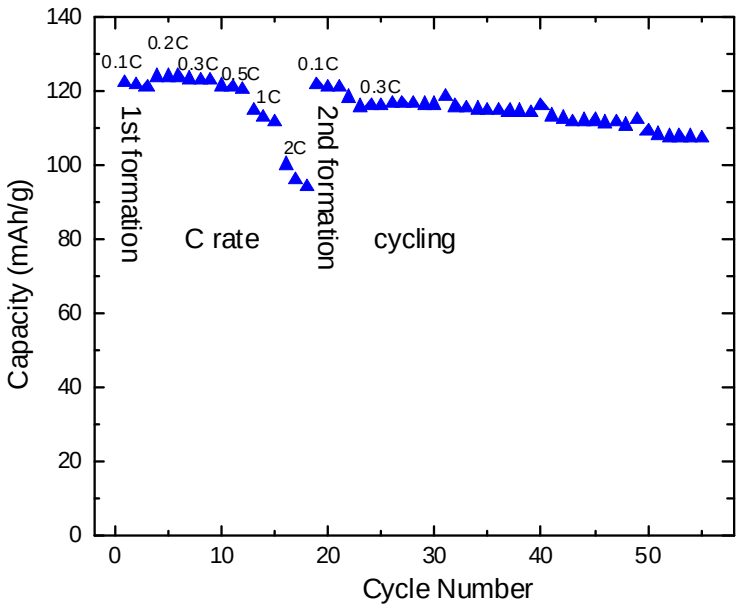

Figure 5. Rate study and cycling performance data for Li/$LiCoO_2$ half cell.

(e) Summary of work in the past quarter related to milestone (e)

Many of the silicon/graphite/binder systems that are being explored are aqueous based slurries. Initial coating trials of these systems were first performed using the standard bench top small scale coater. Several of the slurries and corresponding coatings that showed good adhesion, cohesion, and homogeneity were scaled up using the A-Pro coater in the CFF dry room. There has been initial success in coating Phillips 66 A12 graphite in an aqueous based binder slurry using the A-Pro coater. The aqueous system coated had the following components: 96 wt.% Phillips 66 A12 graphite, 2 wt.% Timcal C-45 carbon black, 1 wt.% CMC (MAC 350), and 1 wt.% SBR (Zeon X-3). A comparison of the aqueous CMC/SBR A12 electrode coin cell half-cell performance versus a PVDF/NMP-based A12 electrode (A-A002 from the CFF Electrode Library) coin cell half-cell performance is provided in Table 2. The CMC/SBR anode had a total coating loading of 4.6 mg/cm^2, coating thickness of 45 µm, and a porosity of 35.0 %. The PVDF Electrode Library anode had a total coating loading of 6.0 mg/cm^2, coating thickness of 53 µm, and a porosity of 38.8 %.

Table 2. Electrochemical performance of CMC/SBR aqueous-based graphite anode compared to PVDF/NMP-based graphite anode in initial characterization cycling tests.

CMC/SBR A12 Graphite Electrode		PVDF A12 Graphite Electrode	
Formation		Formation	
1st Cycle Lithiation Capacity	363 mAh/g of A12	1st Cycle Lithiation Capacity	345 mAh/g of A12
1st Cycle Delithiation Capacity	342 mAh/g of A12	1st Cycle Delithiation Capacity	339 mAh/g of A12
1st Cycle Efficiency	94%*	1st Cycle Efficiency	97%
Rate Study		Rate Study	
C/5	358 mAh/g	C/5	330 mAh/g
C/2	355 mAh/g	C/2	326 mAh/g
1C	348 mAh/g	1C	318 mAh/g
2C	330 mAh/g	2C	310 mAh/g
HPPC		HPPC	
ASI at 50% DOD	47	ASI at 50% DOD	49

* A possible wetting issue may be present

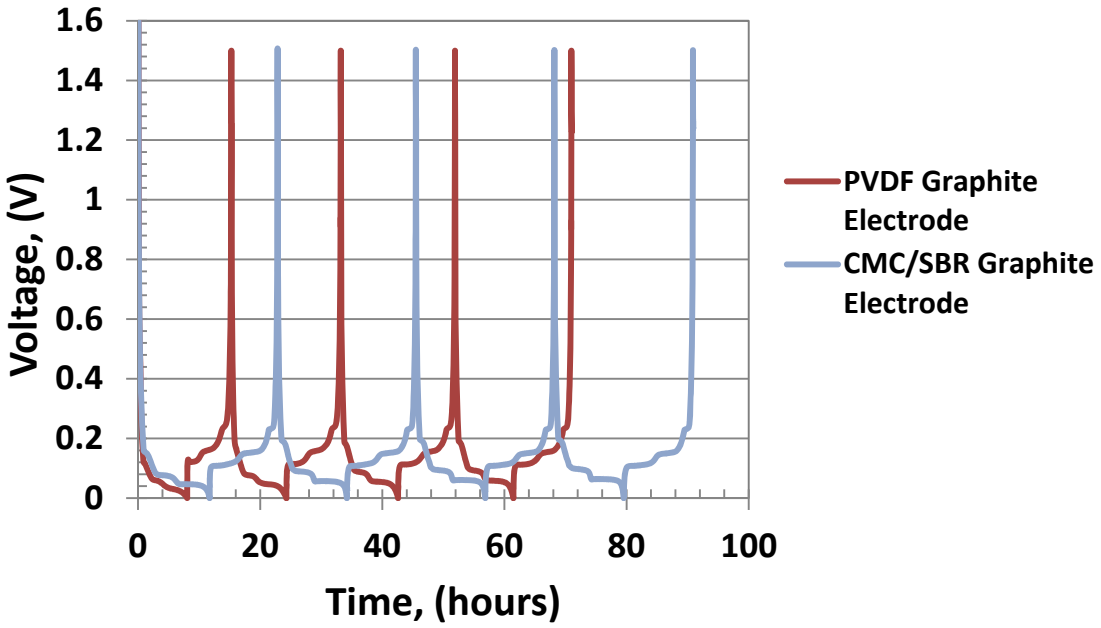

Figure 6. Voltage profile of the PVDF/NMP and the CMC/SBR/aqueous systems using Phillips 66 A12 graphite. The half-cell coin cells used the same procedure for the formation test (0.00V – 1.5 V, 4 cycles at a C/10 rate). The 1C testing value for the PVDF/NMP graphite cell is 0.34 mA/mg (of active material) and has a total active material mass of 8.81 mg. The 1C testing value for the CMC/SBR graphite cell is 0.35 mA/mg (of active material) and has a total active material mass of 7.07 mg.

The data above demonstrate the improved performance of the A12 graphite (no Si or SiO_x) when using the CMC-SBR aqueous binder system. The voltage profile (not normalized) highlights the high capacities achieved with less total active material mass

present in the CMC-SBR aqueous electrode compared to the PVDF/NMP electrode. As expected, the value of the corresponding voltage plateaus are relatively unchanged. The CMC/SBR slurry using A12 graphite shows positive initial results, and now more thorough diagnostic work is to be done to compare the PVDF system to the CMC/SBR system coatings.

The results of using CMC/SBR for aqueous slurry making, its initial application in the CFF using the A-Pro coater, the homogeneous coating quality, and the good initial electrochemical performance are all a positive step forward. The information gained will greatly aid in incorporating Si/SiO_x powders in the aqueous slurry system for coating and ultimately be implemented into pouch cell fabrication in the CFF.

(f) Summary of work in the past quarter related to milestone (f)

Anode: silicon electrode provided by LBNL (Dr. G. Liu)

Dr. Liu (LBNL) invented a conductive binder designed to improve the cyclability of silicon electrodes by tailoring the polymer with dual functionality: conducting electricity and binding closely to silicon particles as they undergo more than a 300 % volume change during the lithiation process. This conductive binder is referred to as PFFOBM. A silicon electrode with 33% PFFOBM was prepared by Dr. Liu and shipped to Argonne. Upon receipt, the electrode was vacuum dried and then assembled in coin cells with 1.2 M $LiPF_6$ in EC/EMC (3:7 by wt.) electrolyte plus 10 wt.% fluorinated ethylene carbonate (FEC). Three formation cycles were conducted on these lithium half cells at a C/10 rate between 1 V and 10 mV. After three formation cycles, the half cells underwent various lower cut-off voltages during cycling: 10 mV, 40 mV, and 200 mV. For the cell with the 200 mV cut-off voltage cycling, a capacity rate test was conducted before life cycling. The delithiation capacity for each cell is shown in Figure 7 (left) below.

All the cells show relatively good cycling performance, regardless of the cut-off voltage, compared to non-conductive binders (data not shown here). It can also be seen from this plot that the cell with the lowest cut-off voltage (10 mV) experienced the fastest capacity fade rate, which is expected due to the excessive volume expansion upon lithiation. When the higher cut-off voltage is used, less lithiation of the silicon particle occurs, leading to less stress and volume expansion in the silicon particle. This will in turn improve the cycle life. In Figure 7 (right), the coulombic efficiency is plotted as a function of cycle number. Another interesting cut-off voltage effect is observed: the coulombic efficiency increases continuously with cycling when 10 mV and 40 mV were used as cut-off voltages. However, the coulombic efficiency jumps up to almost 100 % when the cut-off voltage was changed to 200 mV. It is believed that the coulombic efficiency improvement is related to less stress of the solid electrolyte interface (SEI) at 200 mV. When a low cut-off voltage is used, the high stress as discussed above will pulverize the particle and expose the new surface for new SEI formation, resulting in low coulombic efficiency.

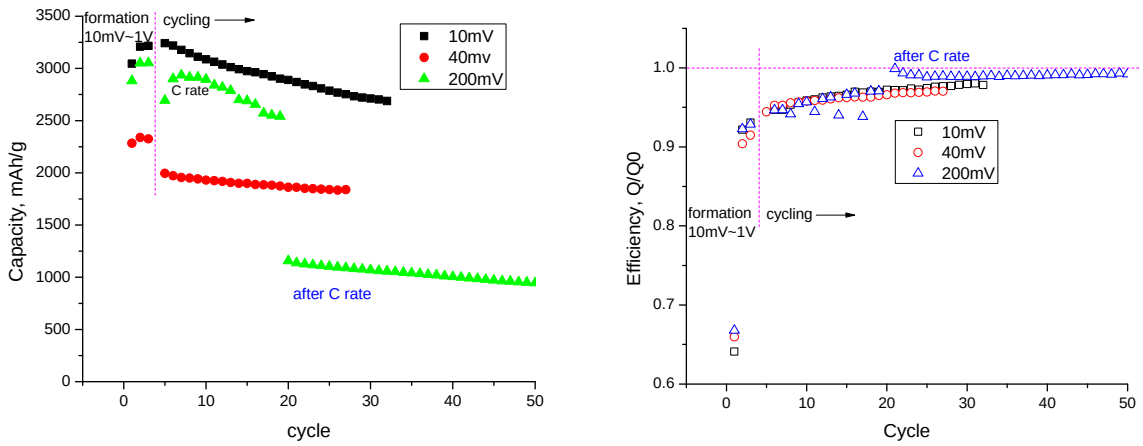

Figure 7. Cycling (left) and coulombic efficiency (right) of silicon electrode with PFFOBM conductive binder from LBNL.

Cathode: Investigation of the high energy density LMR-NMC material will continue.

Aqueous Binder: A12/HE5050 cell with all aqueous binder

In the past, investigations were conducted with an SBR-based aqueous binder (from JSR Micro) for graphite electrodes, and a fluorine acrylic (FA) hybrid latex binder (from JSR Micro) for LMR-NMC (such as Toda HE5050), respectively. Very good electrochemical performance was obtained for both cathodes and anodes in lithium half cells. In this quarter, full cells were made and tested of graphite/HE5050 in coin cells using SBR and FA as binders, respectively. The electrode composition for the graphite anode was 98 wt.% graphite (A12, Phillips 66), 1 wt.% sodium carboxymethyl cellulose (CMC, MAC350, Nippon Paper Chemicals) and 1 wt.% SBR binder. The cathode comprised 92 wt.% of HE5050, 5 wt.% of C-45 carbon black, 2 wt.% of CMC, and 1 wt.% of FA binder. The full cells were tested using established protocols from the Voltage Fade project: one cycle at 10 mA/g between 4.5 V and 2.0 V, followed by 20 mA/g with the same voltage window. The voltage profile is shown in Figure 8 below. There is roughly 85% capacity retention after 50 cycles, which is only slightly less than the full cell using PVDF binder. These results, combined with other favorable information from rate test and hybrid pulse power characterization tests (not shown here), highlight the possibility of designing novel battery systems with high energy, long cycle life, low cost, and environmentally benign.

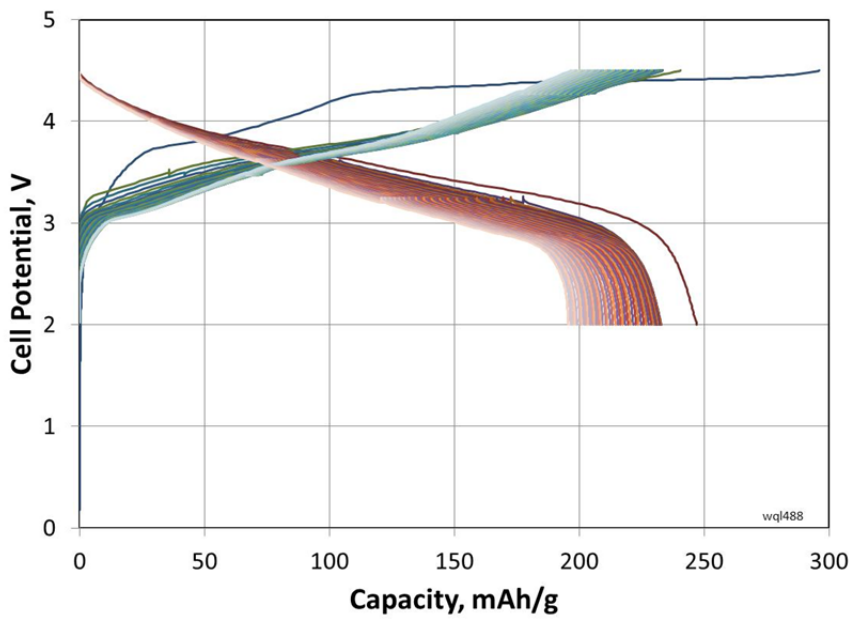

Figure 8. Voltage profile of graphite/LMR-NMC cell using aqueous binders from JSR Micro.

(g) Summary of work in the past quarter related to milestone (g)

The ABR-1 positive electrodes contain 86 wt.% $Li_{1.2}Mn_{0.55}Ni_{0.15}Co_{0.1}O_2$ (HE5050), 4 wt.% SFG-6 graphite (Timcal), 2 wt.% SuperP (Timcal) and 8 wt.% PVDF (Solvay 5130). The ABR-1 negative electrodes contain ~90 wt.% graphite (Phillips 66 A12), 6 wt.% PVDF (Kureha KF-9300) and 4 wt.% SuperP (Timcal). In previous reports it was shown that cell impedance rise is mainly governed by the positive electrode; impedance rise at the negative electrode is relatively small. In AC impedance data, the positive electrode impedance rise appears as an increase in the high-frequency arc width (electronic impedance) and in the mid-frequency arc width (ionic impedance). The following Secondary Ion Mass Spectrometry (SIMS) and Inductively Coupled Plasma–Mass Spectrometry (ICP-MS) data discuss the accumulation of transition metal elements at the graphite electrode during cycling.

Figure 9 shows SIMS sputter depth profiles for carbon, manganese, nickel, cobalt and lithium from negative electrodes harvested from cells that underwent the initial cycles (a), and the 1500 aging cycles (b). In Figure 9a, the carbon signal increases for the first 200 seconds of sputtering, and then reaches a steady state value. The lower carbon signal near the surface is consistent with a solid electrolyte interphase (SEI) that contains a lower carbon concentration than the bulk electrode. In Figure 9b, however, the carbon signal reaches a steady state value indicative of the bulk electrode only after ~8000 seconds of sputtering. The longer sputtering time indicates that the SEI is significantly thicker for the aged sample.

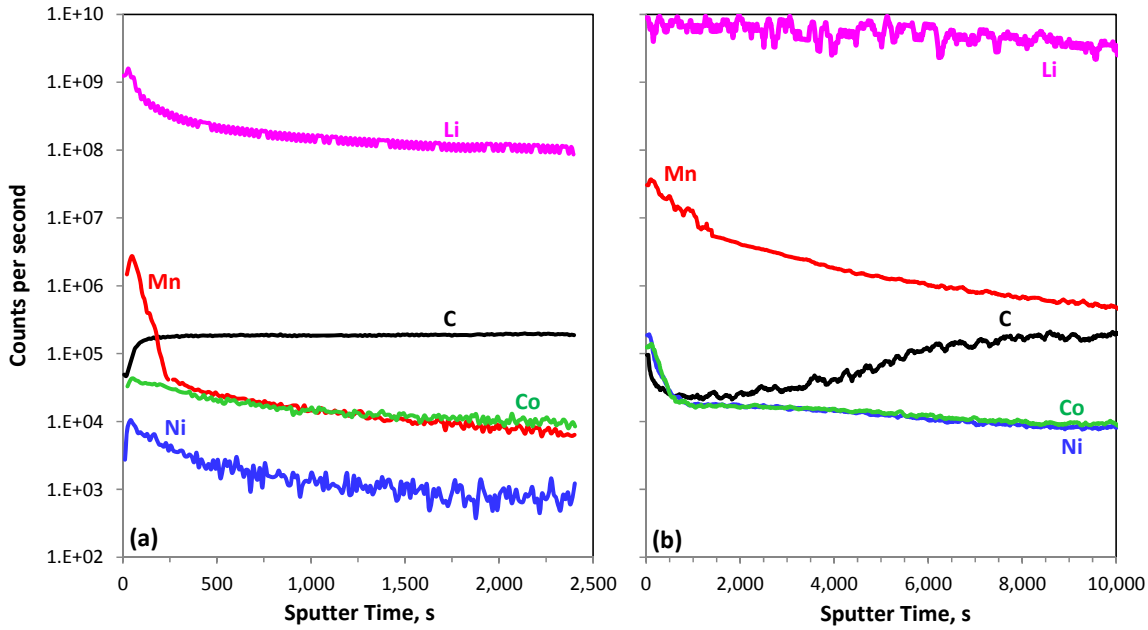

Figure 9. SIMS sputter depth profiles from negative electrodes after (a) Initial cycles, and (b) 1500 cycles. Data for carbon, manganese, nickel, cobalt and lithium are shown. The Y-axis scales are the same for (a) and (b), but the X-axis scales are different.

The Li signal during early sputtering mainly arises from lithium in the electrode SEI near the top surface. At longer sputtering times the signal also includes contributions from lithium remnants deeper inside the electrode. Figure 9 shows that the Li count rate (counts per second, cps) of the aged sample is more than an order of magnitude greater than that of the sample after characterization cycles. The data are consistent with lithium trapping in the negative electrode, especially in the SEI, and explain the significant deterioration of cell capacity that results from extended cycling.

In Figure 9a, the Mn, Ni and Co signals peak after ~50 s sputter time, then decrease relatively rapidly for Mn and more gradually for Ni and Co; the elements display quasi-steady state cps values after ~2000 s sputter time. In Figure 9b also, the Mn, Ni and Co signals peak after short sputter times and then decrease. However, the cps values measured after ~2000 s is more than an order of magnitude larger for Ni and more than two orders of magnitude larger for Mn. That is, the total Mn and Ni counts obtained by integration under the curves are significantly higher for the aged sample than for the sample after initial cycles.

The trends in the SIMS data are confirmed by Inductively Coupled Plasma–Mass Spectroscopy (ICP-MS) data obtained on the negative electrode coatings, which are scraped off the current collector. The measured data are an average of the element concentration contained in the samples, which comprises the graphite, SuperP, PVDF, electrolyte residue, and SEI components; the harvested electrodes were rinsed in DMC to minimize electrolyte residue while preserving the SEI. As expected only trace quantities of Li, Mn, Ni and Co data are measured in the fresh negative electrode, which serves as a

control sample. For the initial–cycle sample, the average Li, Mn, Ni and Co concentrations are 9683, 617, 125 and 63 □g/g-sample, respectively, with a measurement uncertainty of ± 10%.; the corresponding values for a 1500–cycle graphite electrode sample are 25936, 1446, 167 and 71 □g/g-sample, respectively. That is, the Li, Mn, Ni and Co content in the 1500–cycle graphite negative electrode are, on an average, 2.7, 2.3, 1.3 and 1.1 times greater than that in the initial–cycle electrode.

The transition metals at the negative electrode originate from the oxide in the positive electrode, and are an obvious example of metal-ion migration between the electrodes. A simple calculation shows that the Mn, Ni, and Co contents in the graphite electrode are 8.1, 0.9, and 0.4 □g/cm^2, respectively, which are several orders of magnitude smaller than the corresponding contents in the positive electrode. These data indicate that cell capacity loss arising from dissolution of these elements, from the positive electrode into the electrolyte, is negligibly small.

(h) Summary of work in the past quarter related to milestone (h)

The synergistic effects of $LiB(C_2O_4)_2$ (LiBOB), $LiF_2B(C_2O_4)$ (LiDFOB), triphenylamine (Ph_3N), and 1,4-benzodiozane-6,7-diol (BDOD) as functional electrolyte additives in our ABR-1 cells was examined (see Figure 10). The influence of these additives, individually, and in different combinations, was evaluated using galvanostatic cycling of cells containing $Li_{1.2}Ni_{0.15}Mn_{0.55}Co_{0.1}O_2$ ($0.5Li_2MnO_3 \bullet 0.5LiMn_{0.375}Ni_{0.375}Co_{0.25}O_2$)–based positive electrodes, graphite–based negative electrodes, and a $LiPF_6$–based electrolyte. Electrochemical impedance spectroscopy (EIS), linear sweep voltammetry (LSV), and voltage-hold tests were also used. The data showed that cell performance can be significantly improved by choosing additives that separately affect the positive and negative electrodes, thus circumventing the difficulty of finding *one* good bifunctional additive. In addition, the synergistic effects of electrolyte additive combinations can be beneficial to cell performance.

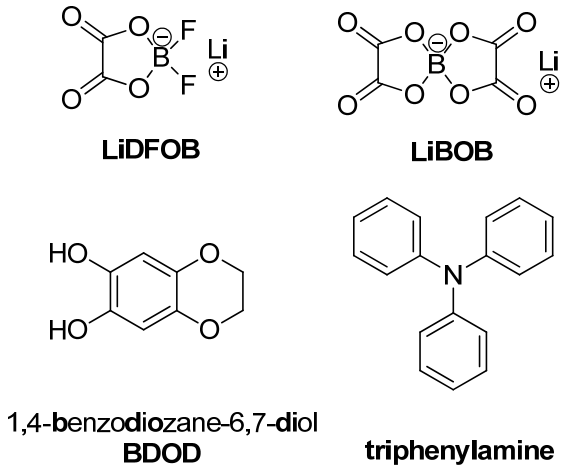

Figure 10. Chemical structures of additives used in this work

The following conclusions can be reached from these various tests:

1. All additive-bearing cells show certain performance improvements over cells containing the baseline electrolyte, both at 30° and 55°C.
2. Cells containing only the LiBOB additive show better capacity retention, but higher impedances, than those containing the structurally-similar LiDFOB additive.
3. The aromatic organic compounds Ph_3N and BDOD are oxidized at the positive electrode before the baseline electrolyte; these compounds are also effective at reducing electrolyte oxidation. However, when used individually, these additives do not reduce cell performance degradation on long-term cycling.
4. The addition of LiDFOB, Ph_3N, and BDOD to LiBOB-containing cells further improves capacity retention (see Figure 11) and lowers impedance rise on extended cycling. These additives may enhance the passivation characteristics of cathode surface films, reducing electrolyte oxidation and protecting the oxide surface.
5. The SEI films formed with additives examined in this study are not completely stable under the test conditions used. Even the best additive combination only slows down performance degradation and does not completely prevent it.

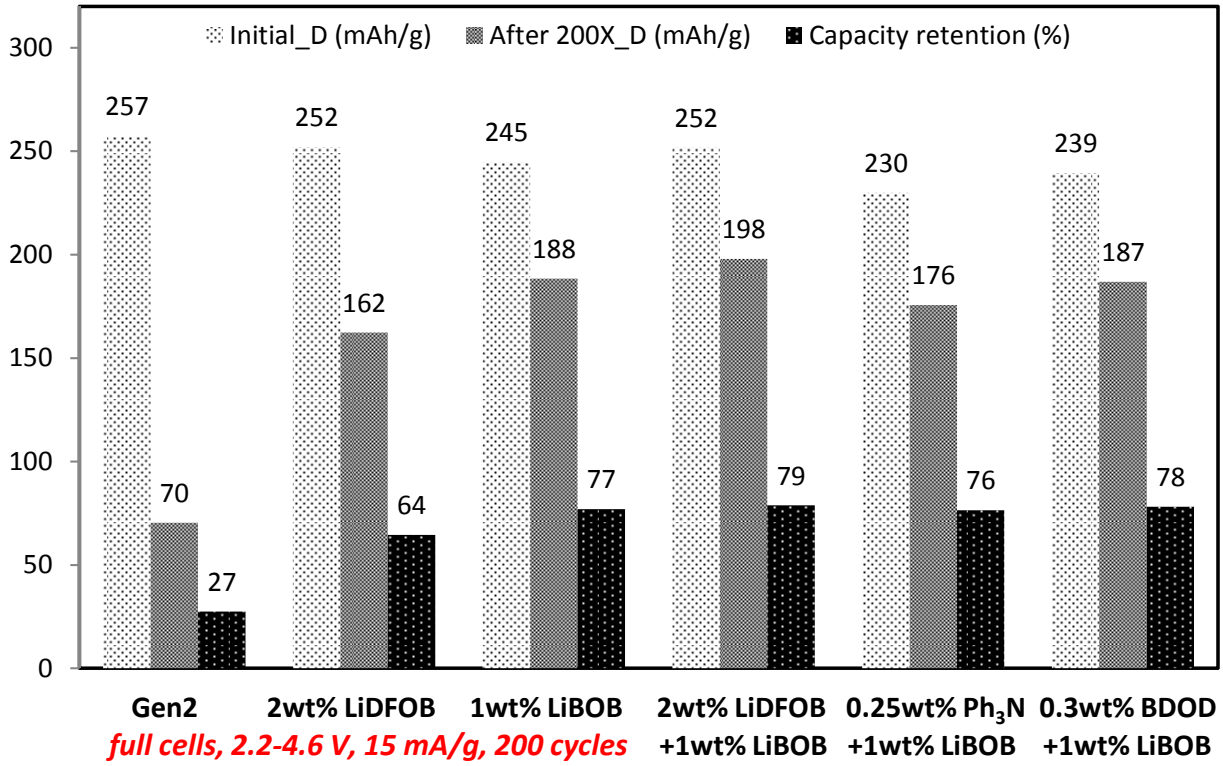

Figure 11. Capacity and capacity retention of full cells cycled at 30°C between 2.2 and 4.6 V at a 15 mA/g rate showing the effect of various additives in the Gen2 electrolyte. The capacity values (and cycling current) are based on the $Li_{1.2}Ni_{0.15}Mn_{0.55}Co_{0.1}O_2$ content in the positive electrode.

(i) Summary of work in the past quarter related to milestone (i)

After the public release of BatPaC v2.1 in the first quarter, available from www.cse.anl.gov/batpac, efforts this quarter have focused on examining and comparing the cost model to the work of Alan Goodrich from NREL on lithium ion battery manufacturing costs.

(j) Summary of work in the past quarter related to milestone (j)

The Electrochemical Impedance Spectroscopy (EIS) electrochemical cell model [1-3] was used to examine the impedance characteristics of the hysteresis between charge and discharge in LMR-NMC positive electrodes [4]. Diagnostic micro-reference electrode lab cell EIS studies were conducted on the baseline HE5050 LMR-NMC electrode at several states-of-charge (SOCs) during the charge and discharge half cycles. In general over the voltage range where the EIS studies were conducted (between 3.3 and 4.0 volts vs. lithium) within the same half-cycle, either charge or discharge, impedance increases as the SOC and electrode potential decreases. The discussion here will be focused on three EIS sweeps: two taken at 3.74 and 3.36 volts (vs. lithium) during the discharge half cycle and one at 3.74 volts during the charge half cycle. Because of the hysteresis between charge and discharge, the two 3.74 volt sweeps are taken at the same electrode potential, but differing SOCs. While the 3.36 volt discharge sweep and 3.74 volt charge sweep are taken at about the same SOC (i.e. same lithium content).

The EIS cell model was developed strictly for intercalation active materials. However, the hysteresis and other characteristics indicate that the LMR-NMC material is obviously more complex. It is applied here to obtain a "snapshot" of the electrode at each SOC. An electrochemical model is currently under development that accounts for the LMR-NMC's more complex behavior. Nevertheless, the SEI portion of the model will probably not change significantly and there is much that can be gained from this approach. The EIS data and electrochemical model fit for the LMR-NMC electrode at 3.74 volts is shown in Figure 12. The interfacial impedance for a lithium ion positive electrode typically consists of two circular arcs (i.e. a high-frequency arc and a mid-frequency arc) with a diffusional Warburg impedance tail at low frequencies.

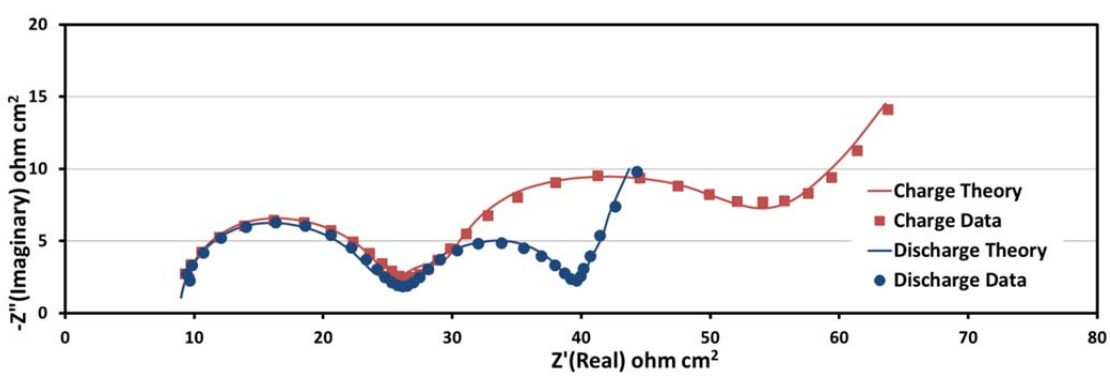

Figure 12. LMR-NMC electrode impedance (100 kHz -10 mHz) at 3.74 volts vs. lithium taken during the charge and discharge half cycles with a micro-reference electrode cell.

The initial EIS electrochemical modeling studies on the LMR-NMC electrodes are discussed in the FY2012 ABR annual report. The work focused on comparing the LMR-NMC electrode to earlier studies on other layered cathode materials and examining possible sources of aging effects. It highlighted the susceptibility of LMR-NMC cathodes to increases in the high frequency impedance owing to the lower overall bulk conductivity of the materials. This manifests in a high contact resistance between the particles and the conductive carbon additives that worsens with continued exposure to high potentials (i.e. electrolyte oxidation). Also included in the high frequency impedance arc are ion migration effects through the surface film on the active material. The lithium ion diffusion effects through the surface film can impact either or both the high and mid frequency arcs. These effects are generally less sensitive to the electrode potential and SOC.

The studies here focus on the changes in the mid-frequency arc and Warburg impedance. The mid frequency arc includes impedance effects from the electrochemical reaction (i.e. Butler Volmer kinetics) and lithium diffusion through active material surface layer. The Warburg impedance is dominated by solid-state diffusion in the oxide particles, but also includes electrolyte salt diffusion. Of all the parameters extracted from the EIS data, changes in the lithium diffusion coefficient (D_{sb}) of the bulk active material are most precisely followed. A general discussion of how the relative time constants for the various phenomena are determined was also discussed in the FY2012 ABR annual report. The size of the impedance for the Butler Volmer kinetics is determined by the exchange current density (i_o). The impact of lithium diffusion through the surface layer is governed by its diffusion coefficient (D_{si}) and the partition coefficient (K_s) for lithium between the bulk material and the surface layer. These parameters are given in Table 3 for the indicated electrode potential and half-cycle.

Table 3. Selected electrochemical model parameters for LMR-NMC electrode at indicated electrode potential and half-cycle.

Positive voltage vs. Li	Half-Cycle	D_{si}	D_{sb}	K_s	i_o
Volts		cm^2/s			mA/cm^2
3.36	Discharge	5.5E-13	2.0E-14	33.0	0.0055
3.74	Charge	6.0E-13	8.5E-14	10.0	0.015
3.74	Discharge	1.4E-12	1.7E-12	10.0	0.035

In general, as you go down the columns in Table 3 the parameters change in the direction of lowering the electrode impedance. Therefore, for the constant SOC data (i.e. first and second lines) the discharge impedance is greater than the charge impedance and the opposite is true for the constant voltage data (i.e. second and third lines), as seen in

Figure 12. How much of a trend this is over the full voltage range is yet to be determined. In Table 3 at an electrode potential of 3.74 volts, both i_o and D_{si} vary by about a factor of two between the charge and discharge half-cycles. Since it is implicitly assumed that both phenomena contribute about equally to the impedance, the changes account for the doubling of the size of the mid-frequency interfacial arc, as seen in Figure 12. Less obvious from examining Figure 12 is the change in the bulk lithium diffusion coefficient (D_{sb}) of the active material by about a factor of twenty, suggesting that the bulk material is significantly different between the charge and discharge half-cycles. An even greater change in the discharge D_{sb} is observed between 3.74 and 3.36 volts. While more studies over a wider voltage range need to be conducted, it is clear that both the interface and bulk LMR-NMC material is changing significantly within and between each half-cycle.

References

1. D. Dees, E. Gunen, D. Abraham, A. Jansen, and J. Prakash, *J. Electrochem. Soc.*, **152** (7) (2005) A1409.
2. D. Abraham, S. Kawauchi, and D. Dees, *Electrochim. Acta*, **53** (2008) 2121.
3. D. Dees, E. Gunen, D. Abraham, A. Jansen, and J. Prakash, *J. Electrochem. Soc.*, **155** (8) (2008) A603.
4. J. R. Croy, K. G. Gallagher, M. Balasubramanian, Z. Chen, Y. Ren, D. Kim, S.-H. Kang, D. W. Dees, and M. M. Thackeray, *Journal of Physical Chemistry C*, **accepted** (2013)

Publications, Reports, Intellectual property or patent application filed this quarter. (Please be rigorous, include internal reports--invention records, etc.)

"A Volume Averaged Approach to the Numerical Modeling of Phase-Transition Intercalation Electrodes Presented for Li_xC_6", by Kevin G. Gallagher, Dennis W. Dees, Andrew Jansen, Daniel Abraham, and Sun-Ho Kang, *Journal of The Electrochemical Society* **159**(12), A2029-A2037 (2012).

"Electrochemical Modeling the Impedance of a Lithium-Ion Positive Electrode Single Particle", by Dennis W. Dees, Kevin G. Gallagher, Daniel P. Abraham, and Andrew N. Jansen, *Journal of The Electrochemical Society* **160**(3), A478-A486 (2013).

"Positive Electrode Passivation by LiDFOB Electrolyte Additive in High-capacity Lithium-ion Cells", by Ye Zhu, Yan Li, Martin Bettge, and Daniel P. Abraham, *Journal of The Electrochemical Society* **159,** A2109-2117 (2012).

"Overcharge Effect on Morphology and Structure of Carbon Electrodes for Lithium-ion Batteries", Wenquan Lu, Carmen M. Lopez, Nathan Liu, John T. Vaughey, Andrew Jansen, and Dennis W. Dees, *Journal of The Electrochemical Society* **159**(5), A566-A570 (2012).

"Electrolyte Additive Combinations that Enhance Performance of $Li_{1.2}Ni_{0.15}Mn_{0.55}Co_{0.1}O_2$-Graphite Lithium-ion Cells" by Y. Zhu, Y. Li, M. Bettge, and D.P. Abraham, *Electrochimica Acta* in press; 10.1016/j.electacta.2013.03.102 (2013).

"Examining Hysteresis in Composite xLi_2MnO_3•$(1-x)LiMO_2$ Cathode Structures", by J. R. Croy, K. G. Gallagher, M. Balasubramanian, Z. Chen, Y. Ren, D. Kim, S.-H. Kang, D. W. Dees, and M. M. Thackeray, *Journal of Physical Chemistry C* **117**, 6525−6536 (2013).

"Structure Evolution of $Li_{1-x}VPO_4F$ Studied by In situ Synchrotron Probes", by Ying Piao, Yan Qin, Chengjun Sun, Yang Ren, Steve M. Heald, Dehua Zhou, Bryant J. Polzin, Steve E. Trask, Khalil Amine, Yinjin Wei, Gang Chen, Ira Bloom, and Zonghai Chen, under review by *Energy & Environmental Science*.

"Understanding Long-Term Cycling Performance of $Li_{1.2}Ni_{0.15}Mn_{0.55}Co_{0.1}O_2$ – Graphite Lithium-Ion Cells", by Y. Li, M. Bettge, B. Polzin, Y. Zhu, M. Balasubramanian and D.P. Abraham, *Journal of The Electrochemical Society* **160**(5), A3006-A3019 (2013).

TASK 2
Calendar & Cycle Life Studies

Project Numbers: 1.1.1 and 2.4 (ES033)

Project Title: Strategies to Enable the Use of High-Voltage Cathodes (1.1.1) and Diagnostic Evaluation of ABRT Program Lithium Battery Chemistries (2.4)

Project PI, Institution: Robert Kostecki, Lawrence Berkeley National Laboratory

Collaborators (include industry): None

Project Start/End Dates: LBNL carried out diagnostics in the ATD Program since its 1999 inception, and the ABRT Program began October 2008

Objectives: Task 1.1.1: To enable increased energy density by addressing the impact of high-voltage cathodes on the conducting carbon matrix. Task 2.4: (i) Determine the key factors that contribute to the degradation mechanism in the PHEV test cells and individual cell components. (ii) Characterize SEI formation on model electrode surfaces to improve understanding of key interfacial phenomena in PHEV cells.

Approach: Task 1.1.1**:** (i) determine the mechanisms for carbon damage and retreat at high potentials. (ii) Investigate mitigating treatments, additives, and procedures. Task 2.4: Use in situ and ex situ advanced spectroscopic and microscopic techniques in conjunction with standard electrochemical methods to characterize components harvested from fresh and tested PHEV cells, model thin-film cells, and special cells used to evaluate SEI formation processes.

Milestones: (i) Determine degradation mechanism in high-voltage cathodes (August 2013), (ii) synthesize a new type of CB with improved interfacial properties (September 2013), (iii) attend review meetings and present diagnostic results obtained in collaboration with ABRT Program participants.

Financial data: FY 2013 funding $600K

PROGRESS TOWARD MILESTONES

The scope of our work in the second quarter included: (i) determination of chemical cross-talk in lithium-ion battery cells using fluorescence spectroscopy and imaging, (ii) further examination of the effect of the oxidative heat treatment of carbon black additives and its positive influence on the electrochemical performance of composite high-voltage cathodes.

To investigate the mechanism of chemical cross talk in high-energy lithium-ion cells, a novel spectro-electrochemical cell was designed and constructed. The ABR baseline cell chemistry i.e., Toda He5050 Li-rich layered NCMO cathode, CPG A12 graphite anode

and EC:DEC 1:2 1M $LIPF_6$ electrolyte was reproduced in a full cell setup. The composite electrodes provided by ANL were used and the cell was cycled galvanostatically following the ABR program protocols. The charge cut-off voltage was set at 4.55 V, whereas the discharge cut-off cell voltage was 2.8 V. Figure 1 shows the voltage profile of the cell versus time (plotted in blue on the right side), and the corresponding fluorescence intensity across the electrolyte gap between the electrodes (middle image). The x-axis of the image represents the distance between cathode and anode whereas the y-axis shows time. The color of each pixel corresponds to the integrated intensity of the fluorescence spectra at this spot (1 micrometer dia) at the particular time and cell state of charge (see legend on the left side).

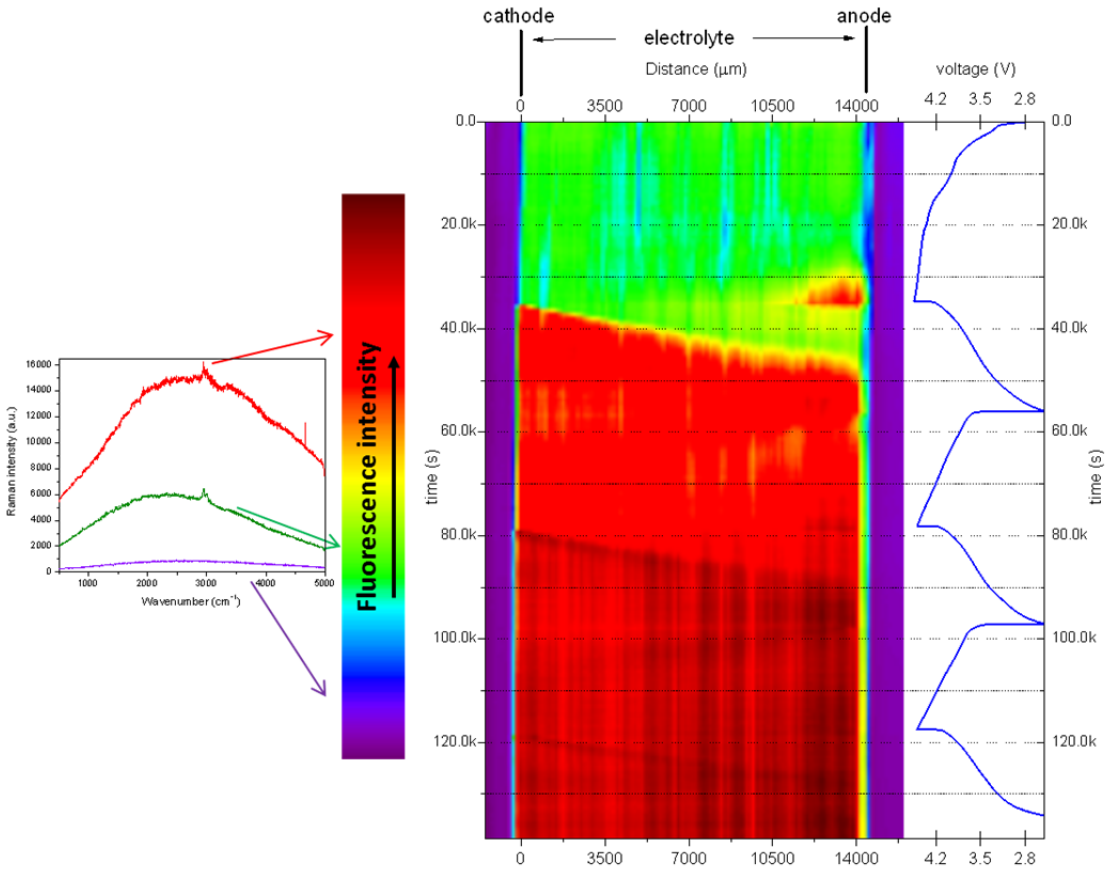

Figure 1. Cross-talk visualization by the means of fluorescence spectroscopy (distance between anode and cathode 14 mm, electrolyte EC:DEC 1:2 1M $LIPF_6$) and corresponding voltage profile for the A12-He5050 full cell cycled galvanostatically between 4.55 and 2.5 V vs. Li/Li^+)

At the end of the first charge, the graphitic anode releases fluorescent species into the electrolyte, which slowly migrate into the electrolyte toward the cathode. Interestingly, no photoluminescence active species were released from the He5050 cathode during the phase transformation. However, upon reversing the current from the beginning of the cell

discharge, the composite cathode starts releasing fluorescent species into the electrolyte, which migrate across the electrolyte gap in the opposite direction of the lithium ions and reach the anode before the end of the first discharge. These species are most likely consumed by interfacial reactions at the anode because no accumulation effect is visible in the following cycles.

A similar process was observed on the $LiNi_{0.5}Mn_{1.5}O_4$ cathode, where some fluorescent species generated by oxidation of the electrolyte precipitated at the surface of the electrode and some dissolved and diffused away into the electrolyte. Further investigations need to determine the composition and origins of these soluble fluorescent species and assess their effect on the composition and stability of the SEI and Li^+ interacalation/deintercalation in graphite.

Other on-going work included efforts to better understand the beneficial effect of carbon dioxide heat treatment of carbon black additives on the electrochemical performance of composite high-voltage cathodes. In addition to the ABR baseline material (Toda He5050, $Li_{1.2}Ni_{0.15}Co_{0.10}Mn_{0.55}O_2$ ($0.5\ Li_2MnO_3$ – $0.5\ LiNi_{0.375}Co_{0.25}Mn_{0.375}O_2$), composite electrodes with $LiNi_{0.33}Co_{0.33}Mn_{0.33}O_2$ (Umicore) as active material were prepared by the group of Vince Battaglia, LBNL. Cells utilizing these electrodes are currently undergoing long-term cycling tests.

TASK 2
Calendar & Cycle Life Studies

Project Number: 1.1, 2.4, and 3.3 (ES034)

Project Title: Life and abuse tolerance diagnostic studies and new electrolytes development for high energy density PHEV batteries

Task 1.1: Develop/Engineer PHEV Electrode Materials, Electrolytes, & Additives
Task 2.4: Life Diagnostics
Task 3.3: Abuse Behavior Modeling and Diagnostics

PI, Institution: Xiao-Qing Yang and Kyung-Wan Nam, Brookhaven National Laboratory

Barrier: Calendar and cycling life, Abuse tolerance

Project Start/End Dates: October 2012 / September 2013

Objects: The primary objectives of the efforts at BNL are: to determine the contributions of electrode structural changes, interfacial phenomena, and electrolyte decomposition to lithium-ion cell capacity and power decline, and abuse tolerance; to develop new diagnostic techniques (in situ and ex situ) for lithium-ion batteries; to collaborate with other ABR teams and the battery developers to understand the technical barriers, especially the voltage fading mechanism of high energy density Li and Mn rich NCM cathode materials during cycling; to explore new approaches to improve the abuse tolerance. The other objective is to design, synthesize and characterize new electrolyte for PHEV oriented lithium-ion batteries with better performance and safety characteristics. Special attention will be given to the new electrolytes for high voltage cathode materials.

Approach: Our approach is to use a combination of *in situ, ex situ* and time-resolved synchrotron based x-ray techniques to characterize electrode materials and electrodes taken from baseline ABR Program cells. *Ex situ* soft X-ray absorption spectroscopy (XAS) will be used to distinguish the structural differences between surface and bulk of electrodes using both electron yield (EY) and fluorescence yield (FY) detectors. Time-resolved X-ray diffraction (TR-XRD) technique will also be used to understand the reactions that occur in charged cathodes at elevated temperatures in the presence of electrolyte. In situ x-ray diffraction will be used to monitor the structural changes of the electrode materials during charge-discharge cycling at different conditions. A combination of TR-XRD, in situ soft and hard X-ray absorption (XAS), in situ transmission electron microscopy (TEM) techniques during heating will be applied to study the thermal stability of the electrode materials. These approaches developed at BNL will be utilized to study various cathode-anode chemistry pair systems of ABR projects through extended collaboration with other ABR members, such as Dr. Khalil Amine, Dr. Daniel Abraham, Dr. Chris Johnson, and Dr. Zhengcheng Zhang at ANL. We

will continue to develop new synchrotron based x-ray techniques such as combined in situ x-ray diffraction and mass spectroscopy during heating for the thermal stability of cathode material studies. We will continue to develop TEM based in situ diagnostic tools to study the structural changes at both surface and bulk of the electrode particles with high spatial resolution.

Milestones:

(a) By April 2013, complete the studies of thermal decomposition of charged $Li_{1.2}Ni_{0.15}Mno_{0.55}Co_{0.1}O_2$ (Toda HE5050) cathode materials during heating using combined Time-Resolved XRD and Mass Spectroscopy, **Completed.** (b) By April 2013, complete the ex situ soft x-ray XAS studies of $Li_{1.2}Ni_{0.15}Mno_{0.55}Co_{0.1}O_2$ (Toda HE5050) cathode material during charge-discharge cycling to distinguish the structural change differences between the surface and the bulk, **Completed.** (c) By September 2013, complete the in situ hard x-ray XAS studies of $Li_{1.2}Ni_{0.15}Mno_{0.55}Co_{0.1}O_2$ (Toda HE5050) cathode material for the voltage fading mechanism and structural instability during extended cycling, **on schedule.** (d) By September 2013, complete the studies of thermal decomposition of charged $Li_{1.2}Ni_{0.17}Mno_{0.53}Co_{0.1}O_2$ (ANL-HE) cathode materials with and without AlF_3 coating during heating using combined Time-Resolved XRD and Mass, **on schedule.**

Progress toward milestones for the second quarter of FY2013:

Summary of work in the past quarter related to milestone (a)

In the second quarter of FY2013, the mile stones (a) and (b) have been completed. Using ex situ soft x-ray absorption spectroscopy (XAS), the structural change differences between the surface and the bulk of $Li_{1.2}Ni_{0.15}Mno_{0.55}Co_{0.1}O_2$ (Toda HE5050) cathode material after multiple charge-discharge cycling were studied. Soft-XAS measurements were carried out at beamline U7A of the National Synchrotron Light Source (NSLS). The beam size was 1 mm in diameter. The estimated incident X-ray energy resolution was ~ 0.2 eV. Data were obtained in partial electron yield detection (PEY, surface probing) and fluorescence yield detection (FY, bulk probing) simultaneously. Figure 1 shows the O K-edge XAS of $Li_{1.2}Ni_{0.15}Mno_{0.55}Co_{0.1}O_2$ (Toda HE5050) cathode material after multiple charge-discharge cycling obtained from PEY method and FY method. The pre-edge peaks below ~ 534 eV of these spectra correspond to the transition of oxygen 1s electron to the hybridized state of transition metal 3d and oxygen 2p orbitals, whereas the broad higher peaks above ~ 534 eV correspond to the transitions to hybridized states of oxygen 2p and transition metal 4sp orbitals. O K-edge XAS spectra of PEY show two distinct peak features in the pre-edge region. The one at ~ 532.2 eV corresponds to hybridized state of Ni^{2+} 3d – O 2p orbitals and the other at ~ 528.8 eV is ascribed to hybridization of higher oxidation state, $M^{3+, 4+}$ 3d – O 2p orbitals (M=Ni, co, and Mn). As the cycling number increased, the intensity of 532.2 eV peak increases in the expense of the intensity of 528.8 eV peak, indicating the growing amount of rock-salt structured Ni-O type phase at the surface created by cycling. The O K-edge XAS spectra of FY exhibit similar trend as that in PEY data, but never reached the stage where the 532.2 eV peak become the dominating one over the 528.8 eV peak as seen after 130 cycles in PEY.

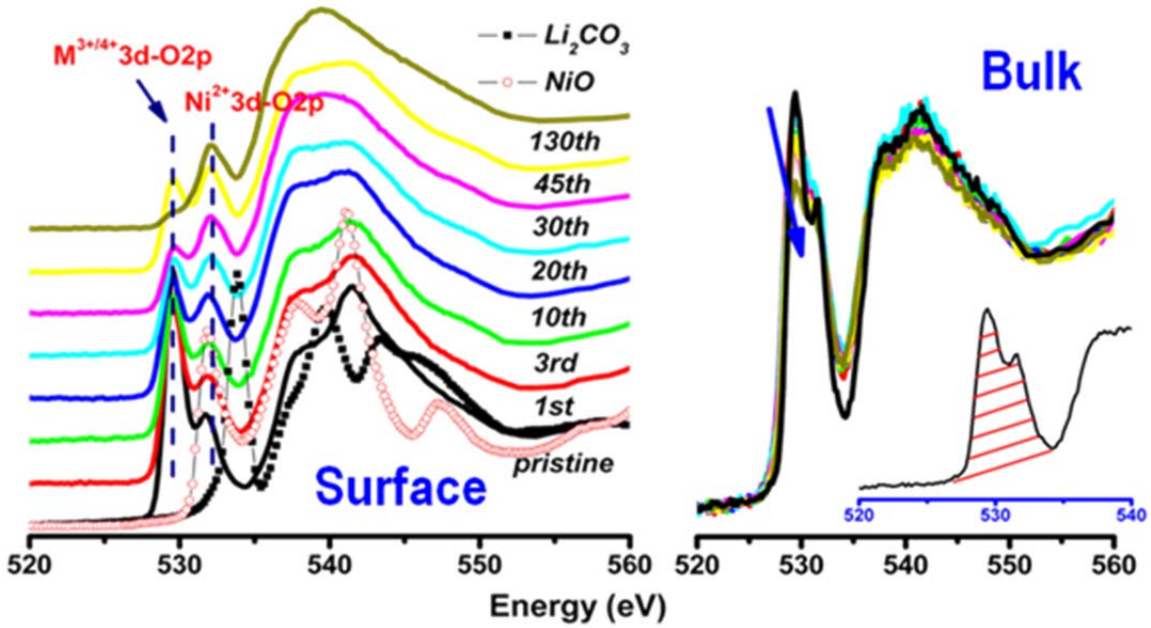

Fig. 1. Normalized O K-edge soft XAS spectra of $Li_{1.2}Ni_{0.15}Mno_{0.55}Co_{0.1}O_2$ (Toda HE5050) cathode material after multiple charge-discharge cycling using (a) partial electron yield detection (PEY, surface probing) and (b) fluorescence yield detection (FY, bulk probing) method.

TASK 2
Calendar & Cycle Life Studies

Project Number: CSP Project 18502, CSP Agreement 23060, ORNL FWP CEVT110 (ES165)

Project Title: Roll-to-Roll Electrode Processing NDE and Materials Characterization for Advanced Lithium Secondary Batteries

Project PI, Institution: David Wood, Oak Ridge National Laboratory

Collaborators:

- **Equipment Suppliers: Ceres Technologies, Keyence, FLIR**
- **Battery Manufacturers: Dow Kokam, A123 Systems**
- **Materials Suppliers: TODA America**
- **National Laboratories: Argonne National Laboratory, National Renewable Energy Laboratory**

Project Start/End Dates: 10/1/11 to 9/30/14

Objectives: Due to high scrap rates of 10-20% or more associated with lithium secondary cell production, new methods of quality control (QC) must be implemented. Often flaws in the electrodes are not detected until the formation cycling when the entire series of manufacturing steps has been completed, and the associated scrap rates drive the costs of lithium secondary cells to an unacceptable level. If electrode flaws and contaminants could be detected in line near the particular processing steps that generate them, then the electrode material could be marked as unusable and the processing equipment could be adjusted to eliminate the defects more quickly. ORNL is considering in line analysis methods such as X-ray fluorescence spectroscopy (XRF) for electrode component uniformity and metal particle detection and laser thickness sensing of the electrode wet thickness measurement. In addition, on-line laser thickness measurement and IR imaging of wet and dry electrode coatings are being implemented for thickness uniformity and coating flaw detection. These methods have been effectively utilized in other industries such as photovoltaic, flexible electronics, and semiconductor manufacturing, but the equipment and measurement methods must still be tailored for lithium secondary cell production. The object of this project is to raise the production yield of lithium secondary battery electrodes from 80- 90% to 99% and reduce the associated system cost by implementing in line XRF and laser thickness control. In addition, ORNL is providing its diagnostics capabilities and expertise to address materials issues with ABR cathode materials.

Approach: Ceres Technologies has been identified as a top manufacturer of in line XRF instruments for roll-to-roll applications and has a great deal of experience with the photovoltaics industry. ORNL will work closely with them to establish this technology for the lithium secondary battery industry by producing tape casted and slot-die coated electrode rolls (anodes and cathodes) with deliberately introduced flaws to test the

appropriateness of the method and the equipment modifications to the standard model. All key process parameters, such as line speed, coating thickness range, metal particle density, elemental homogeneity, etc., will be examined. In-line XRF data will also be correlated with ex-situ XCT data to gain a complete chemical and structural picture of the electrode as it is coated and dried.

Keyence has been selected as the partner for developing a set of laser thickness sensors for lithium secondary battery electrode production. ORNL has purchased sensors with point scanning capability from Keyence and integrated them directly into the slot-die coating line for the proof-of-concept experiments. The next step is to implement sensors with the capability of scanning multiple points or a full line scan across the web.

The output data from the wet layer thickness measurements using the laser sensors will be used to mark regions that are out of specification during the coating process. The coated electrode rolls with markings will be fed into the in line XRF equipment to determine if wet regions out of specification match with dry regions that are determined to be out of specification. Ultimately a feedback mechanism will be designed that considers whether the wet or dry thickness is a better input for adjusting the dispersion flow rate into the slot-die coater. The IR imaging QC will be correlated with thickness variation data to determine any further systematic flaw formation mechanisms such as pinholes, divots, and large agglomerates.

ORNL characterization capabilities and offline diagnostics consisting of acoustic emission detection, in-situ and ex-situ X-ray diffraction, neutron scattering, magnetic property determination, and high-resolution microscopy will be utilized to investigate cathode materials issues with ABR developed materials (specifically TODA HE5050).

FY13 Milestones:

1) Determine feasibility of measurement of deliberately introduced metal contaminants into cathodes with in-line XRF using ORNL tape caster line (January 2013 – delayed to July 2013).
2) Correlation of wet and dry thickness using laser line-scan thickness measurement (wet thickness) and in line XRF (dry thickness) to within ±10% (July 2013).
3) Ceres Technologies to complete final design of in-line XRF system for secondary lithium battery electrode production (July 2013).
4) Transfer technology associated with each of the three techniques (in-line laser thickness, XRF, and IR imaging) to industry partner (TBD) pilot/production line (September 2013).

Financial data: $300k/year (FY12-FY13)

PROGRESS TOWARD MILESTONES
Summary of work in the past quarter related to milestones (2) and (3)

1. **Adapting fiber optic sensor to measure the wet electrode thickness across the electrode width.**

The laser caliper system was successfully mounted on the slot-die coater and the wet thickness from the cathode and anode coating were monitored (previous quarterly report). However, in order to acquire the thickness of an entire area of wet electrode while coating, a triangular scan is necessary. The "gold standard" in industrial web-coating thickness measurements may be the use of a laser caliper constructed of two laser triangulation sensors. These systems are inherently tolerant of significant fluctuations in the position of the web because the thickness measurement involves mathematical processing of two position measurements obtained from sensors that are capable of operating effectively over a wide range of standoff distances. Unfortunately, the hardware for these systems is quite expensive. Moreover, the two sensors in the caliper system must be precisely aligned to each other to ensure accurate web thickness measurement. This makes it difficult to move the sensors from place to place on the web, as each position would require precision realignment. To facilitate coating thickness measurements across a wide coating area, a secondary, fiber-optic sensor was employed. This sensor was positioned relative to a roller that the electrode web foil must pass over prior to being measured by the laser caliper (see Figure 1). Thus the sensor measures a thickness relative to the position of the roller. Several associated errors must be taken into account with this method; but it allows high-resolution thickness measurements to be obtained at virtually any position on the coated electrode surface using a sensor that is an order of magnitude cheaper to employ than a laser caliper. The fiber-optic displacement probe uses a combination of emitter and detector fibers to measure the distance to a surface based on the amount of reflected light received by the receiver fibers. Since our electrode coatings are black and wet, it is anticipated that the reflectivity will be low and may be variable. Consequently, we have elected to use a reflectance-compensated fiber-optic displacement sensor (Philtec muDMS-RC25). To facilitate translational movement across the coated electrode surface, a high-precision ball-bearing translation stage and associated rail was mounted in the slot-die coating system (Figure 1). A mounting structure was designed to hold the optical sensor directly over the apex of the roller, which was employed as the reference measurement surface. The sensor itself has submicron resolution, but the alignment of the rail to the roller axis is known to have an angular displacement, and the roller itself is known to be eccentric by a few microns. Both of those errors were characterized as the measurement system was being implemented. The proposed measurement methodology that is being developed will be to first place the fiber-optic displacement probe in position so that it measures the same electrode section as the laser caliper. This will allow the fiber-optic sensor to be calibrated to the higher-precision laser caliper. After that, the sensor can be moved to other positions along the electrode surface and corrected for the measured angular error between the precision translation rail and the roller axis. The roller eccentricity will be compensated for by acquiring data over one full roller rotation for a given location. Averaging data over one full rotation of the roller will eliminate the eccentricity error.

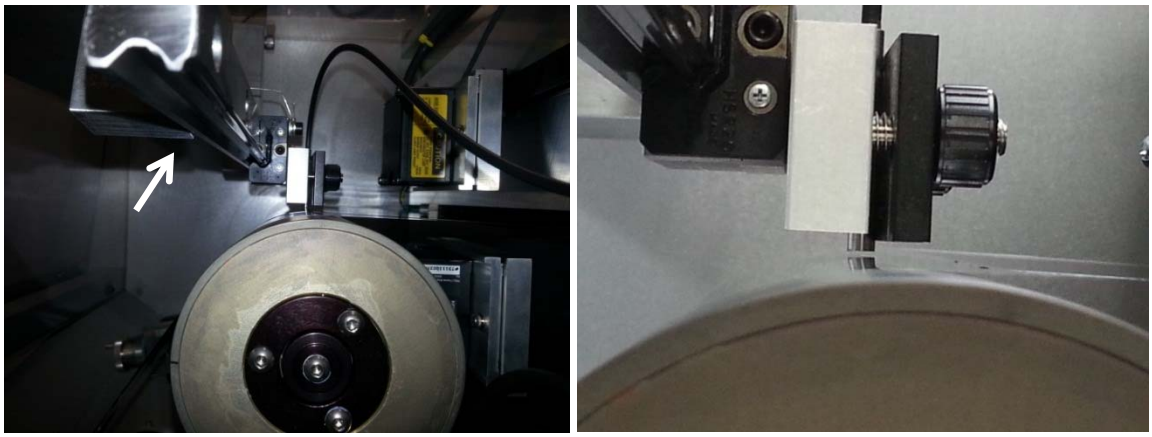

Figure 1. Set-up of fiber optic probe sensor on the slot-die coater to measure the thickness. This sensor is mounted on a rail (designated by arrow) where it can be moved from one position to another.

In Figure 2, the initial data acquired by fiber optic probe sensor is shown. This data was calculated at a fixed point for one full rotation of the roller; then the sensor was moved to different positions, acquiring data for a full rotation of the roller at each of seven positions. In the next step, data from each rotation was averaged to get the thickness of the coating for a full roller rotation.

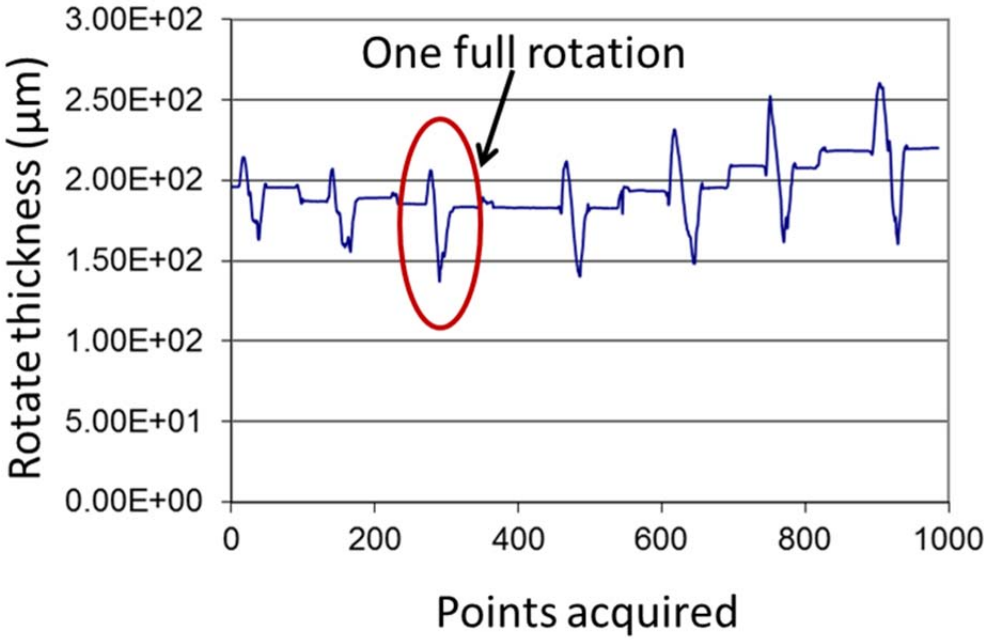

Figure 2. Wet thickness data across the electrode web acquired from fiber optic sensor (one full roller rotation at each web width position).

2. XRF with Ceres Technologies to measure cathode transition metal uniformity and electrode coating areal weight uniformity.

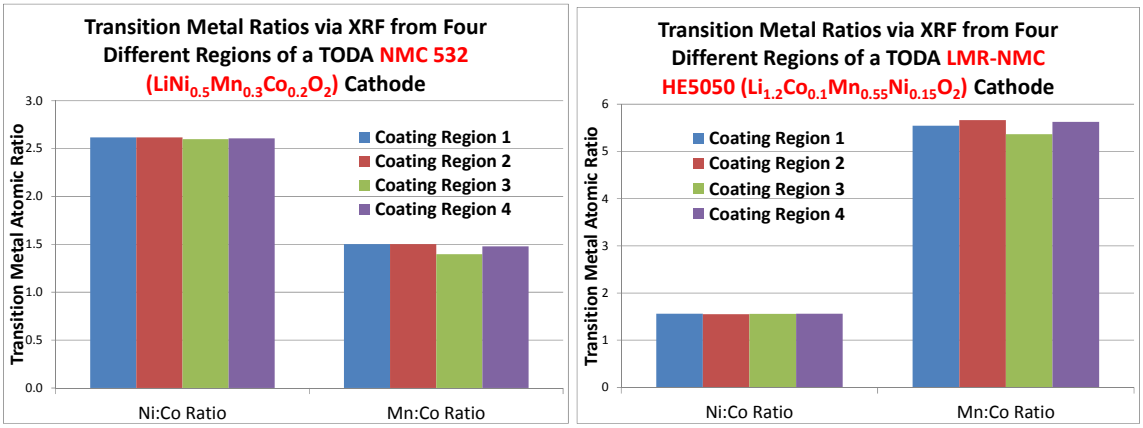

Figure 3. Transition metal ratios for two different NMC cathodes (traditional NMC left and LMR-NMC right) taken *off-line* at different regions of the coating width.

ORNL has contributed to designing an in-line XRF measurement system with Ceres Technologies specifically designed for lithium ion battery cathode coatings. The instrument was used to monitor the transition metal (TM) ion composition at different coating positions (regions 1-4) for two different cathode types, a traditional NMC coating and a LMR-NMC coating. In Figure 3 (left), we show the Mn to Co ratio and Ni to Co ratio for a TODA NMC 532 cathode which was found to be ~2.5 and 1.5 respectively. These results demonstrate excellent compositional uniformity across the electrode coating. The same compositional analysis was also completed on a LMR-NMC cathode (TODA HE5050), and the ratios between Mn to Co and Ni to Co in four different regions were found to be the nominal values of 1.5 and 5.5, respectively.

3. Characterization of TODA HE5050 by neutron diffraction for understanding of the voltage fade problem.

Additionally, we are implementing ORNL's advanced characterization capabilities to understand the voltage fading phenomenon in the TODA HE5050 cathode. In previous quarterly reports we have presented *in situ* XRD, magnetic susceptibility and advanced TEM characterization on this active material. In this report, we will discuss some of our recent results on neutron diffraction analysis. We have implemented the neutron powder diffraction (NPD) technique to obtain a deeper understanding on phase transformation mechanism leading to voltage fade in TODA HE5050 ($Li_{1.2}Co_{0.1}Mn_{0.55}Ni_{0.1}5O_2$). Full pouch cells of dimension 84.4 mm × 56.0 mm were assembled at the ORNL Battery Manufacturing Facility (BMF). HE5050 (electrode areal loading ~ 10 mg/cm^2) was paired with a ConocoPhillips A12 graphite anode. All cells underwent a formation cycling procedure, and were then cycled between 2.5 V and 4.7 V at 20mA/g (voltage profile results are shown in Figure 4).

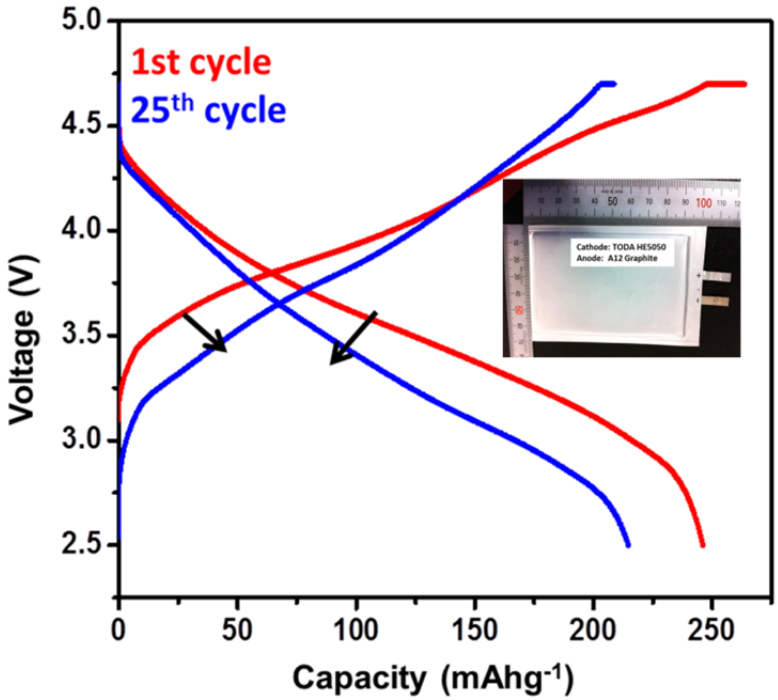

Figure 4. Charge-discharge voltage profiles during first and 25th cycles showing significant voltage fade (denoted by arrows). The *inset* shows the pouch cell made at the ORNL BMF.

The pouch cell cycling was stopped at different states of charge after two and 25 cycles, and the cells were disassembled in an argon-filled glove box. Cathodes were washed with dimethyl carbonate (DMC) several times and dried in the glove box. The cycled cathode materials were harvested from the current collector, ground, and subsequently placed in a 6 mm vanadium sample holder for neutron diffraction experiments. These experiments were conducted at the POWGEN beam line at the ORNL Spallation Neutron Source (SNS). The diffraction data collected from the materials was simulated by the Rietveld method using EXPGUI software. Different crystal models were considered for the phase analysis, and lithium position, oxygen occupancies, and transition metal ion migration were also taken into consideration. Here we present the results from the pristine HE5050 material.

While refining the structure of the pristine HE5050 material, the monoclinic phase with Li_2MnO_3 or $Li[Li_{1/3}Mn_{2/3}]O_2$ composition (C2/m space group) was used, and the refinement of the experimental ND pattern was initiated by assuming one transition metal (Mn) atom present as explained by Strobel. However, the agreement parameters obtained were not satisfactory (Rwp= 13%, χ^2 =11) and the fitting was not well represented. It is obvious that the pristine HE5050 compound contains Co and Ni along with Mn atoms and the neutron scattering factors of these three metal atoms are distinct, and, hence, assuming only Mn atom in Li_2MnO_3 type structure did not result in a good fit. Perhaps this indicates the metal sites are occupied by Co, Mn and Ni transition metal atoms. Hence, keeping the unit cell dimension unaltered, Mn, Co, and Ni were allowed to

occupy in the 2b and 4g sites (metal sites) and Li in the 2c and 4h sites (lithium sites) which resulted in an improvement in the profile fitting. The Wyckoff positions of the oxygen were refined and values showed no difference as compared to the values reported by Whitfield and Strobel. Interestingly, displacing Ni from TM to the lithium sites showed significant improvement in the fitting and good agreement parameters were achievable. The site occupancy factor (SOF) of all individual atoms was refined by applying constraints to the particular sites. The obtained crystallographic information is presented in Table 1, and it was observed that Ni atoms present in 2b sites are rich in composition as compared to the Ni atoms present in the 4g sites. It is believed that Ni atoms prefer the lithium site and this might be due to the similar ionic radii of Ni^{2+} and Li^{+} in the octahedral coordination. The structural parameter of the TODA HE5050 pristine material can be represented as:

$$\{Li_{1-x}Ni_x\}^{2c}\{Li_{1-y}Ni_y\}^{4h}[\{Li_{0.364}Ni_{0.266}Mn_{0.3694}\}^{2b}\ \{Li_{0.128}Ni_{0.0494}Mn_{0.6726}Co_{0.15})^{4g}]O^{4i}O^{8j}$$

where x= 0.0043; y= 0.01. The refined ND pattern with this model is shown in Figure 5. The overall composition was calculated as $Li_{1.199}Co_{0.099}Mn_{0.562}Ni_{0.140}O_2$, which is in good agreement which is nominal composition. We are currently refining the data from the cycled materials, and these results will be presented in the next quarterly report.

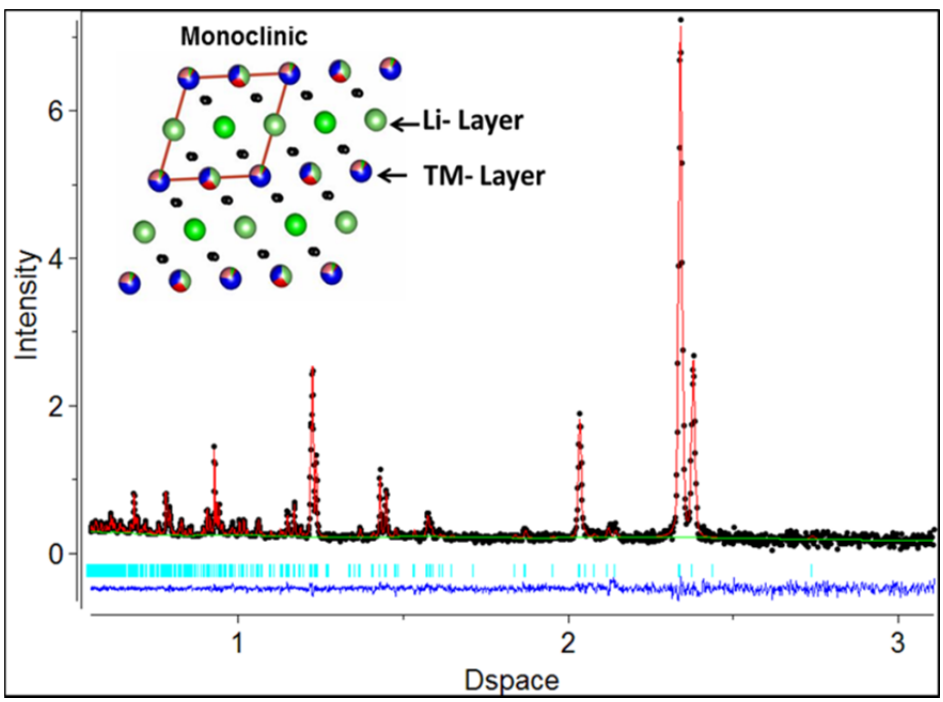

Figure 5. Simulated ND pattern of TODA HE5050 pristine material. The input structural parameter was $\{Li_{1-x}Ni_x\}^{2c}\{Li_{1-y}Ni_y\}^{4h}[\{Li_{0.364}Ni_{0.266}Mn_{0.3694}\}^{2b}$ $\{Li_{0.128}Ni_{0.0494}Mn_{0.6726}Co_{0.15})^{4g}]O^{4i}O^{8j}$ where x= 0.0043 and y= 0.01. In the model, the different colors represent different transition metal ions occupying a single site.

Table 1. The refined crystallographic parameter, unit cell dimensions, and refinement agreement parameter values for TODA HE5050 pristine material.

Crystal System: Monoclinic SG: C2/m a=4.94565(19), b=8.56182 (31), c= 5.03138(13), β =109.2908 (25), V=201.086 (12), Z= 12						
Composition: $Li_{1.199}Co_{0.099}Mn_{0.562}Ni_{0.140}O_2$						
Agreement parameters: R_{WP}= 5.05% Rp= 6.69 χ^2 =1.50						
Site	**Atom**	**x**	**y**	**Z**	**SOF**	**Uiso**
2c	Li	0	0	0.5	0.9957	
	Ni				0.0043	0.01173
4h	Li	0	0.655100	0.5	0.9900	
	Ni				0.0100	0.01248
2b	Li	0	0.5	0	0.364	
	Ni				0.2666	0.00297
	Mn				0.3694	
4g	Li	0	0.166000	0	0.128	
	Ni				0.0494	
	Mn				0.6726	0.00763
	Co				0.15	
4i	O1	0.222689	0	0.223208	1	0.00499
8j	O2	0.253909	0.322246	0.225611	1	0.00568

4. Future work for next quarter:

1. Calibrate the fiber optic sensor over the roller rotation and compare thickness results with the laser caliper sensors.
2. Test the ability of XRF to detect the metal contamination in the electrodes.
3. Provide the mechanism of voltage fade in TODA HE5050 by detailed analysis of neutron diffraction data.

Publications, Reports, Intellectual Property or Patent Applications filed this quarter.

1. D. Mohanty, A. Safa-Sefat, J. Li, S. Kalnaus, R.A. Meisner, D.L. Wood, and C. Daniel, "Investigating the Voltage Fading Mechanism in a $Li_{1.2}Co_{0.1}Mn_{0.55}Ni_{0.15}O_2$ High-Voltage Lithium Ion Battery Cathode via Magnetic and Diffraction Studies," *Chemistry of Materials*, In Preparation, 2013.
2. D. Mohanty, L.C. Maxey, R.B. Dinwiddie, J. Li, and D.L. Wood, "Improved QC of Slot-Die Coated Lithium Ion Battery Electrodes by IR Thermography and Laser Thickness Techniques," *Analytical Methods* , Under Review, 2013.
3. D. Mohanty, S. Kalnaus, R.A. Meisner, K.J. Rhodes, E.A. Payzant, D.L. Wood, and C. Daniel, "Structural Transformation of a Lithium-Rich $Li_{1.2}Co_{0.1}Mn_{0.55}Ni_{0.15}O_2$ Cathode During High Voltage Cycling Resolved by In-Situ X-Ray Diffraction," *Journal of Power Sources*, **229**, 239–248 (2013).
4. D. Mohanty, S. Kalnaus, R.A. Meisner, A. Safa-Sefat, J. Li, K.J. Rhodes, E.A. Payzant, D.L. Wood, and C. Daniel "Structural Transformation in a

$Li_{1.2}Co_{0.1}Mn_{0.55}Ni_{0.15}O_2$ Lithium-Ion Battery Cathode During High-Voltage Hold," *RSC Advances*, **3**, 7479–7485 (2013).

5. D. Mohanty, A. Safa-Sefat, S. Kalnaus, J. Li, R.A. Meisner, E.A. Payzant, D.P. Abraham, D.L. Wood, and C. Daniel, "Investigating Phase Transformation in $Li_{1.2}Co_{0.1}Mn_{0.55}Ni_{0.15}O_2$ Lithium-Ion Battery Cathode During High-Voltage Hold (4.5 V) via Magnetic, X-ray Diffraction and Electron Microscopy Studies," *Journal of Materials Chemistry A*, **1**, 6249–6261 (2013).

TASK 3
Abuse Tolerance Studies

Project Number: 3.2 (ES036)

Project Title: Abuse Tolerance Improvements

Project PI, Institution: Chris Orendorff, Sandia National Laboratories

Collaborators (include industry): ANL, INL, BNL, ORNL, NREL, Physical Sciences Inc.

Project Start/End Dates: 10/1/2012-9/30/2013

Objectives: The objective of this work is to develop inherently abuse tolerant lithium-ion cell chemistries. This involves understanding the mechanisms of cell degradation and failure, determining the effects of new materials & additives on abuse response, and cell level abuse testing and cell characterization to quantify improvements

Approach: Materials to full cell characterization to determine inherent safety and reliability of the most advanced lithium-ion chemistries. Approaches include a suite of battery calorimetry techniques (microcal, DSC, TGA/TDA, isothermal, ARC), abuse tests (electrical, mechanical, thermal), and analytical diagnostics (electrochemical characterization, optical spectroscopy, mass spectrometry, computed tomography, electron microscopy, etc.)

Milestones:
(a) LiF/ABA electrolyte development (ON GOING, on schedule)
(b) Evaluation of coated materials (ON GOING, on schedule)
(c) Ionic liquid electrolyte development (ON GOING, on schedule)
(d) Abuse testing and characterization of FRION electrolytes (starting Q3)
(e) Abuse tolerance of high energy materials (ON GOING, on schedule)

Financial data: Total budged $1.0M; received $500K

PROGRESS TOWARD MILESTONES

(a) LiF/ABA electrolyte development. Work in Q2 has continued to improve overall LiF/ABA performance in cells as we move toward delivering LiF/ABA to MERF for scale-up. One issue that initially presented a challenge with LiF/ABA was capacity fade at the negative electrode because of poor SEI formation. Electrolytes formulations have been made to improve SEI film formation including those with nominal quantities of $LiPF_6$. Figure 1 shows cyclic voltammetry data (current density vs. potential) for LiF/ABA cycled from 0-4.5 V (vs. Li/Li+) for 1 M LiF/ABA in EC:EMC and 1 M LiF/ABA + 10 mM $LiPF_6$ in EC:EMC. The addition of 10 mM $LiPF_6$ appears to stabilize the LiF/ABA at negative potentials because of good SEI formation (comparable to 1.2 M

$LiPF_6$ in EC:EMC electrolyte). Work will continue by demonstrating the impact of improved SEI formation in full cells in Q3 and Q4 FY13. In addition, the synthesis of LiF/ABA has been improved during Q2 to enhance LiF/ABA performance. Figure 2 shows the conductivity (mS/cm) of LiF/ABA and $LiPF_6$ in EC/EMC as a function of temperature. Early generations of LiF/ABA-1A have ambient temperature conductivities on the order of 6 mS/cm. Improved LiF/ABA-1B has a room temperature conductivity of 11 mS/cm; approaching that for $LiPF_6$. Performance of these improved ABA electrolytes will be determined in full cells in Q3 and Q4 to better understand the impact on cell capacity and rate capability.

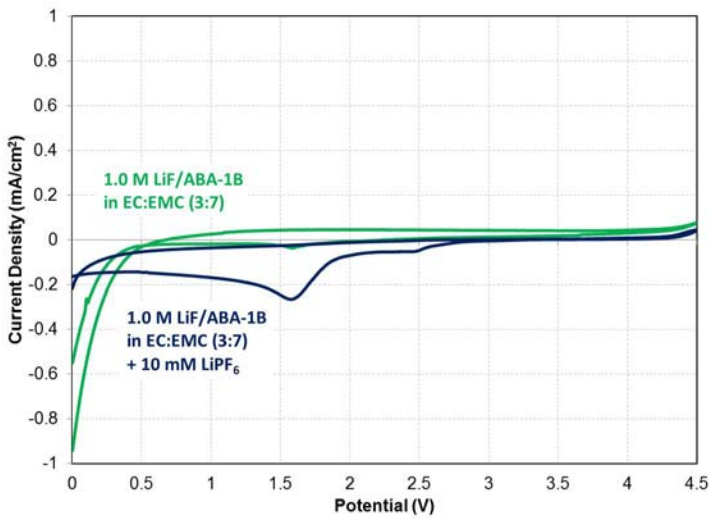

Figure 1. Cyclic voltammetry of 1.0 M LiF/ABA and 1.0 M LiF/ABA + 10 mM $LiPF_6$ in EC:EMC (vs. Li/Li^+)

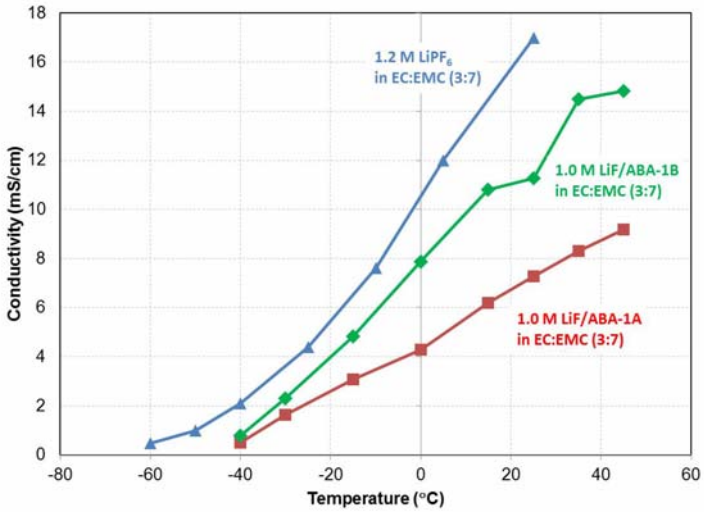

Figure 2. Conductivities (mS/cm) of 1.2 M $LiPF_6$ (blue), 1.0 M LiF/ABA-1A (red), and 1.0 M LiF/ABA-1B (green) in EC:EMC (3:7).

(b) Coated materials. For a number of years, the ABR program has focused on material coating strategies to improve cell performance and reliability. In earlier work, we have shown AlF3-coated NMC to have improved safety performance, as well. The NREL led coatings programs have focused on Al_2O_3 atomic layer deposition (ALD) coatings and the objective of our contribution is to evaluate the effect of these coatings on thermal stability and safety. NMC 111 (Toda) and graphite (CP A10) electrodes are coated with Al_2O_3 ALD to give ~0.3 nm and 0.8 nm thick coatings on each electrode, respectively. Figure 3 (left) shows DSC data for the coated and uncoated graphite electrode. Results show a significant reduction in the heat generation at the onset of SEI decomposition (~100 °C). Figure 3 (right) shows ARC data for 18650 cells with Al_2O_3 ALD and uncoated electrodes. The coated cell shows and increase in the exotherm onset temperature by ~20 °C, which is consistent with a stabilized SEI at the anode interface. The high rate cathode decomposition remains unchanged in the coated cell. This is likely due to the fact that the coating is not thick enough (nominally ~0.3 nm) to influence the decomposition of the positive electrode. Work will continue in Q3 to vary the thickness of Al_2O_3 ALD on NMC electrodes to improve the cathode thermal stability.

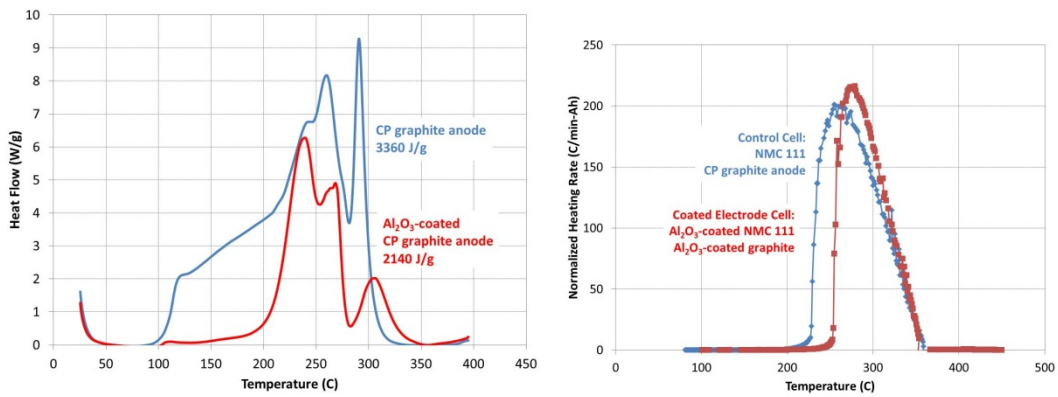

Figure 3. DSC of Al_2O_3 ALD coated graphite and ARC of Al_2O_3 coated graphite and NMC electrodes in 18650 cells.

(c) Ionic liquid electrolyte development. Q2 continued the development of ionic liquids (ILs) with improved voltage stability and useable electrolyte formulations of the candidate ionic liquids (ILs). Figure 4 (left) show cyclic voltammetry data of the candidate ILs prepared in FY12 and 13. The newest candidate, IL-3, shows the most promising voltage stability at both high and low potentials. IL-3 is stable to 5V which is comparable to carbonate solvent mixtures (no salt) and near the lithium potential without significant cation reduction. Electrolyte formulations of EC:EMC and IL-3 have been prepared to determine their performance in coin cells (NMC111/graphite full cells). Figure 4 (right) shows specific capacity of for these coin cells with 0-60% IL during formation. Results show that up to 40% IL the specific capacity during formation is identical to the EC:EMC control cell. At 60% IL, the performance begins to decay rapidly. Work in Q3 will continue to evaluate these 40% IL-3 electrolyte formulations over longer cycle life and for safety performance (thermal stability and flammability).

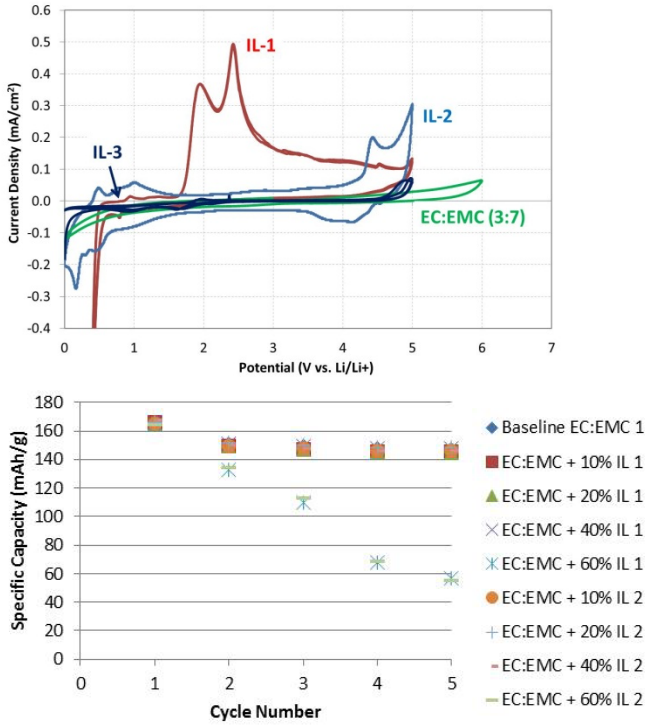

Figure 4. Cyclic voltammetry of candidate ionic liquids (neat) and EC:EMC solvent and specific capacity of electrolyte formulations in NMC 523/graphite coin cells up to 60% IL.

(d) FRION electrolyte development. A candidate FRION (flame retardant ion) electrolyte (developed at Case Western under the BATT program) was sent to ANL in Q2 for screening and electrolyte formulation. This electrolyte will be sent to Sandia for 18650 cell building and safety performance testing. ARC and flammability measurements will be performed on the FRION and control cells to determine the impact of the FRION on cell thermal stability during runaway and the efficacy of the flame retardant electrolyte in cells during ignition testing.

(e) High Energy Materials. One objective for FY13 is to determine baseline safety performance and thermal stability of high energy lithium-ion materials (lithium-rich LMO, Si-composites, and high voltage LMNO). The largest barrier to the success of this effort to date has been the availability and access to these high energy materials. In Q2 we received a small quantity of lithium-rich LMO positive material from Toda (HE5050). Initial work has focused on baseline materials characterization. Figure 5 shows DSC data for HE5050 at 4.6 V. Results show a relatively high onset temperature for decomposition and specific heat release of 1860 J/g (comparable to NMC 523 at 4.2 V).

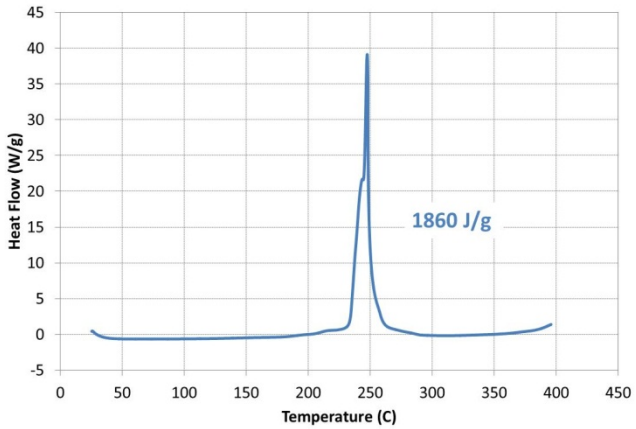

Figure 5. Representative DSC data for HE5050 cathode electrode at 4.6 V.

TASK 3
Abuse Tolerance Studies

Project Number: 3.3 (ES037)

Project Title: Overcharge Protection for PHEV Batteries

Project PI, Institution: Guoying Chen, Lawrence Berkeley National Laboratory

Collaborators: Robert Kostecki, John Kerr, Vince Battaglia, Marca Doeff, Gao Liu, Quy Ta and Brian Nguyen (American Dye Source, Inc.).

Project Start Date: March 2009

Objectives: Develop a reliable, inexpensive overcharge protection system. Use electroactive polymers for internal, self-actuating protection. Minimize cost, maximize rate capability and cycle life of overcharge protection for high-energy Li-ion batteries for PHEV applications.

Approach: Our approach is to use electroactive polymers as self-actuating and reversible overcharge protection agents. The redox window and electronic conductivity of the polymer will be tuned to match the battery chemistry for non-interfering cell operation. Rate capability and cycle life of the protection will be maximized through the optimization of polymer composite morphology and cell configuration.

Milestones:

a) Investigate rate performance and cycle life of Li-ion cells protected by electrospun electroactive-fiber-composite separators (January 2013). **Complete**

b) Evaluate alternative placements of the fiber-composite membranes in battery cells (March 2013). **Complete**

Financial data: $240K/FY2012

PROGRESS TOWARD MILESTONES

We previously reported that poly[(9,9-dioctylfluorenyl-2,7-diyl)-co-(1,4-phenylene)] (PFOP) has an onset oxidation potential of 4.25 V, which is one of the highest value reported so far. When the polymer was scanned at 5 mV/s between 0.1 to 4.5 V *vs.* Li/Li^+, no obvious changes were observed on the cyclic voltammogram (Fig. 1a), suggesting improved low-voltage stability and the possibility of using single-layer polymer composite for overcharge protection. A PFOP composite membrane was prepared by impregnating a concentrated chloroform solution of the polymer into a microporous Celgard membrane and then used as the separator in a "Swagelok-type" $LiFePO_4$ half-cell with 1M $LiPF_6$ in 1:1 (v/v) ethylene carbonate (EC) and diethyl

carbonate (DEC) electrolyte. The cell was charged and discharged at 0.65 C rate and 80% overcharge. A steady-state potential was reached at 4.3 V which remained nearly constant during the test, suggesting reversible internal shorting established by PFOP (Fig. 1b). Excellent capacity retention was also observed. The improved low-voltage stability of the polymer allows for stable single-polymer protection, which eliminate the need of the bilayer configuration that was previously adopted to protect the high-voltage polymer from degradation at the anode potential.

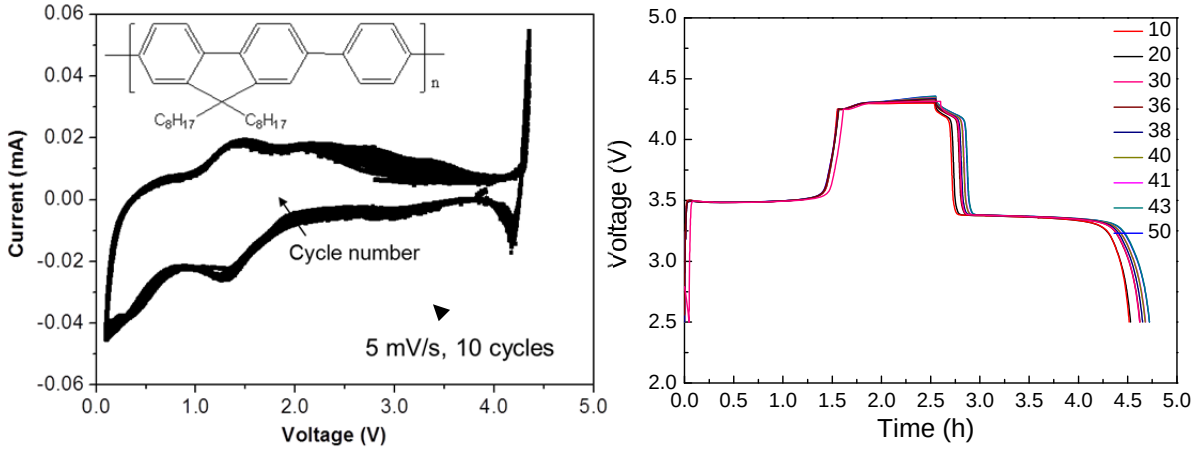

Figure 1. a) Cyclic voltammogram of PFOP in 1M $LiPF_6$ in EC: DEC electrolyte and b) cycling profiles of a $LiFePO_4$ half-cell overcharge-protected by the PFOP composite separator.

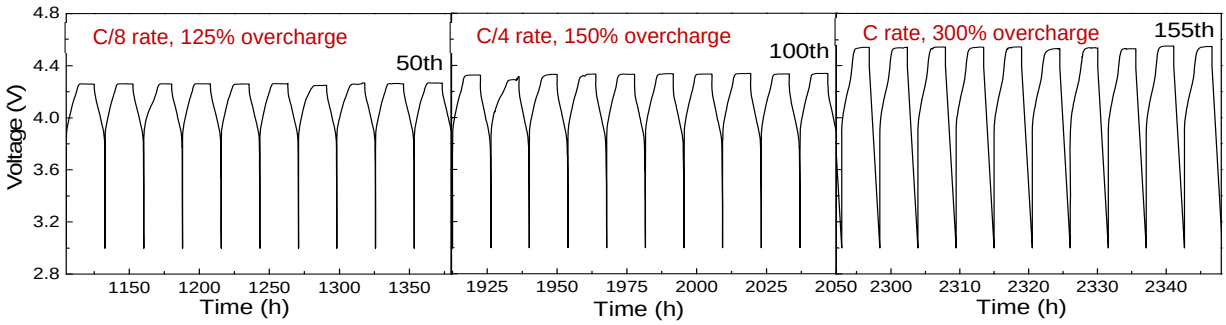

Figure 2. Varying-rate cycling profiles of a $Li_{1.05}Mn_{1.95}O_4$/Li pouch cell overcharge-protected by the PFO/P3BT glass-fiber composites.

The scalability of overcharge protection based on electroactive fiber composite separators was also evaluated. A $Li_{1.05}Mn_{1.95}O_4$-Li pouch cell with an electrode area of 3cm x 4cm, which is ten times larger than that in the "Swagelok-type" cell, was equipped with the combination of the PFO/P3BT glass-fiber composites, a configuration previously used in the "Swagelok-type" cell tests. Fig. 2 shows the room-temperature voltage profiles of the cell at the various cycling rates. At C/8 rate and 125% overcharge, the cell was reversibly protected at 4.3 V during the first 50 cycles. The steady-state voltage increased with the current density, reaching 4.35 and 4.55 V at C/4 and C rates, respectively. Stable protection was achieved at all rates tested. Compared to the previous protection achieved

on the pouch cells equipped with the PFO/P3BT Celgard composites, the upper cell limiting voltage was significantly reduced, further confirming lowered internal resistance and improved performance in the fiber composites.

Publications, Reports, Intellectual property or patent application filed this quarter. (Please be rigorous, include internal reports--invention records, etc.)

1. B. Wang, T. J. Richardson and G. Chen, "Stable High-Rate Overcharge Protection for Rechargeable Lithium Batteries," *Physical Chemistry Chemical Physics*, **15** (18), 6849 (2013).

2. G. Chen and T. J. Richardson, "High-Rate Overcharge-Protection Separators for Rechargeable Lithium-Ion Batteries and The Methods of Making The Same," PCT Application based on US Provisional Application 61/647,389, May 2013.

3. G. Chen, "Overcharge Protection for Safer Li-ion Batteries," Energy Storage and Distributed Resources Department Seminar, Berkeley, CA, February 2013.

4. G. Chen, "Overcharge Protection for PHEV Batteries," DOE Hydrogen Program and Vehicle Technologies Program Annual Merit Review and Peer Evaluation Meeting, Washington, DC, May 2013.